INTEGRATED STRATIGRAPHIC ANALYSIS OF A MIOCENE-AGE SANDY SHALLOW MARINE DEPOSITIONAL SYSTEM IN SOUTHERN DELAWARE

by

Tyler J. Buchanan

A thesis submitted to the Faculty of the University of Delaware in partial fulfillment of the requirements for the degree of Master of Science in Geology

Spring 2019

INTEGRATED STRATIGRAPHIC ANALYSIS OF A MIOCENE-AGE SANDY SHALLOW MARINE DEPOSITIONAL SYSTEM IN SOUTHERN DELAWARE

by

Tyler J. Buchanan

Approved: ____
Peter P. McLaughlin, Jr., Ph.D.
Professor in charge of thesis on behalf of the Advisory Committee

Approved: ____
Ronald E. Martin, Ph.D.
Professor in charge of thesis on behalf of the Advisory Committee

Approved: ____
Neil C. Sturchio, Ph.D.
Chair of the Department of Geological Sciences

Approved: ____
Estella Atekwana, Ph.D.
Dean of the College of Earth, Ocean, and Environment

Approved: ____

Douglas J. Doren, Ph.D.
Interim Vice Provost for Graduate and Professional Education

ACKNOWLEDGMENTS

I would first like to thank my advisors, Dr. Peter McLaughlin and Dr. Ronald Martin. Without Pete's knowledge of regional palynology and stratigraphy, along with his assistance during field work, I would have never been able to finish this project. Conversations with Ron were imperative for developing my understanding of stratigraphic principles and micropaleontology. Their continuous support, guidance, and commentary were much appreciated during the entirety of this project. I also thank Dr. Katharina Billups for her helpful feedback as a committee member.

I also want to thank the Delaware Geological Survey's staff, especially Mr. Charles "Tom" Smith for his help in palynomorph processing, and Mr. Paul "Steve" McCreary for his drilling expertise. Without their knowledge and assistance, this project would not have been possible.

I am forever grateful for the unshakable love and support from my family and friends along this journey. It is amazing what the support of loved ones helped me to achieve, and I will never forget those who helped me attain this goal.

TABLE OF CONTENTS

Appendix

LIST OF TABLES

LIST OF FIGURES

ABSTRACT

This study examines the stratigraphy and palynology of three Miocene geologic units that occur in the Delaware Coastal Plain: the Calvert, Choptank, and St. Marys Formations. The goal of this investigation is to examine the stratigraphic record of these ancient shallow-marine units in detail in a nearly-continuous cored borehole at Abbott's Mill Historical Site, in Milford, Delaware. This study utilizes lithostratigraphy, fossil palynomorphs, and sequence stratigraphy to understand the age, depositional environments, and regional correlation of these units.

Pollen and spores were analyzed to interpret the paleoclimate. Vegetation is dominated by *Quercus*, *Pinus*, and *Carya*. The lower to middle Miocene Calvert Formation is interpreted to be a warm-temperate to subtropical environment, whereas the middle Miocene Choptank Formation represents a decline in temperature and moisture. The middle to upper Miocene St. Marys Formation represents a warm-temperate, slightly moist climate regime. Three zones were recognized using cluster analysis of the pollen data. Zone 1 (middle Choptank to St. Marys) is characterized by little to no exotic taxa, with high abundances of *Carya*, Cyperaceae, and *Quercus*. Zone 2 (middle Calvert to lower Choptank) has abundant *Pinus*, *Tsuga*, and *Picea*, with decreased *Quercus* and *Carya*. Zone 3 (lower to middle Calvert) contains the greatest abundances of exotic species including *Engelhardia*. Dinoflagellates cysts allow a refined subdivision of the Miocene stratigraphy, with zones identified from dinoflagellate Zone DN2 (lower Miocene) through Zone DN9 (upper Miocene).

Nine stratigraphic sequences were identified in this borehole, representing cycles of sea-level rise and fall in an overall wave-dominated, sandy, shallow-marine shoreline environment. The Calvert Formation is characterized by several coarsening-upward sections, with offshore clays transitioning to shallower silty sands. The Choptank Formation sediments are shelly, foreshore sands with breaks of muddier, finer-grained sections. The St. Marys Formation consists of interbedded silty sands and clays, representative of estuarine to marsh environments. Sequences identified here, constrained by the pollen and dinoflagellate biostratigraphy, correlate well with sequences identified at Marshy Hope and Bethany Beach. Results from this integrated stratigraphic analysis assist in better understanding the subsurface geology and hydrostratigraphy of southern Delaware.

Chapter 1

INTRODUCTION

The Miocene-age Calvert, Choptank, and St. Marys Formations are three geologic units that occur in the Mid-Atlantic Coastal Plain, specifically in Maryland and Delaware. The units are exposed in outcrop along the famous Calvert Cliffs along the western shore of the Chesapeake Bay. These units are known to dip gently to the southeast, where they occur in the subsurface in Delaware (McLaughlin and Velez, 2006; McLaughlin et al., 2008). Studies in Delaware have recognized that these units are fairly well correlated throughout the subsurface of the state (McLaughlin and Velez, 2006; McLaughlin et al., 2008), however aquifer continuity and paleoenvironmental changes in these units are not well understood in all of the Delaware Coastal Plain.

During June 2016, a nearly continuous record of Miocene sediments was recovered from a borehole at Abbott's Mill Historical Site in Milford, Delaware using wireline coring techniques. This comprehensive, multidimensional study incorporates stratigraphy, sedimentology, chronostratigraphy, and palynology in order to determine and better understand depositional and environmental changes, as well as palynomorph assemblages, within Miocene-age sediments recovered at this locality. Sequence stratigraphy is utilized to determine depositional environmental shifts through the Miocene-age Calvert, Choptank, and St. Marys Formations. These determined sequences are used to correlate the stratigraphy from this site across to the Marshy Hope borehole (Nb53-08) to the west, and the Bethany Beach borehole (Qj32-

27) to the southeast. In correlating these boreholes, not only can the Miocene lithostratigraphic units be better constrained, but economically important groundwater aquifers can be connected. This study also aims to provide context for palynomorph assemblage changes across the three sites, utilizing both pollen and dinoflagellates as a basis for climactic shifts through time.

The hypotheses of this study are as follows:

1. The palynological zonation created at this borehole will correlate to other boreholes around the region, namely Marshy Hope and Bethany Beach.

2. Dinocyst zones determined from this study are predicted to correlate to the Miocene dinocyst zonation created for the Salisbury Embayment by de Verteuil and Norris (1996).

3. Palynological data will help constrain the correlation of the hydrostratigraphic framework (aquifers and confining units) at Abbott's Mill to the hydrostratigraphy previously established for boreholes at Marshy Hope and Bethany Beach.

The objective of this study is to use sequence stratigraphy, sedimentology, biostratigraphy, and palynology to identify and better constrain the depositional and environmental history of northern Sussex County. Furthermore, aquifer geology can be better constrained as well, allowing the ability to more accurately map and drill the economically important groundwater from the subsurface.

Aquifers in southern Delaware are significant suppliers of water for residential, business, and agricultural uses. Several continuous aquifers occur throughout the Miocene-age sediments in this region, including the Upper Choptank, Lower Choptank, Milford, Frederica, Federalsburg, and Cheswold Aquifers (McLaughlin and Velez, 2006, McLaughlin et al., 2008). As such, it is possible to correlate aquifers together using information gained from this study. Using palynological assemblages, sequence stratigraphy, and sedimentology allow for better correlation of unstudied and understudied areas of lower Delaware, and a more detailed picture of the subsurface geology of the area.

1.1 Stratigraphy

Sequence stratigraphy is the study of stratigraphy in the context of unconformity-bound packages. The development of these unconformity-bond packages reflects the effects of changes in base level on sedimentation, usually due to sea level rise and fall but in some cases tectonics. The resulting variations in accommodation space and sediments supply contribute to the formation of stratigraphic surfaces and facies changes between these surfaces (Browning et al., 2006). A sequence is identified as a succession of relatively conformable, genetically related strata capped by unconformities, up to several hundred meters thick. These sequences can be divided into systems tracts, which themselves are capped by other stratigraphic surfaces (Coe et al. 2005; McLaughlin and Velez, 2006).

This study utilizes sequence stratigraphy to divide the sediments of the Abbott's Mill borehole into genetically related strata. Delineation of sequences allows for correlation from this borehole to other boreholes around the region. The sediments of this borehole represent a shallow-marine clastic depositional system. McLaughlin et al. (2008) have created a generalized sequence stratigraphy model for southern Delaware that will be utilized in this study (Figure 1.1).

Surfaces and systems tracts can be identified within sequences occurring in the borehole. Sequence boundaries (SB) are created by relative sea-level fall and subsequent erosion of previously deposited sediments, resulting in an unconformity, or a period of time unrepresented in the sedimentary record. Sediments from onshore, whether from a fluvial environment or eroded from the newly exposed coast, are deposited further out in the depositional basin (Coe et al., 2005). When relative sea level rises, sedimentation migrates towards the land above the SB, resulting in a marine flooding surface called a transgressive surface (TS). This surface is evident in a shift from progradational to retrogradational stacking patterns (Coe et al., 2005). The highest level that relative sea level rises during deposition of a sequence produces a surface known as the maximum flooding surface (MFS), which corresponds to the most landward position of the coast (Coe et al., 2005).

The sediments that accumulate between these various surfaces can also be labeled as specific systems tracts. Highstand systems tracts (HST) occur between a maximum flooding surface and a sequence boundary, where sediments represent progradation out towards the basin. This systems tract represents a slowing rate of rising sea level and lower accommodation space for sediment accumulation (Coe et al., 2005).

Frequently found above a sequence boundary is a lowstand systems tract (LST), which represents a period between sea-level fall and sea level rise, so oftentimes there is evidence of subaerial exposure and erosion towards the top of the section (Coe et al., 2005). In southern Delaware however, it is common in the Miocene-age units to have a poorly defined to usually nonexistent LST (Fisher, 2016, McLaughlin et al., 2008, McLaughlin and Velez, 2006). This is because Delaware is in a relatively updip position on the continental margin and lowstand deposition would have moved farther basinward with the relative fall of sea level.

Between a transgressive surface and a maximum flooding surface is the transgressive systems tract (TST). A shift in sediments landward from the basin occurs during TST deposition because sea-level is rising.

These depositional cycles can be identified in core samples and geophysical logs. Thus, the formations present in this study are identified by analyzing lithologies and interpreting geophysical logs from the Abbott's Mill borehole. Sequences identified in this borehole are used to correlate this location to Bethany Beach and Abbott's Mill.

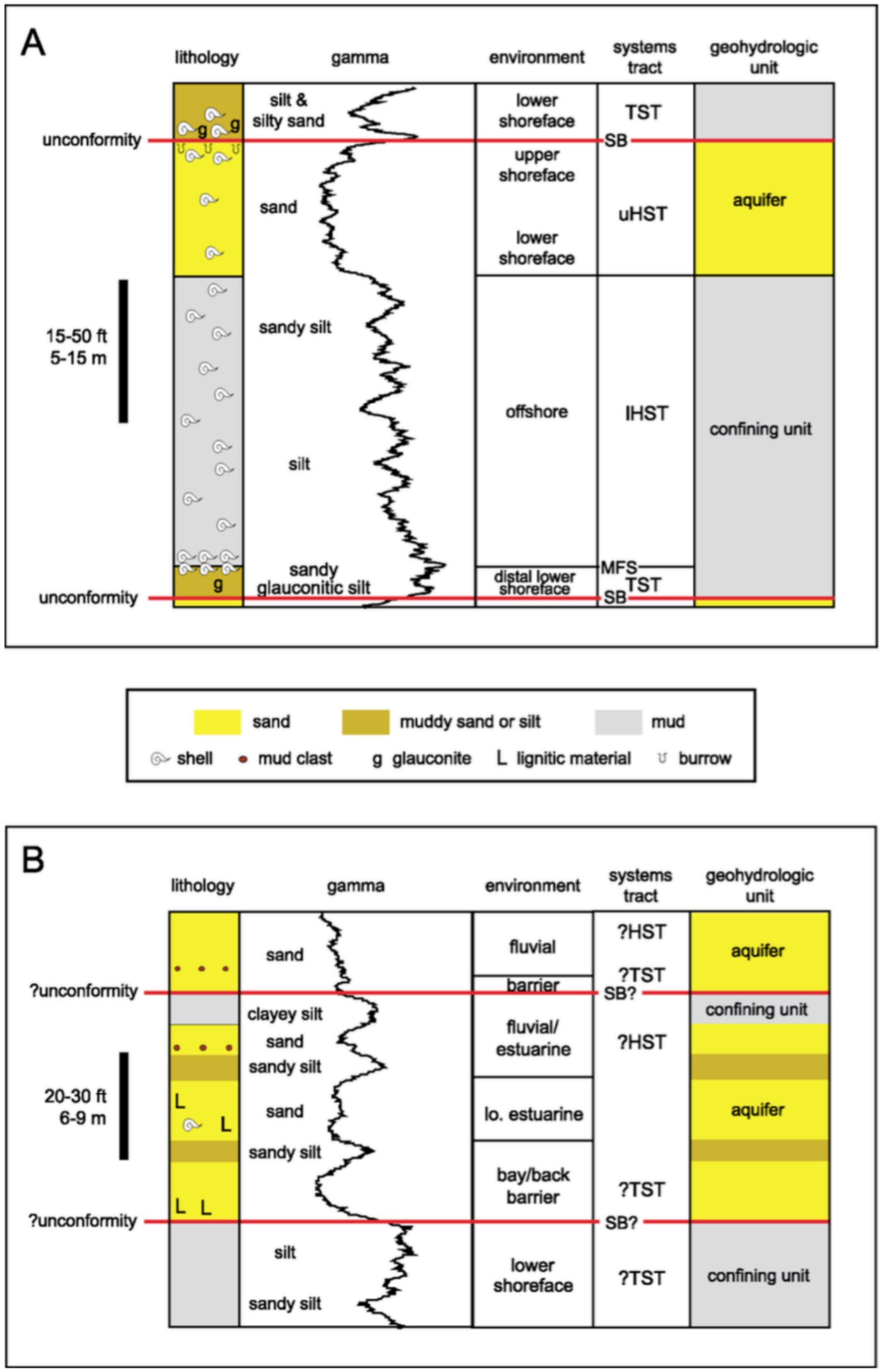

Figure 1.1: Generalized sequence stratigraphy model for Miocene-age units in southern Delaware (McLaughlin et al., 2008). A represents the shallow-marine lower to middle Miocene sections. B represents the shallow to marginal-marine upper Miocene sections.

1.2 Palynology

Palynological identification begins with an understanding of pollen and spore morphology. Pollen grains are identified in several different steps. Pollen grains are shed in dispersal units, which may be a monad (single), tetrad (four), or polyad (several) grains. Grains can contain no apertures (thin, recessed, regions across the surface) to more than five. These apertures have varying types. The outer layer of the pollen wall, called the tectum, can be atectate (no tectum), eutectate (continuous tectum), or semitectate (discontinuous tectum). Pollen grains also come in a wide range of sizes, and several different shapes. The ornamentation of a grain, along with the other morphologic features, can be used to identify a particular pollen or spore grain down to the species level, but in this study, ornamentation was used to determine genera, and in some cases, family level taxonomy. Figures 1.2 and 1.3 show morphological types of pollen and spores. Morphologic features include variations in colpi (furrows), pore sizes and amounts, and shape. Size of a grain can also be used to identify pollen grains; however sizes can vary within the same taxa (Faegri and Iverson, 1989).

In order to interpret paleoenvironments based on palynological assemblages, it is important to understand the deposition of the grains themselves. Pollen, in general, is transported in three main ways. How it is dispersed depends on the plant species itself. The first method of dispersal is self-pollination, where not much pollen is produced, and typically pollen is dropped by the plant onto itself to reproduce. These plant species are called autogamous (Faegri and Iverson, 1989). The second type is pollination by animals (entomophilous or zoophilous) where pollen attaches to insects and animals to be carried to another plant for reproduction (Faegri and Iverson, 1989). The third, and by far the most important in terms of the pollen record, is pollination by wind, also known as anemophilous pollination. Plants that use this form of pollination produce large amounts of pollen to be taken by the wind to reproduce (Faegri and Iverson, 1989). There is a slim chance that the execution of pollination is successful, resulting in most of the pollen grains being carried away by water or wind and incorporated in the sediment. Autogamous and zoophilous plants do not contribute significantly to the fossil pollen record. Typically, pollen transported by the wind is the most common pollen found in paleodeposits.

The amount of pollen and spores in the air in a given area is known as pollen rain (Faegri and Iverson, 1989). These grains are generally silt-sized or smaller, allowing them to be transported by wind and water rather easily. The path length of pollen transport falls into three categories. Gravity pollen is pollen that falls straight down off the plant and lands on the ground. The second is local, where the pollen may be picked up by the wind, but travels less than 100 meters from the source. The final category is regional pollen, where pollen is picked up by the wind and can be kept in the air for long distances. Pollen grains can also be transported by water, such as rivers or ocean currents, which can transport grains far distances from their source plant (Faegri and Iverson, 1989). Miocene sediments at Abbott's Mill represent a shallow continental shelfal environment. Therefore the majority of pollen and spores found were deposited by modes of wind and water transportation.

Identification of pollen, spores, and dinoflagellates can be used to determine palynofacies, which help identify variations in environment and climate over time based on changing assemblages (Traverse, 2008). Palynological zonations created at Bethany Beach and Marshy Hope are used to correlate this site to these other sites across lower Delaware. Dinoflagellates identified at this site are compared to the dinocyst zonation put forth by de Verteuil and Norris (1996) to create a zonation for this site to compare to Bethany Beach and Marshy Hope. The zones identified by de Verteuil and Norris (1996) have been dated, and are therefore useful in helping constrain the ages of the sediments at Abbott's Mill.

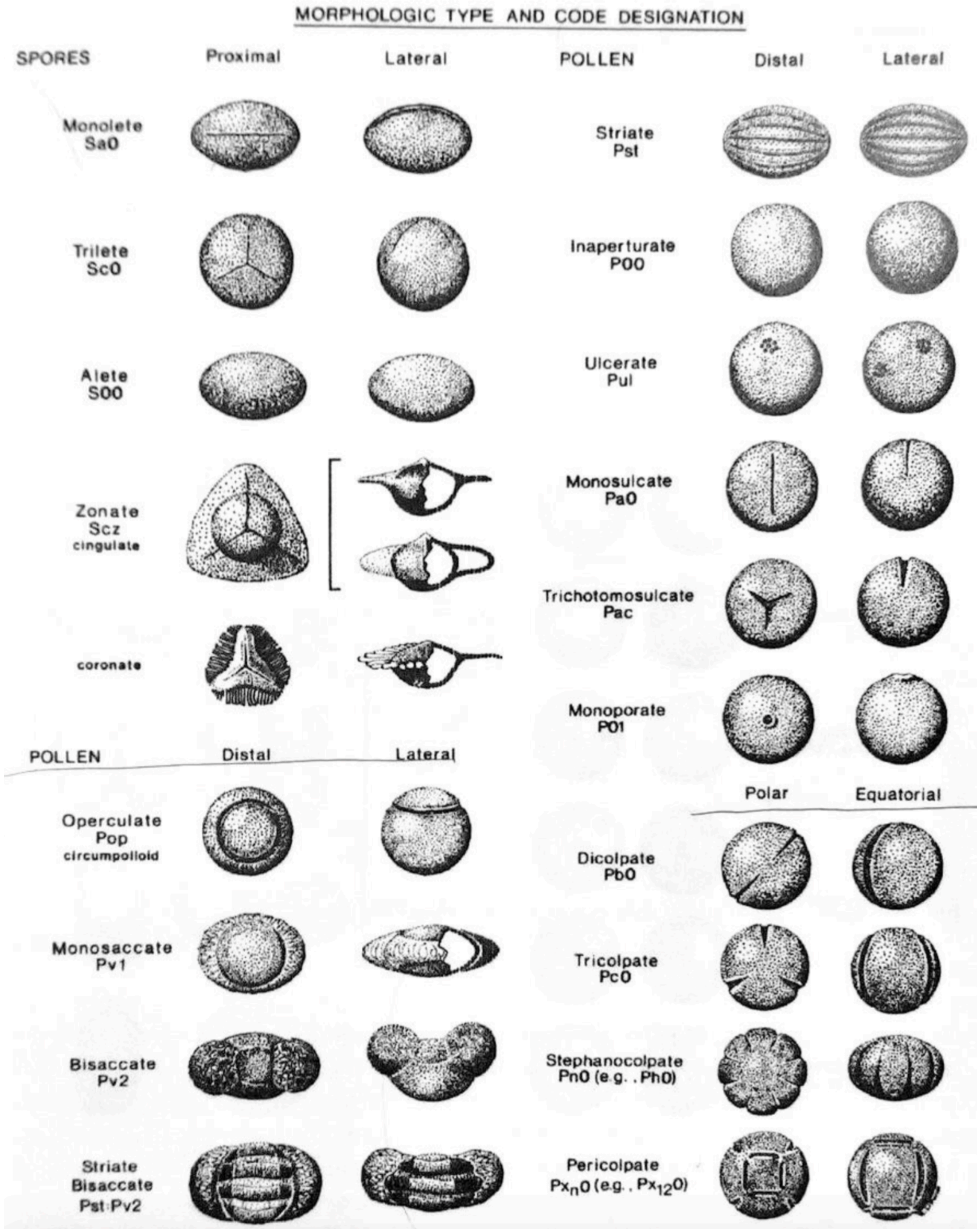

Figure 1.2: Morphologic features of pollen and spores (Traverse, 2008).

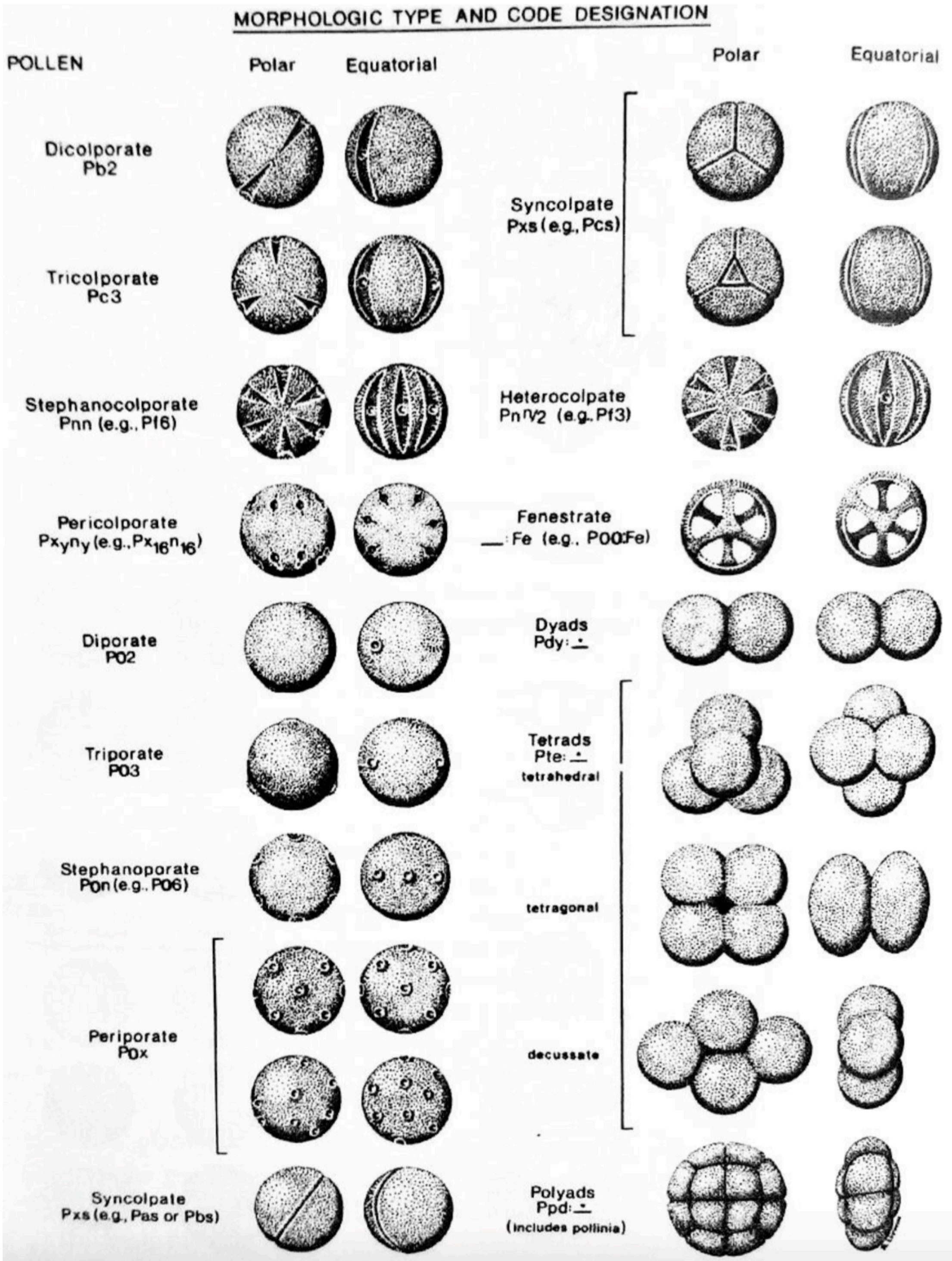

Figure 1.3: Morphologic features of pollen and spores continued (Traverse, 2008)

Chapter 2

BACKGROUND

2.1 Previous Work

In Delaware, a few studies have been completed regarding Miocene-age deposits (McLaughlin and Velez, 2006, McLaughlin et al., 2008, Fisher, 2016, McLaughlin et al., 2019). McLaughlin and Velez (2006) focused on hydrostratigraphy of Kent County. Aquifers were identified and mapped throughout the subsurface. These aquifer correlations, along with updated data from McLaughlin et al. (2019) were used to identify aquifer units present in this borehole, based on comparisons of lithologies and geophysical logs.

A deep borehole drilled with continuous coring at Bethany Beach, Delaware provides an important geological reference for the Oligocene to Pleistocene section (Figure 2.1) (Miller et al., 2003; Browning et al., 2006; McLaughlin et al., 2008). Those previous studies studied the subsurface lithology, palynology, and sequence stratigraphy. The study found eleven Miocene-age shallow-marine stratigraphic sequences. Sequence C1 is heavily burrowed at the base, where above the unconformity is a thin glauconitic transgressive systems tract (TST), transitioning into a thick coarsening upward highstand systems tract (HST). Sequence C2 is predominantly silty, with a thicker TST. The lower sequence boundary (SB) of C2 is identified by a gamma peak, which is caused by residually radioactive minerals in the sediments. The upper SB was determined by a heavily bioturbated contact between muddy sand and a sandstone. Sequence C3 was identified by a thin TST transitioning to a clean sandy section of a HST. The bottom of Sequence C4 was identified by silty lower shoreface sands overlying a cemented sand bed, with a thin TST and thicker coarsening upward HST. The contact between C4 and C5 shows heavy burrowing and a gamma increase. A deepening event can be seen, with a MFS that shallows to a sandy upper shoreface sand. These clean sands were interpreted as the bottom of the Choptank Formation. Sequence C6 is subtle, and saw a shift from the clean sands below to cemented shelly sand. Sequence C7 is a nearly completely HST, with a coarsening upward trend rich in shelly material, similar to the next sequence, C8, which contains two coarsening-upward packages. The base of Sequence C9 was determined by basal cemented quartz sandstone and a sharp gamma peak. The sequence contains a heavily burrowed MFS with glauconite, which was also noted to be the contact between the Choptank and St. Marys Formations. The base of Sequence C10 is heavily bioturbated, on top of an indurated zone. The TST is thin, with glauconite sands, transitioning to a MFS where phosphate grains are noted. The final Miocene sequence, M1, is marked by another highly burrowed surface. The TST is thin, and contains glauconitic clays. A MFS is recognized, and is noted to be the contact between the St. Marys and Cat Hill Formations. Typically, sequences were identified by peaks on the gamma log, along with sediment compositions. These interpretations of sequences are the basis for the approach used in this study's sequence stratigraphic analysis. McLaughlin et al (2008) were also able to identify three distinct pollen zones with subzones in each (Zones 4 to 6) within the Miocene section that will be used for correlation to the borehole at Abbott's Mill.

A Master's Thesis related to this project was completed on a borehole from Marshy Hope, Delaware (Fisher, 2016). This study related sedimentology, sequence stratigraphy, and palynology. The borehole was correlated to Bethany Beach, and the author's identified dinoflagellate zonations were compared to zonations put forth by de Verteuil and Norris (1996). Three pollen zones (Zones 1 to 3) and seven stratigraphic (Sequences 1 to 7) sequences were found in her study, most of which were correlated to the interpretations made for the Bethany Beach cores by McLaughlin et al. (2008). This study's interpretations were also considered when determining sequences in this study.

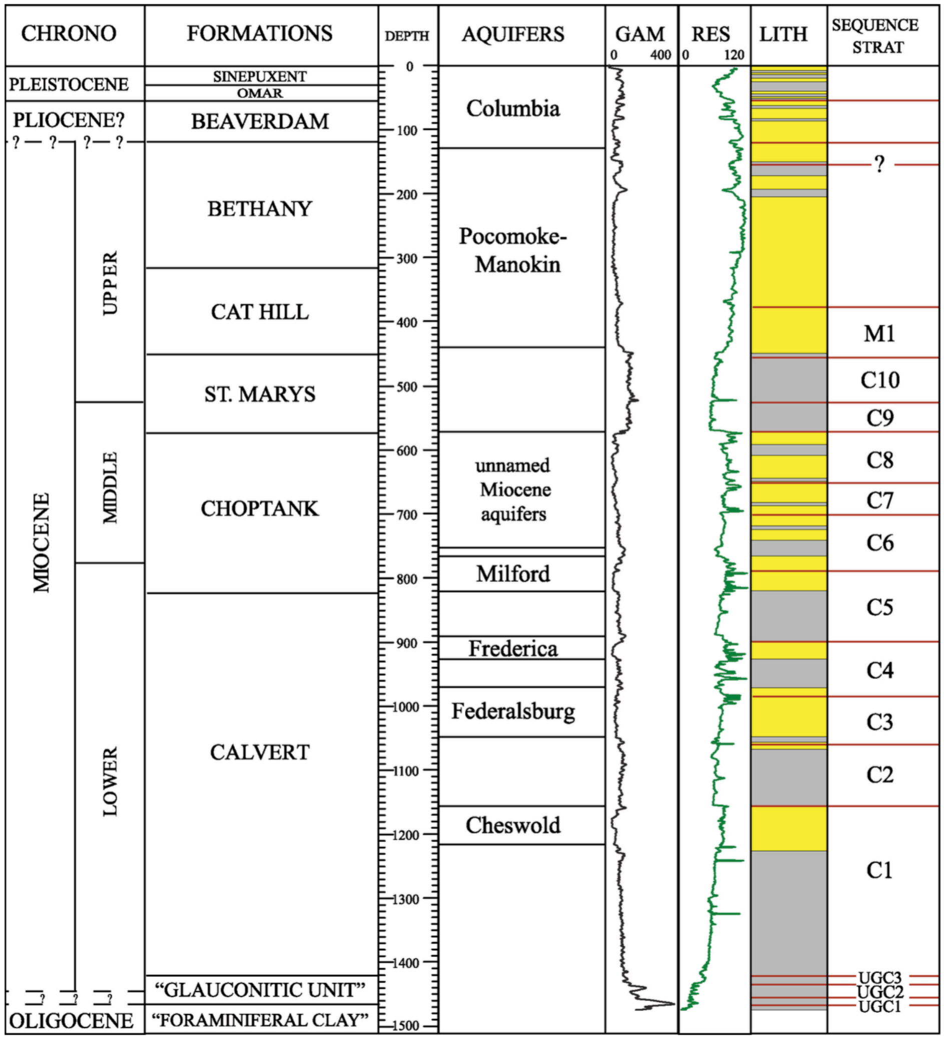

Figure 2.1: Summary stratigraphic column for the Bethany Beach borehole, Qj32-27 (McLaughlin, et al., 2008)

2.2 Mid-Atlantic Coastal Plain Stratigraphy

The Mid-Atlantic Coastal Plain includes New Jersey, Delaware, Maryland, and Virginia from the Atlantic Ocean to the Fall Line. This region includes the geologic structure known as the Salisbury Embayment, a regional geologic depression that underlies the coastal portions of the region. The Salisbury Embayment is a low area between the Normandy Arch and the Norfolk Arch and adjoins a deep basin that underlies the outer continental shelf, the Baltimore Canyon Trough. (Figure 2.2). During most of the Miocene, the Salisbury Embayment was covered by the sea and accumulated a succession of marine shales and sands. Sea-level rise and fall had a large effect on depositional processes in the Salisbury Embayment, producing alternations between shallower-marine sandy intervals, and deeper shelf intervals rich in silt and clay. Several studies, mentioned below, have linked Miocene age sequence boundaries to growth and waning of ice sheets. Positive shifts of global 18δO increases have been measured and are linked to the growth of continental ice sheets and subsequent sea- level fall (Miller et al., 2005, Browning et al., 2006, Browning et al., 2013).

The Calvert, Choptank, and St. Marys Formations (all part of the Chesapeake Group), are Miocene-age marine units recognized in Maryland, where they were named, as well as in Delaware and Virginia (Figure 2.3). Shattuck first described these units in Shattuck (1902) and in Shattuck (1904) subdivided the section along the Calvert Cliffs in Maryland into twenty-four informal lithologic units that are now referred to as Shattuck Zones. These Shattuck Zones were divided based on sediment color and type, abundance of shell materials, and molluscan species assemblages. These zones have been used for over the past one hundred years because most are readily identifiable throughout Maryland's coastal plain and in outcrop. The Calvert, Choptank, and St. Marys Formations are usually found to be shallow-marine deposits, from inner tidal to shallow shelf to deeper shelf, trending deeper towards the south-southeast across Maryland, Delaware, and Virginia. These environments are characterized by overall shallowing, with higher frequency shoaling and deepening trends within, later in the Miocene (Kulpecz et al., 2009, McLaughlin et al., 2008, Browning et al., 2006). A map of the region depicting relevant locations can be seen in Figure 2.4.

Comparable to the Calvert, Choptank, and St. Marys Formations, Miocene formations in New Jersey include the Kirkwood and Cohansey Formations. The Kirkwood Formation represents a deltaic environment, while the Cohansey Formation is indicative of more beach-barrier island and fluvial environments (Browning et al., 2008). The Kirkwood beds contain, like the Calvert-Choptank succession, alternations between sandier intervals deposited at shallower water depths and muddier intervals deposited at deeper paleowater depths. Glauconite is commonly found between Oligocene and Miocene units, at the base of both the Calvert and the equivalent Kirkwood Formation (Sugarman et al, 1993, Sugarman et al., 1997, Harris and Whiting, 2000, McLaughlin et al., 2008). Three major sequences are present in the Kirkwood Formation, occurring at 19.2 to 22.5 Ma, 15.5 to 17.4 Ma, and 11.5 to 13.6 Ma, with several smaller-scale sequences occurring throughout the Miocene (Browning et al., 2008). These sequences reflect a typical cycle found in New Jersey, where the sequence generally coarsens upward, representing a basal transgression followed by regression during which deltaic deposits prograde over shelfal deposits (Sugarman et al., 1993, 2005).

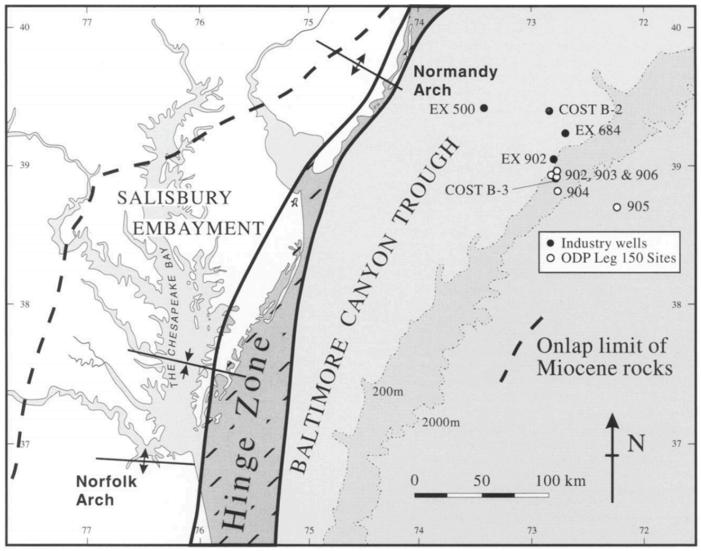

Figure 2.2: Map of the mid-Atlantic United States depicting the structural elements of the Salisbury Embayment (de Verteuil and Norris, 1996).

In Kent County, Delaware, the Calvert and Choptank Formations contain four significant aquifers: Cheswold, Federalsburg, Frederica, and Milford. Aquifers here consist of layers of shallow-water sands coupled with deeper-water fine-grained confining units, representing environmental transitions from upper and lower shoreface sands to deeper, offshore silts and clays. These aquifer units, along with the Choptank and Lower Calvert aquifer units, were identified in this study. Most abrupt transitions from an aquifer sand to a fine-grained confining unit is considered to be a sequence boundary, representing a drop in sea-level, a hiatus, and a marine flooding over the hiatus (McLaughlin and Velez, 2006). These aquifers, much like the formations themselves, trend dipping towards the south to southeast. The facies represented in these formations also trend in a similar fashion, generally with nearshore facies to the north-northwest and offshore facies to the south-southeast (McLaughlin and Velez, 2006).

The Bethany Beach cores provide an integrated stratigraphic framework from near the center of the Salisbury Embayment that helps to correlate Miocene units regionally. The Miocene lithostratigraphy described at Bethany Beach consists of six formations (Miller et al., 2003; Browning et al., 2006; McLaughlin et al., 2008). From lowest Miocene up, the formations and their depositional environments are: the inner shoreface to offshore middle neritic Calvert Formation, the nearshore shallow marine to estuarine to shoreface Choptank Formation, the low-energy shelfal or estuarine beds of the St. Marys Formation, the nearshore Cat Hill Formation, the shallow marine to estuarine Bethany Formation, and the possibly Pliocene fluvial to estuarine Beaverdam Formation (McLaughlin et al., 2008).

As mentioned previously, the Calvert, Choptank, and St. Marys Formations can be seen best in outcrop at Calvert Cliffs, on the western side of the Chesapeake Bay, where they were first described. Kidwell (1997) studied these deposits in detail and identified eleven facies types at Calvert Cliffs, including storm-dominated shelf, shoreface sands, and intertidal flats. Though Kidwell (1997) described sequences within these deposits and noted abrupt shallowing of sea-level between each, she indicated that there was no evidence of subaerial exposure at the sequence boundaries. Also noted by Kidwell (1997) were several "shaved" stratigraphic sequences, specifically in the St. Marys Formation, representing the partial truncation of the transgressive systems tract and the removal of the highstand systems tract. Several major shell deposits can be recognized in these formations, which record condensed transgressive records of intertidal to subtidal environments (Kidwell, 1989).

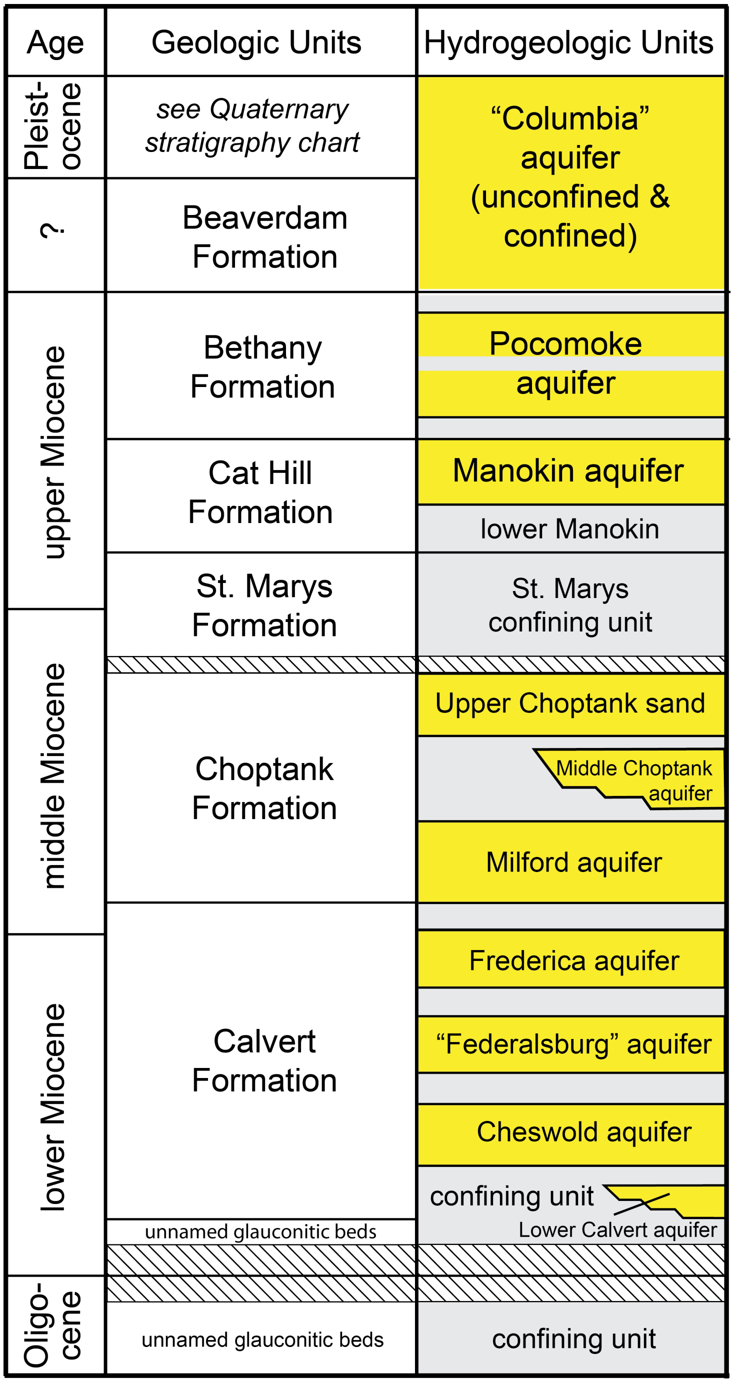

Figure 2.3: Formations and aquifers present in the subsurface of southern Delaware (McLaughlin et al., 2019 in press).

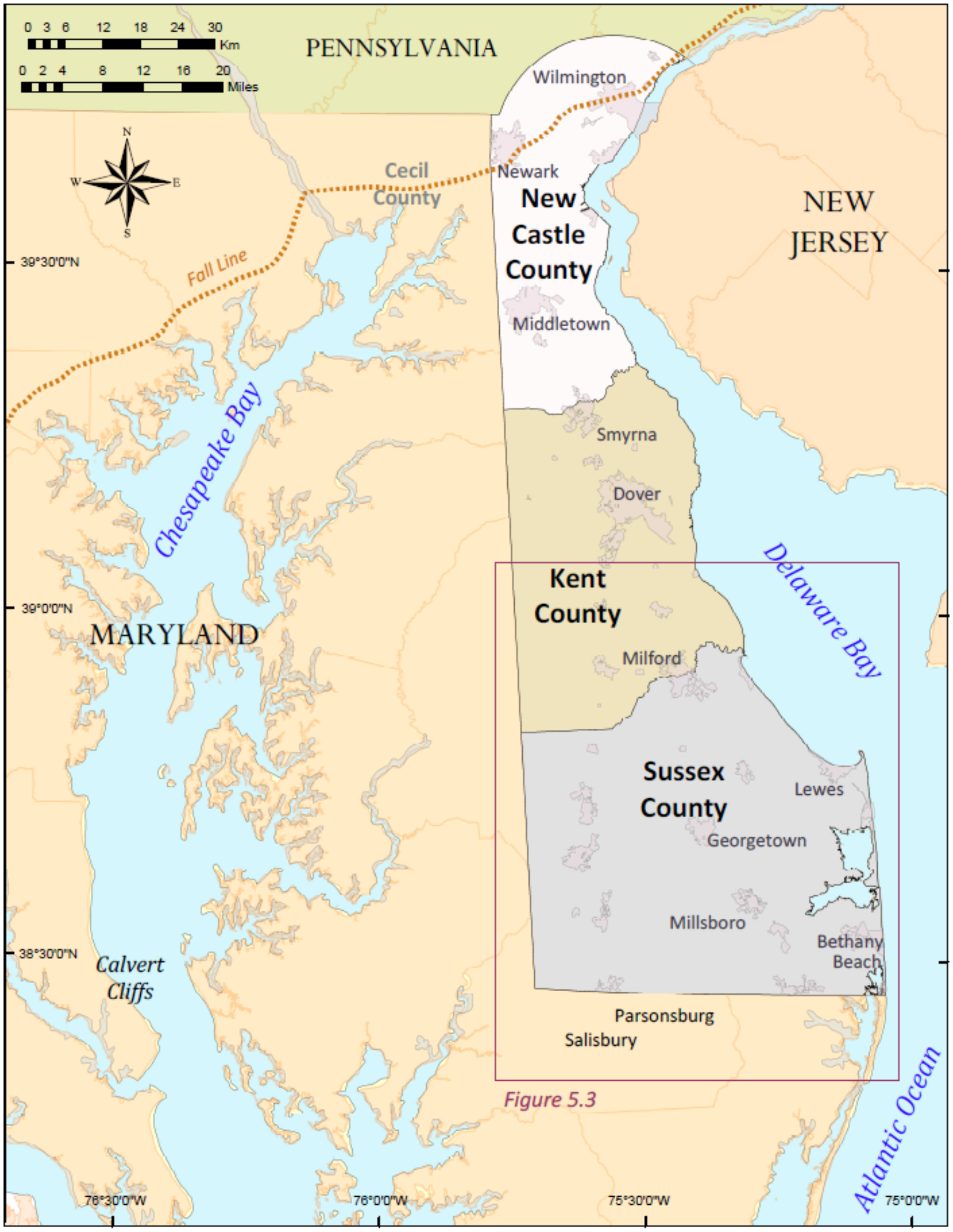

Figure 2.4: Map of Delaware and surrounding areas, discussed in this study.

2.3 Mid-Atlantic Coastal Plain Palynology

Several studies have been conducted in the Mid-Atlantic region of the United States regarding Miocene palynology. Results from these studies were useful for comparison to the results of this borehole, given the proximity. These studies have used samples from nearshore boreholes collected by the International Ocean Drilling Program (IODP), onshore boreholes, and outcrops.

In 1996, de Verteuil and Norris created a dinocyst zonation from Miocene age deposits in the Middle Atlantic Coastal Plain and offshore boreholes in the adjacent Baltimore Canyon Trough. This zonation features ten interval zones, mostly between the highest stratigraphic occurrences (HOs) of two species, and can be used for Miocene age deposits throughout the Salisbury Embayment (de Verteuil and Norris, 1996; Figure 2.5). Within these zones, several highest occurrences (HOs) and lowest occurrences (LOs) can be found, averaging two to four per zonation. In total, 32 HOs and 24 LOs occur within these zones. The study presented here also uses the de Verteuil and Norris zonations as a basis for the dinocyst data.

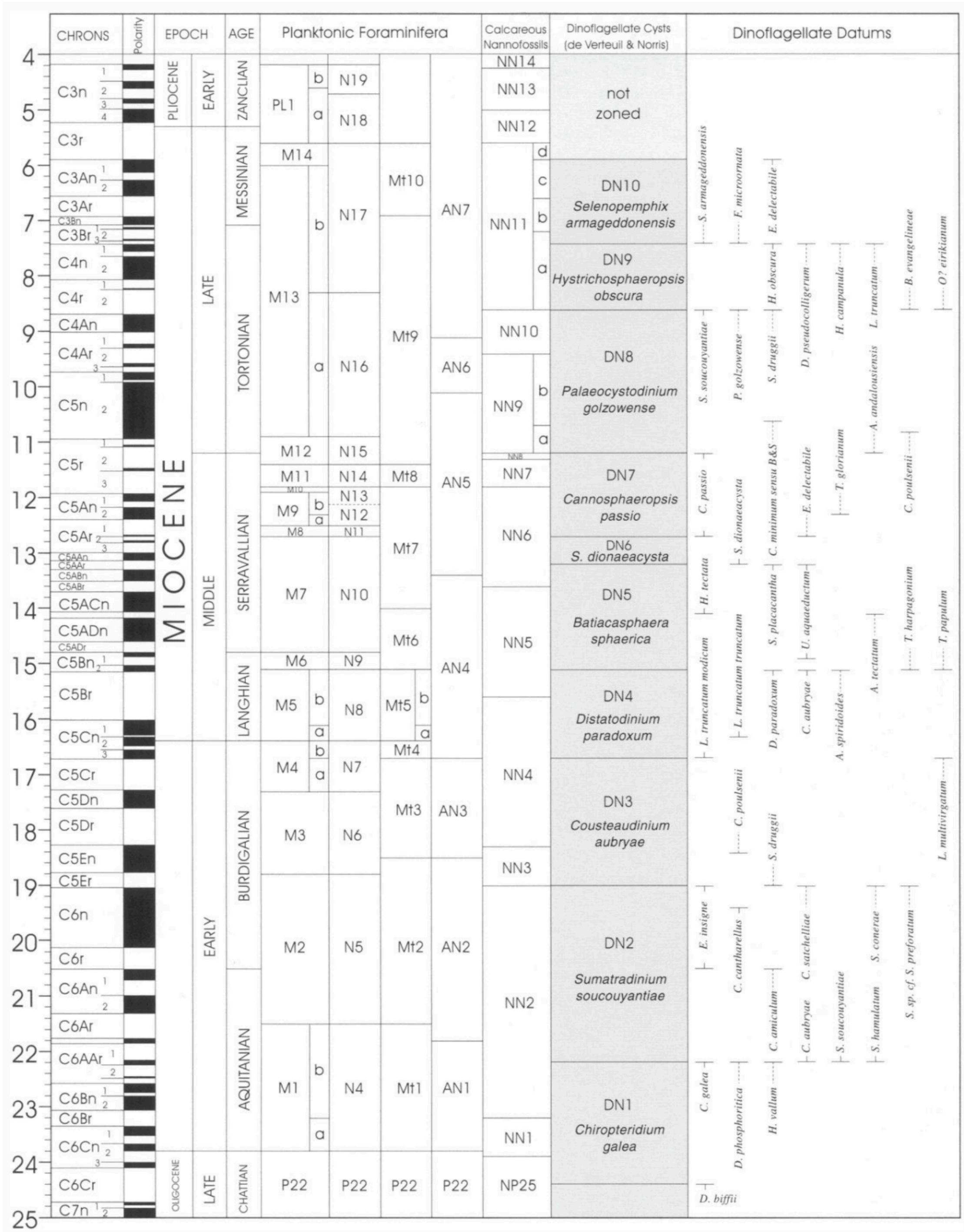

Figure 2.5: Dinoflagellate cyst zonation put forth by de Verteuil and Norris (1996). Dinoflagellate datums show the highest and lowest occurrences of certain dinoflagellate species.

In the Mid-Atlantic Coastal Plain, including Maryland, Delaware, and New Jersey, most pollen taxa that can be identified from Miocene sediments can be seen within modern vegetation assemblages. Groot (1992) summarized the palynology of the Calvert Formation described an assemblage dominated by forms common in the region today, with *Quercus*, *Pinus*, and *Carya* comprising up to 80% of the terrestrial pollen. However, several taxa seen in Miocene sediments are extinct or exotic to the region. For example, *Engelhardia* and *Sciadopitys* no longer occur in the Mid-Atlantic, but, they are present in Asia (Groot, 1992).

In a study conducted by Pazzaglia et al. (1997) in the northwestern reaches of the Coastal Plain in Cecil County, Maryland, forty-eight samples were taken from the quartz-rich, sandy gravel Bryn Mawr Formation. Assemblages, as well as the abundance of fungi, pyrite nodules within specimens, absence of marine taxa, and occurrence of gypsum, led them to consider this area a brackish estuarine environment. Further, the assemblages present were indicative of a warm-subtropical, wet climate.

Pazzaglia et al. (1997) summarized the Chesapeake Group palynoflora as part of his analysis of the Bryn Mawr Formation assemblage. That comparison indicated that Choptank Formation samples are generally characterized by high relative abundances of *Quercus*, *Pinus*, and *Carya* (Groot et al., 1990 in Pazzaglia et al., 1997). Whereas the St. Marys contains high abundances of *Quercus*, *Carya*, *Pinus*, and non-arboreal pollen, in order of descending amounts (Groot et al., 1990 in Pazzaglia et al., 1997). Overall, pollen assemblages of the mid-Atlantic Coastal Plain have changed very little since the Miocene, aside from a few now regionally exotic species. However, proportions of these taxa and specific species found in the region have varied throughout the Miocene.

McLaughlin et al. (2008) used the palynology as a proxy for identifying sequence stratigraphy by using both pollen and dinoflagellates, and by relating dinocyst occurrences to the zonation put forth by de Verteuil and Norris (1996). Like results reported in Groot (1992) and Pazzaglia et al. (1997), it was found that in the early Miocene, *Quercus* dominated, transitioning to increasing *Pinus*, then an increase in both *Quercus* and *Carya* in the late middle Miocene. Towards the end of the Miocene, *Liquidambar* and polypodiacean fern spores become common, representing a freshwater swamp-like environment (McLaughlin et al., 2008).

More recently, studies have focused on the Miocene palynology from the New Jersey shallow shelf (IODP Expedition 313). McCarthy et al. (2013) compared Miocene age sequence boundaries to the dinocyst zonations created by de Verteuil and Norris (1996). Each sequence was noted to have a distinct palynological assemblage, with varying abundances of terrestrial to marine species (T:M ratios). Generally terrestrial palynomorphs were more abundant, representing a strong terrigenous flux to the shelf, perhaps due to river input. High levels of nonsaccate pollen support the interpretation of an inner neritic environment, given that nonsaccate pollen tends to be less buoyant (McCarthy et al., 2013). From the same expedition, another study was done by Kotthoff et al. (2014) focusing on vegetation and climate variations through the Oligocene to Middle Miocene. Vegetation and climate dynamics were examined from 33 to 13 Ma using 61 samples from this drilling offshore New Jersey. Shifts in assemblages allowed correlation to several Miocene cooling events (Mi-1, Mi-1a, and Mi-1aa). The palynological assemblages lead researchers to determine that lowlands generally consisted of oak-hickory forests and highlands were dominated by conifers until the beginning of the middle Miocene. Lower Miocene palynoflora was interpreted to show an increase in conifers, with a decrease in marine taxa, representing falling sea-level. The uppermost lower Miocene was interpreted to show a decrease in mean annual temperatures (MATs), with an increase of *Carya* and Poaceae, representing increasing humidity and the presence of grasses. By the middle to uppermost middle Miocene, *Quercus*, *Carya*, and *Pinus* dominate, and the presence of Taxodiaceae, Cupressaceae, *Liquidambar*, and others indicated the growth of swamp forests and warm temperate conditions (Larson et al., 2011).

Chapter 3

METHODS

3.1 Field Methods

A series of cores were collected from an area belonging to the Abbott's Mill historic site, outside of Milford, Delaware, from June 5 to June 15, 2017 (Figure 2.3). A near-continuous wireline core of 630 feet was extracted by the Delaware Geologic Survey's (DGS) drill rig in five- to ten-foot increments. Before the drilling commenced each day, notes were made regarding the date and time, weather conditions, and people on-site. Subsequently, notes were taken of start and stop times and depths of each core as it was recovered, along with notes of any unusual operation by the drill rig. Cores were removed from the core barrel into slotted core trays and washed to remove surface mud cake. After, cores were described, noting information such as rock/sediment types, texture information including grain size, sorting, and roundness, color using the Munsell Chart, sedimentary structures, and accessory minerals and fossils. These initial observations will be confirmed or modified later in the DGS sediment laboratory. Cores were then stored in two foot PVC sections labeled with the location and depths, and placed in core boxes for transportation.

Wireline geophysical logs including gamma, resistivity, and spontaneous potential were obtained from the core once the drilling was completed. Gamma logs indicate natural radioactive levels between different types of sediments in the borehole. Muddier sediments tend to have higher gamma values that reflect the presence of trace amounts of radioactive elements such as uranium, thorium, and potassium-40. Gamma values in coarser-grained sediments are typically low. This logging tool was run inside of the drilling rods after drilling to ensure that a log was recorded in case of hole collapse after withdrawal of the rods.

The Multi-Parameter Electric-Log Tool is used to obtain electric logs in uncased boreholes and records five different resistivity logs, spontaneous potential, and natural gamma. The resistivity logs strongly reflect the fluid content of the formation, with fresh-water bearing intervals such as aquifer sands producing a high-resistivity signal in contrast with low-resistivity clay zones. The point resistance and short-normal (16 in) resistivity curves have higher vertical resolution, but also only measure resistivity at or near the wall of the borehole, so may be affected by drilling mud invasion or mud cake on the side of the hole. The long-normal (64 in) and lateral resistivity curves measure resistivity from a zone several feet around the hole, but have reduced vertical resolution. Another curve produced by this tool, spontaneous potential, is a measure of voltage differences between the tool and an electric ground, and basically traces clay versus sand content, with clay intervals usually represented by a bend of the curve to the right (higher values) and fresh-water sands by a bend in the curve to the left (lower values. This logging tool was run in the open hole after the conclusion of drilling and withdrawal of the drilling rods.

3.2 Laboratory Methods

Cores were first reanalyzed for sedimentological characteristics in the laboratory, using similar identification methods as to what were used in the field. This was completed to verify notes made in the field and to identify any details that were originally overlooked. Grain size analysis was conducted on 85 samples, taken every 8 to 10 feet, on average. This was done by first disaggregating samples and drying them.

Weights were recorded and the sample was subsequently wet sieved to separate clay and silt from the sands. When the clay and silt fraction would not wash out, a small amount of dish detergent was used to help disaggregate the finer sediments. After being dried and weighed again, samples were dry sieved to separate very fine (.067 to .125 mm), fine (.125 to .25 mm), medium (.25 to .5 mm), coarse (.5 to 1.0 mm), and very coarse (1.0 to 2.0 mm) sands, as well as granules and above (greater than 2.0 mm). The weights of each were recorded and were used to determine grain size distributions for each sample (Table A.1). These same samples were also used for lithologic analysis. One hundred grains were counted for every sample, noting composition of each grain (Table A.2). Samples consisted of varying combinations of quartz, lithic fragments, glauconite, opaque heavy minerals, carbonated fragments, feldspar, foraminifera, phosphate fragments, and organic material. Abundance curves for both grain size distributions and sample compositions were created in Strater 5.

Forty-four samples were taken approximately every ten feet for palynological analysis when the recovered core material was appropriate. These subsamples were taken from clay or silt sections; pollen grains and dinoflagellate cysts are not well represented in sands because they tend to stay in suspension longer than sand-size particles. To avoid cross-contamination from other sections of the core, subsamples were separated from the core and thoroughly cleaned of surface cake and foreign sediments.

To prepare samples for palynological analysis of pollen and spores, a standardized sample processing procedure is used to demineralize the samples and remove extraneous organic matter. Batches of up to 16 samples can be processed simultaneously at the Delaware Geologic Survey's palynology lab. Samples were dried, weighed, and spiked using a known quantity of polystyrene microspheres in solution.

The solution was composed of 10.0 g of Dextran powder (to keep microspheres in suspension), 0.2 ml of Triton X (to reduce foaming) and 2.73 ml of concentrated microspheres in suspension, added to 100 ml of distilled water. Given this, approximately 10,000,000 microspheres should have been present in the solution. The solution was enough to make 100 samples, with a calculated average of 93,900 microspheres/ml. This microsphere spike allows for the notation of palynomorph concentrations in each sample per gram of sediment when grains are counted. The formula for calculating the pollen concentration per gram can be found in Figure 3.1.

$$C_t = \frac{\left(\frac{Tc}{Lc}\right) \times M_s}{Wt_s}$$

Where:

Ct = the pollen concentration

$\frac{Tc}{Lc}$ = the ratio of pollen counts to microsphere counts in each slide

Ms = the number of microsphere grains added to the full sample

Wt_s = the weight of the sample in grams.

Figure 3.1: Formula to calculate the pollen concentration per gram.

Mineral material was first removed from the sample. Carbonates are removed by using 37% hydrochloric acid (HCl). Some of the sand is removed by washing and retaining the finer than sand fraction until clean sand could be discarded. The retained fines were then treated with 48% hydrofluoric acid (HF) and then 20% HCl. Remaining sample residues were then split in half so pollen and dinoflagellate slides could be created.

The pollen sample split was treated with 35% nitric acid (HNO_3) for oxidation. A treatment of 5% ammonium hydroxide (NH_4OH) for several minutes removed humic acid. To make the grains stand out, samples were subjected to acetolysis using acetic and sulfuric acids ($C_2H_4O_2$ and H_2SO_4, respectively). Lastly, samples were floated using zinc chloride (ZnCl). This allowed pollen grains to separate from the residual mineral matter in the solution. Pipettes were used to collect the remaining organic material at the top of each sample. Each residue of organic material collected was stained with safranin and double-mounted onto a microscope slide using polyvinyl alcohol medium (PVA) and sealed with a UV-reactive epoxy.

The dinoflagellate sample splits were washed through a 25-micron sieve to remove clay particles and finer organic material. No additional treatments were necessary, although more washing could have been possible if clay particles inhibited dinoflagellate identification. The samples were stained with safranin and double-mounted on slides in a similar fashion to pollen grains.

Roughly 100 to 300 pollen grains were identified and counted in each sample depending on the evaluation of taxa diversity and available grains for reasonable quantitative analysis. Samples with relatively few pollen and spore grains resulted in smaller counts, where in some slides, nearly every grain had to be counted to reach 100 identifiable taxa. Samples with fewer than 100 identifiable grains were omitted from the study. Two Delaware Geological Survey photographic pollen databases were consulted to help pollen and spore identification, the Quaternary Pollen Catalogue Database and the DGS Extant Palynomorph Database were consulted during identification. Pollen were identified at the genus level or in some cases at the family level. Counting allowed for the determination of relative abundances of each taxa within each sample.

Dinoflagellates were identified and counted using information from several research papers (de Verteuil and Norris, 1996; Munsterman and Brinkhuis, 2004; Dybkjær and Piasecki, 2010; Louwye and de Schepper, 2010). Slides were scanned completely, and dinoflagellate species occurrences were marked with either X (present) or P (possible) for each sample.

In all, data from 36 pollen/spore samples and 42 dinoflagellate samples were used for analysis in this study. Data were recorded in a Microsoft Excel spreadsheet, where the data could be easily manipulated and exported to other programs. Palynomorph diagrams, depicted as abundance bar graphs, were created using the software program C2. Pollen zonations were created in the software program PAST. Zonations were determined by a multivariate cluster analysis method, using the Bray-Curtis Similarity Index and Paired Grouping (UPGMA) algorithm.

Chapter 4

RESULTS

4.1 Lithology

The borehole at Abbott's Mill (Me22-25) produced a nearly continuous sediment record down to 630 ft, collected in 5 and 10 foot intervals. These cores were recovered and described in the field in June 2017, and later reexamined in the laboratory between January and March 2018. Descriptions of the lithology were noted and photos were taken at the drilling site. Eighty-five samples were taken systematically from the cores, typically in 5 ft to 10 ft increments where sediments were available. The lithology categories used in this study follow the Wentworth Scale and include the following: clay and silt (sometimes combined as mud, which is used for this study), very fine sand, fine sand, medium sand, coarse sand, and granules and coarser (Wentworth, 1922). Compositional makeup of each sample was also determined using the following categories: quartz, lithic fragments, opaque heavy minerals, mica, carbonate material, feldspar, foraminifera, organic debris, glauconite, and phosphate. Given the predominance of quartz sands with interbeds of silts and clays, along with common carbonate material and foraminifera-rich sections, sedimentary facies at Abbott's Mill are interpreted as a shallow-marine, wave dominated siliciclastic environment. The results of the sediment grain and compositional analyses, along with the gamma log, can be found on Figure 4.1. Raw grain size data and compositional make-up of each sample can be seen in Appendix Tables A.1 and A.2, respectively.

4.1.1 Calvert Formation

In this borehole, the Calvert Formation encompasses over half of the section, from 630 ft up to approximately 272 ft. The formation is characterized by several coarsening-upward sections, with silty clays transitioning to silty sands. Seemingly abrupt changes in lithologies may be linked to sequence boundaries, which will be discussed further on. Interbedded silt and clay layers, along with bioturbated sections, are common. Fractions of whole shells and shell fragments are seen throughout, as well as a few gravelly sand layers. In this study, the Calvert Formation is described in informal subunits; a lower, a middle, and an upper section.

4.1.1.1 Lower Calvert Formation

Lower Calvert Formation sediments occur from 630 ft to 465.95 ft. The first unit in this section is characterized by a distinct upward coarsening trend from an approximately 60-ft thick zone of silt and clay to silty sands and ultimately clean sands at the top. The lowest sample was taken at 629.9 ft. It is composed of silty, medium grain, quartz sands, with few (1% each) opaque heavy minerals, feldspar, and mica grains, with 1% shell fragments (Figure 4.1). The first package, which generally coarsens upwards, is found from 629 ft up to 496.7 ft. A layer of very dark to dark grayish brown, slightly sandy silt occurs from 629 ft to 603.2, with few thin (less than one inch) bioturbated sections. Foraminifera and mica grains constitute less than 1% of samples in this section. Carbonate shell material increases from 2% up to 13% at 618 ft, then it decreases down to 2% at 604 ft. This section is capped by a dark brown to black silty sand glauconite-rich lamination at 602.45 ft, which contains upwards of 20% glauconite grains (Figure 4.1).

Above the contact at 602.45 ft, a gradual coarsening upward package occurs to 530 ft. Dark olive gray clay with interbeds of very dark gray silty sand persists up to 550 ft. At this point, the lithology consists largely of very dark gray silty sands with interbeds of dark olive gray clay, similar to what is found from 602.45 ft to 530 ft. Localized laminations of shell hash were found at 538.1 ft, 537.7 ft, 537.45 ft, and 531.4 ft. Sparse bioturbation was noted, mostly subvertical burrows less than 1 cm in diameter. A few woody black clasts up to 3 cm long were also present. Shell fragments varied from <1% to 3% in this section, with 1% to 3% mica and opaque heavy minerals (Figure 4.1). From 530 ft to 496.7 ft, the lithology is silty sands with lithified sand (sandstone) sections. Sandstone sections, which occurred at 515.4 ft and 510 ft, ranged from .25 ft to 2.35 ft respectively. These sections were dark olive gray to grayish brown and contained up to 3% glauconite and up to 30% densely packed broken and complete bivalve shells. Unconsolidated sands contained up to 7% shell fragments, with 1% or less of phosphate, opaque heavy minerals, mica, and organic debris present throughout (Figure 4.1). Sands were fine- to medium grained, with a high mud fraction, coarsening up to coarse sands. Frequent burrowing is noted towards the bottom of the section.

The package from 496.7 ft to 465.95 ft was comprised of interbedded sandy silts and silty sands, with one 1.4 ft sandstone section at 481.9 ft. Sediment color transitions from olive gray silts with very fine interlaminated sands to gray, medium- to coarse-grained sands and sandstone. From 497.6 ft to 482.8 ft, the lithology is silt, with increasing sand fractions, from 10% to 30%. Very few (<1%) shell fragments are observed (Figure 4.1). Fine-grained sand laminations increase in size up to .5 inches. Sandy lithologies become dominant from 482.8 ft to 465.95 ft, with a section of partially cemented, shelly sandstone from 481.9 ft to 483.2 ft. The sandstone section correlates to a sharp increase in the resistivity values. In samples collected, shell fragments constitute up to 34 percent of the total composition. Cross-laminations are seen at 467.1 ft. This section contained areas of horizontally deposited, large bivalves, decreasing upwards, where shells became fragmented. One to 2% glauconite was found throughout, which was sometimes found to coat shell material. Opaque heavy minerals and phosphate comprised 1% to 2% of the section as well (Figure 4.1). The sandy sections that occur from 530 ft to 465.95 ft are considered to be part of the Lower Calvert Aquifer complex.

4.1.1.2 Middle Calvert Formation

The middle Calvert Formation sediments occur from 465.95 ft to 371.3 ft. The lowest package of the middle Calvert consists of a massive-bedded clay layer with thin, 0.3 inches or smaller, sandy laminations, transitioning to muddy sands and very fine grained quartz sandstone. Up to 447.1 ft, the lithology was a very heavily bioturbated dark gray clay layer, with burrows being infilled by very dark gray medium sands. Burrows range from 0.05 to 0.15 ft in thickness. The clays contained less than 1% opaque heavy minerals, with typically 1% or less of organic debris. Dark gray to gray sands occur from 447.1 ft to 445.6 ft, with 1% or less glauconite, opaque heavy minerals, and phosphate throughout (Figure 4.1). From 445.6 ft to 420 ft, several small (0.2 to 0.9 ft) sections of sandstone were recovered. This section may not all be sandstone, however, as drilling processes may have removed any unconsolidated sediments, leaving behind only the cemented grains. Peaks in the resistivity logs from 445.6 ft to 430 ft, and approximately 425 ft to 420 ft suggest these are the depths where the sandstone was recovered from, meaning the cores in these areas may not be accurate to the lithologies at that depth. A trough in the resistivity log between 430 ft and 425 ft suggests a silty lithology, which could have been blown away by drilling operations. The sandstones recovered were grayish brown transitioning down to olive brown and then gray. Shell fragments decreased up section, from 7% to 3%, consisting of bivalve pieces and gastropods. Rounded, less than 4 mm, phosphate pieces contributed 1% to total grain composition throughout (Figure 4.1). This section is capped by similar sands to the top of the section, from 420 ft to 415.65 ft. The sandy sections from 447.1 ft to 415.65 is considered to be the Federalsburg Aquifer.

The second package of the middle Calvert Formation consists of a coarsening upwards package from 415.65 ft to 371.3, transitioning from very dark gray silts with frequent very fine grained sand laminations 1 to 2 mm in thickness, to muddy, matrix supported sandstone and slightly muddy sands. Samples taken at 410 ft, 400 ft, and 390 ft show 1% organic matter consistently, with variations in opaque heavy minerals from 1% to 2%, and mica from 1% to 3%. Cores from 390 ft to 415 ft all recovered less than 0.6 ft of material in each, however based on the acquired core and the well logs, it is likely that the entire section was silts with interlaminations of very fine quartz sands. From 386 ft to 387.1 ft, a section of gray sandstone was recovered. Frequent burrowing was noted, with 1% opaque heavy minerals present (Figure 4.1). The sandstone is marked by a decrease in the gamma and a sharp increase in the short resistivity. Very dark grayish brown silty sands capped the section, with samples at 383 ft, 377 ft, and 371 ft consisting of 2% to 4% opaque heavy minerals and 3% to 5% carbonate shell material (Figure 4.1). The section was also sparsely bioturbated throughout. The sands of from 415.65 ft to 447.1 ft are interpreted to be part of the Federalsburg Aquifer. The sandstone and sandy sections from 386 ft to 371.3 ft are considered to be the Lower Frederica Aquifer. Recovery was low for the cores in this section, ranging from .1 ft to .85 ft for the four cores recovered between 390 ft and 415 ft. Based on the moderate values on both the gamma and resistivity logs, it can be determined that the lithology remains relatively consistent through this section.

4.1.1.3 Upper Calvert Formation

Between 371.3 ft to 272.0 ft, the sediments of the upper part of the Calvert Formation show an alternation between thick (25 to 50 ft-thick) sand and muddy intervals. The first package of this section occurs from 371.3 ft to 303.1 ft, consisting of a coarsening upwards trend from dark brown, slightly sandy clay to dark gray, slightly gravelly, poorly sorted sands. Samples taken from the clay at 365 ft, 359 ft, 354 ft, 350 ft, 343 ft, and 338 ft show a very gradual decrease in mud-sized fractions, from 99% to 71.5% upward. The clay contains 1% to 2% opaque heavy minerals, and 2% to 3% lithic fragments and mica. Within the sediments there are high percentages of organic material and low (8% in the sample at 354 ft) to no shell material present in samples taken from 359 ft, 338 ft, and 336 ft. However, at 353 ft, there is one very fine sandy lamination (less than 5 mm) with approximately 30% shell hash, which is represented by a spike on the resistivity logs (Figure 4.1). Other thin laminations (3 mm or less) occur throughout, though these are mainly interlaminated very fine grain sands. There is a relatively abrupt transition at 337.1 ft. Sands are medium to fine, but quickly coarsen upwards to 335 ft where sands become less muddy with medium to very coarse grains. Sparse quartz granules are also present. Sands begin to become gravelly at 330 ft continuing up to the top of the section. Samples at 323 ft and 310 ft showed granule abundances at 18% and 37.6% respectively (Figure 4.1). In all of the samples in this interval, larger sand grain sizes dominated. In the sample at 310 ft, the majority of the larger grain size fractions were carbonate shell material, which made up 30% of the sample. This coarsening upward can be seen by a quick decrease in the gamma and an increase across the resistivity logs starting at approximately 334 ft. Phosphate and opaque heavy minerals made up 1% to 3% of contents throughout the section (Figure 4.1). Bioturbation is also present throughout this section; however, it is poorly preserved. Based on the wetness and larger grain sizes of the sands, and the interpretation of the geophysical logs, the sand layer from 337.1 ft to 303.1 ft is considered to be the Frederica Aquifer.

The top of the Calvert Formation from 303.1 ft to 272 ft is a fine-grained section of very dark grayish brown. From 303.6 ft to 300 ft, several shell beds are noted, consisting of small shell fragments. Upwards, burrowing becomes common, with burrows having a diameter up to .2 ft, infilled by very dark gray silts. Starting at 285.2 ft, silt fractions become dominant and shell fragments are not observed, and lenticular cross-lamination is common. One spiral burrow (Gyrolithes) was observed at 282.2 ft. Samples at 297 ft, 290 ft, 284 ft, 280 ft, and 275 ft contain from 57% to 99% mud fractions, containing up to 3% carbonate material and 1% to 5% mica (Figure 4.1). Sediments were not recovered between 275 ft and 271.1 ft, but based on the geophysical logs, there is an abrupt change in lithology from clays and silts to sands, where the contact between the Calvert and Choptank Formations.

4.1.2 Choptank Formation

The Choptank Formation is comprised of sediments from 272.0 ft to 138.0 ft, with sediments consisting of overall shelly sand with breaks of muddier, finer-grained sand sections. Three coarsening upwards packages are noted within this formation. The lowest package, from 272 ft to 225.7, is a coarser section which overlies the fine material at the top of the Calvert Formation. This section is also described as the Milford Aquifer. The lithology is found to be muddy, generally fine- to medium-grained sands, gradually transitioning to more gravelly sands starting at 250.5 ft. Shell fragments increase up section from less than 1% to 12% in the sample taken from the top of the Unit at 240 ft (Figure 4.1). Organic rich laminations are frequent up to 235.8 ft, but are not noted above this point. Gravel begins to become present above 235.8 ft, culminating to 8.59% of the sediment fraction in the sample at 240 ft. The granule fraction is composed of rounded grains of phosphate, glauconite, and milky quartz, indicating a shallow, high-energy environment. The gamma and resistivity logs follow expected patterns, and the gamma begins to increase at the top of the unit, where phosphate and glauconite are present. Throughout the sands are very dark to dark gray, and samples were noted to have low (1% to 3%) compositions of phosphate granules and opaque heavy minerals (Figure 4.1). The samples at 240 ft, 235 ft, and 230 ft were found to have relatively high carbonate material increasing upwards, from 12% at 240 ft to 40% at 230 ft. Granules of rounded phosphate, glauconite, and quartz are present, and shell material constitutes roughly 60% of the composition in the sample at 235 ft (Figure 4.1). The top of this package exhibits a .5-inch oxidized, orange-brown, silty sand layer with less than 5% carbonate material, which has been interpreted as an exposure surface.

The second coarsening-upward package, from 225.7 ft to 185 ft, consists mainly of dark gray, muddy laminated sands to greenish gray coarse shelly sands. The base of the section contained 55% carbonate shell pieces, some glauconized, with minor foraminifera (2%) and phosphate (3%) components in the sample at 224 ft. The sample at 205 ft shows upwards of 8% glauconite, which is the highest found in any sample taken from this borehole, and also occurs in the sample at 192 ft (Figure 4.1). Shell material decreases in the middle of the section to around 9% average, and increases at the top to 32%, seen in the sample at 192 ft (Figure 4.1). These sands are interpreted as the Middle Choptank Aquifer.

The highest coarsening-upward package is dark greenish gray clayey silts transitioning to shelly, dark gray medium sands, from 185 ft to 138.0 ft. Throughout the section, opaque heavy minerals constitute 1% to 2% of the composition, while in samples at and above 168 ft, phosphate constitutes 1% to 5%. From the base of the unit up to 167.2 ft, the lithology is composed of silts with a high percentage of clay content and slight sand fractions of very fine-grained quartz (Figure 4.1). The dark greenish gray section has lenticular cross-lamination preserved throughout, representative of a low energy environment. At 168.2 ft, a large clam shell was cut through, which was deposited whole and horizontally. A sample taken at 168 ft showed upwards of 5% phosphate composition, which is the highest abundance in any sample taken from the borehole.

From 167.2 ft to 138 ft, sandy lithologies dominate, with few millimeter scale cross-laminations of clay decreasing in abundance towards the top of the section. The color transitions from very dark gray to light gray, and then back to greenish gray and greenish black towards the top of the section. Carbonate shell fragments begin to increase around 155 ft, as seen in the increase from 6% to 32%, in samples at 162 ft and 138 ft, respectively (Figure 4.1). Horizontal deposition of shells was noted at the top of the section. Increasing resistivity and decreasing gamma levels corroborate with the coarsening of grain sizes. The sandy section from approximately 169 ft to 138 ft is considered to be the Upper Choptank aquifer, based on lithologies and the geophysical logs.

4.1.3 St. Marys Formation

The Saint Marys Formation occurs from 138 ft to 70 ft, and is characterized by interbedded silty sands and clays. The sandy units in this section may act as unnamed confined aquifer units. The silty sand section from 138 ft to 125.45 ft consists of heavily bioturbated, very dark greenish gray, very fine sands. The sample at 132 ft showed 3% carbonate shell material, 2% opaque heavy minerals, and 1% feldspar grains (Figure 4.1). The sand transitioned to gray, shelly sands from 125.45 ft to 113.75 ft, with low (0% to 3%) concentrations of phosphate, opaque heavy minerals, and organic material in samples from this interval. Carbonate material decreased upward, comprising 23% in the sample at 125 ft, down to 10% at 114 ft. It was noted that glauconite made up 5% of the sediments towards the top of the section (Figure 4.1).

A section of muddy to slightly gravelly sands occurs from 113.75 ft to 105.65 ft. the bottom of this section was composed of gray sands with glauconite filled burrows with low (1%) compositions of phosphate and plant fragments. Grain sizes coarsen upwards with 2 to 5 mm granules of quartz, chert, and bone phosphate found at 105.65 ft, representing less than 5% of the abundance for each. The sample at 106 ft confirms these notes, with 3% lithic fragments and 2% phosphate present (Figure 4.1). At this point, the color also transitions to very dark gray to the top of the section.

From 105.65 ft to 70.0 ft, dark gray, silty sands, with interlaminated few cm or less, sandy clays dominate. Samples taken from this section were all poorly sorted. Of the samples taken at 100 ft, 92 ft, 85 ft, and 77 ft, quartz made up 93% or greater of the composition. Feldspar abundance fell from 3% at 100 ft to 0% at 77 ft. Organic matter varied from 0% to 2%, and opaque heavy minerals comprised 1% of the make-up in each sample (Figure 4.1). The entire section was heavily bioturbated, with larger, light gray, sand-infilled burrows present at the top of the section where the formation contact is found.

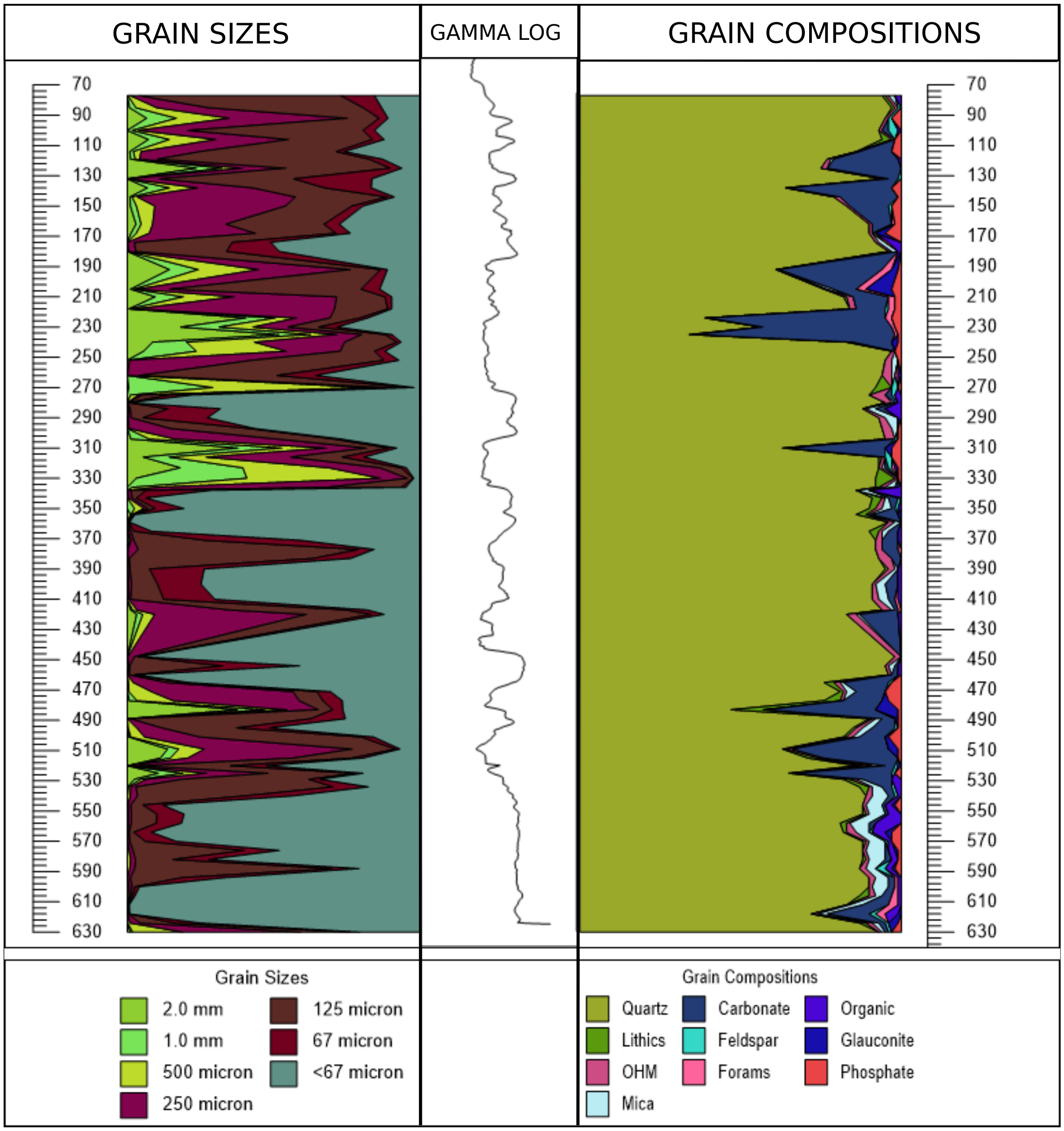

Figure 4.1: Grain size and composition data for the samples recovered from Me22-25.

4.2 Palynology

Forty-three samples were recovered from the borehole at the Abbott's Mill site (Me22-25) for use in pollen analysis. Of the 43 recovered samples taken from the borehole, 37 samples were usable in pollen and spore analysis. The six unusable samples contained pollen, however the total abundance of grains for each were less than 100, so the samples were omitted from the study. Raw pollen data can be seen in Table A.3, and the pollen diagram is shown in Figure 4.2. Photos of 13 representative pollen taxa can be seen in Plate 1 in Figure A.1.

4.2.1 Calvert Formation

Twenty-five samples were taken from the Calvert Formation, which occurs from the bottom of the borehole at 630 ft to 272 ft. Arboreal pollen dominates every sample, with *Quercus*, *Carya*, and *Pinus* being the three most abundant taxa in every sample. Nine samples were taken from the lower part of the Calvert Formation, from 630 ft to 548 ft. Through this section, arboreal pollen shows a general slight decrease when compared to non-arboreal pollen, from 90% down to 85% (Figure 4.2). However, *Quercus*, *Pinus*, and *Carya* abundances stay relatively the same. Exotic species constitute 11% to 17% of the total pollen sum in each sample, with *Engelhardia*, *Pterocarya*, Taxodiaceae-Cupressaceae-Taxaceae (TCT), *Symplocos*, and *Podocarpus* all present. *Engelhardia*, *Pterocarya*, and *Symplocos* constitute less than 1% to 4% of the total pollen sum in each sample, though *Pterocarya* and *Symplocos* both decrease up section. TCT is the most abundant exotic taxon, with abundances ranging from 4% to 8% consistently throughout the section. *Acer*, *Alnus*, *Cornus*, *Ilex*, *Tsuga*, and *Ulmus* are all lesser constituents, and each constitute less than 5% of the total abundance per sample. *Fraxinus* and *Liquidambar* each make up 1% or less of the pollen sum in these samples (Figure 4.2). Sediments from 548 ft to 520 ft produced no useable palynomorphs due to sandier lithologies (Figure 4.1).

Eleven samples were selected from the middle Calvert Formation, from 520 ft to 354 ft. This section shows two distinct pollen assemblage trends, so the middle Calvert can be subdivided further into lower middle and upper middle parts separated by a section of non-fossiliferous sediments from 450 ft to 417 ft. The six samples in the lower middle Calvert section, from 520 ft to 450 ft., show a steady decrease in arboreal pollen from 92.5% to 84%. Exotic taxa within this section make up 12% to 26% of the total pollen sum. *Engelhardia* has its highest abundance in the borehole in the sample from 485 ft, reaching 11.6%. *Pterocarya* and *Symplocos* make up to 5% of the total pollen sum in each sample, while *Podocarpus* abundance stays under 1%. TCT abundance stays between 7.5% and 11.3% of the total. *Acer*, *Alnus*, *Cornus*, *Ilex*, *Tsuga*, and *Ulmus* constitute no more than 3% to 4% of the total pollen sum of each sample. Poeaceae grass pollen shows an increased abundance from the lower Calvert, with abundances as high as 2.3% of the total pollen sum (Figure 4.2).

The upper middle Calvert section, from 417 ft to 302 ft, shows a general increase in arboreal pollen, as well as a sharp decrease in deciduous taxa, from 79.2% to 51%. Coniferous taxa increase with this trend, as *Pinus* sums total between 10% and 20% in this section, except for the sample at 417 ft. *Picea* also reach up to 5.8% of the total pollen sum. Exotics also show an increase, from 11.9% to 26% at the top of the middle Calvert section. *Engelhardia* constitutes between 1.3% and 10.9% of the total pollen sum for each sample, while *Pterocarya*, *Podocarpus*, and *Symplocos* contribute less than 5% for each taxon. TCT remain consistent with the lower part of the section constituting up to 11% of the total pollen sum in some samples. Carya represents approximately 7% to 11% of each sample, and Quercus remains the most dominant taxa, contributing 23% to 53.5% of the total pollen sum for each sample.

Acer, *Ilex*, and *Tsuga* are the only other significant deciduous taxa present, but these taxa are never over 5% of the total pollen sum (Figure 4.2). Poeaceae levels remain similar to the lower part of the middle Calvert Formation, however the highest abundance (4.8%) within the borehole is found in the sample at 365 ft (Figure 4.2). No samples were recovered between 354 ft to 302 ft due to little recovery and sandy sediment types.

The upper Calvert Formation produced four samples from 302 ft to 272 ft. Arboreal pollen remains dominant, constituting 83% to 90% of the total pollen sum in every sample. Of the arboreal pollen in these samples, 70% to 77% of the abundances were deciduous taxa. *Carya* reaches its highest abundance in the borehole in the samples at 287 ft and 280 ft, reaching 18% of the total pollen sum. *Quercus* is noted to decrease through the section, from 45.1% to 25.1% of the total (Figure 4.2). Conifers begin to increase at the top of the section, up to 25% of the total arboreal pollen abundance in each sample. *Pinus* and *Picea* levels increase as well, averaging around 10% and 2.5% respectively, similar to what is seen in the upper section of the middle Calvert. Exotic taxa make up between 16.7% to 18.2% of each sample in this interval, with TCT taxa relatively high (up to 11.3%), and *Engelhardia* and *Pterocarya* constituting up to 6% of the sum. *Podocarpus* and *Symplocos* contribute 2% or less each of the total pollen sum. *Symplocos* is no longer noted above 287 ft. *Acer*, *Alnus*, Poaceae grass, polypod fern spores, and *Ilex* contribute less than 3% of the total sum in each sample. *Liquidambar* abundances are the highest for the borehole in this interval, the highest being 5.5% at 275 ft (Figure 4.2).

4.2.2 Choptank Formation

Seven pollen-rich samples were recovered from the Choptank Formation, which occurs from 272 ft to 138 ft. No fossiliferous samples were produced from 275 ft to 222 ft. Arboreal pollen dominates in all samples, constituting 88% to 97% of the pollen in samples (Figure 4.2). Non-arboreal pollen shows a general decrease compared to the Calvert Formation. Like the upper Calvert Formation, *Carya* abundance is increased compared to the lower and middle Calvert, making up 11 to 15% of each sample. *Quercus* was slightly more abundant in the Choptank compared to the upper Calvert, averaging around 37% within these samples. *Pinus* pollen also is increased from below, with abundances generally increasing from 12% to almost 16% (Figure 4.2).

Exotics in these samples constitute 3% to 13% of the total assemblages, which is an overall decrease from the Calvert Formation below. *Pterocarya* has its highest abundances within the borehole in the sample at 190 ft (8.8% of the total pollen). TCT abundance drops from 8% at the lowest sample at 222 ft to 2% at the highest sample at 146 ft. Few *Engelhardia* grains were identified, only occurring in the samples in the upper part of the formation, with abundances never reaching over 1%. *Podocarpus* and *Symplocos* were not noted in these samples (Figure 4.2).

Acer, *Alnus*, *Ilex*, *Picea*, and *Ulmus* each contribute less than 4% of the total pollen sum. *Liquidambar* follows this same pattern except in the sample at 160 ft, where it constitutes 9% of the total pollen. Cyperaceae shows a decrease in abundance throughout the Choptank, which carries though into the St. Marys Formation, from 7.8% to 2% in the highest sample of the borehole (Figure 4.2).

4.2.3 St. Marys Formation

Five samples were recovered and analyzed from the St. Marys Formation, which occurs from 138 ft to 70 ft. No samples were fossiliferous from 112 ft to 82 ft. The useable samples are dominated by arboreal pollen, with high abundances of *Carya*, *Quercus*, and *Pinus*. Exotic species have low abundances in this interval, making up 4% to 9% of the pollen assemblage (Figure 4.2).

Like the Choptank Formation samples, *Carya* has relatively high abundances compared to the Calvert Formation, making up 13% to 17.5% of the total species make-up. *Quercus* is the most dominant taxa in the St. Marys samples, with abundances ranging from 34% to 54% throughout. *Pinus* shows a general increase up section from 13.5% to 26.5% in the highest borehole sample. *Picea* remains fairly constant throughout, ranging from 0% to 2% (Figure 4.2).

Engelhardia, *Pterocarya*, and TCT are the only exotic species found in the samples from the St. Marys Formation. Neither *Symplocos* nor *Podocarpus* are present. *Engelhardia* make up less than 1% of each sample, while *Pterocarya* constitutes 2% to 3% in every sample. TCT is the most abundant exotic pollen constituting 2% to 7% of the total abundance, increasing up section (Figure 4.2).

Cyperaceae pollen shows a slight decrease up section, from 4.5% to 2%. *Acer* shows the opposite pattern, generally increasing from 1.3% to 4%. *Alnus*, *Liquidambar*, *Ulmus*, and polypod ferns are also present in these sample; however, their abundance in each sample never exceeded 5% (Figure 4.2).

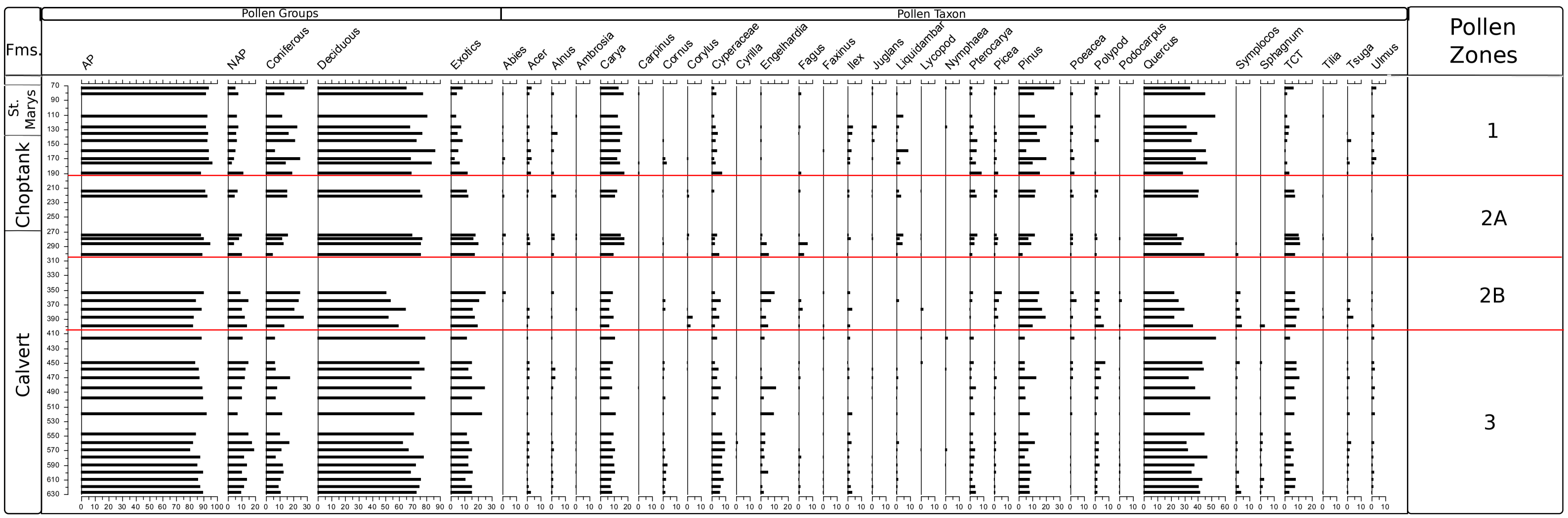

Figure 4.2: Pollen diagram for borehole Me22-25. Identified pollen zones can be found on the right. Solid red lines divide the zones. AP represents arboreal pollen, while NAP represents non-arboreal pollen.

4.2.4 Pollen Zonation

Multivariate cluster analysis was used to determine pollen zonations for the pollen and spore samples at Abbott's Mill. Results from the analysis determined three distinct zones (labelled 1, 2, and 3), with Zone 2 being divided into subzones 2A and 2B (Figure 4.3). These zonations are linked to the pollen diagram (Figure 4), which shows how the relative pollen and spore taxa abundances characterize each zone.

Zone 3 includes 16 samples across the lower and middle Calvert Formation, from 628.0 ft to 417.0 ft. This Zone had the highest abundances of Cyperaceae and *Engelhardia* compared to the others. *Abies*, *Picea*, and *Tilia* all had the lowest to no representation throughout Zone 3, compared to the other Zones. Polypod fern spores show a steady increase up through the Zone, as does Poeaceae and TCT, though the increase in TCT is more sporadic.

Zone 2 is divided into two subzones, 2A and 2B. Zone 2B includes 5 samples from the upper Calvert Formation, from 400.0 ft to 354.0 ft. Compared to Zone 3, Zone 2B has significantly higher abundances of *Pinus*, *Tsuga*, and *Picea*. *Symplocos* abundance increases and *Pterocarya* decreases. The Zone also shows a decrease in *Quercus* and *Carya*. Zone 2A incorporates 6 samples from 302.0 ft to 215.0 ft, spanning the uppermost Calvert to middle Choptank Formations. Similar to Zone 2B, Zone 2A has comparable abundances of total exotic taxa, though *Engelhardia* abundances decrease to zero percent at the top of the Zone, and *Pterocarya* shows increases throughout the Zone. TCT and Cyperaceae stay relatively the same, as do abundances of *Pinus*, *Picea*, *Quercus*, and *Carya*.

Zone 1 incorporates 10 samples from the middle Choptank Formation to the top of the St. Marys Formation, from 190.0 ft to 74.0 ft. Exotic taxa decline in this

Zone, which can be seen in the decrease in *Pterocarya*, the lower abundances in *Engelhardia* and TCT, and the absence of *Symplocos* compared to the other Zones. *Pterocarya* is the only exotic taxa with similar abundances to Zone 2. *Cyperaceae*, *Quercus*, *Ilex*, and *Ulmus* increase compared to Zone 2, similar in abundances to Zone 3. *Alnus*, *Juglans*, *Liquidambar*, and *Pinus* all have their highest abundances in this Zone.

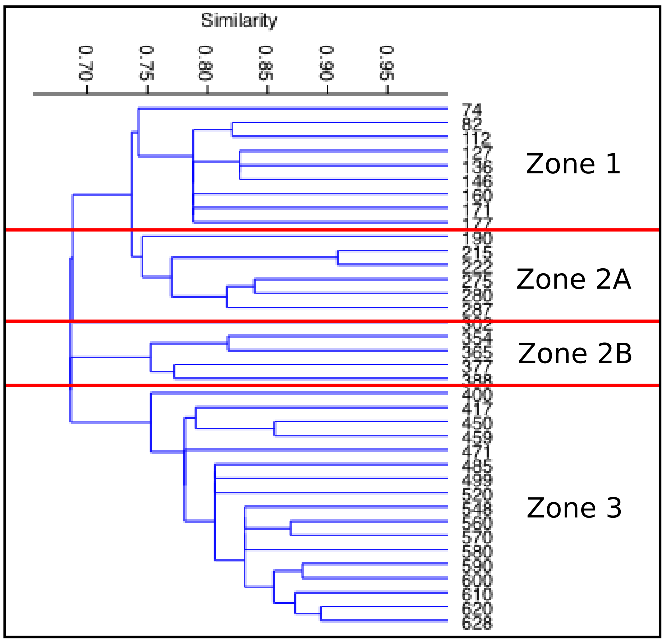

Figure 4.3: Similarity of pollen samples determined by multivariate cluster analysis in borehole Me22-25.

4.3 Dinoflagellate Cyst Zonation

Of the 43 samples taken for dinoflagellate identification in Borehole Me22-25, 42 contained identifiable dinoflagellate cysts. Several studies were referenced in order to identify dinoflagellates (de Verteuil and Norris, 1996; Munsterman and Brinkhuis, 2004; Dybkjær and Piasecki, 2010; Louwye and de Schepper, 2010). Species were identified as either present or absent in the samples, and as such, only one sample was found to be barren of any dinoflagellates. The species identified were used to determine zonations throughout the borehole using the dinocyst zonations created for Calvert Cliffs by De Verteuil and Norris (1996) (Figure 2.4). Zones DN 2 to DN 9 were found to occur in this section (Figure 4.4). Occurrence data can be found in Table A.4. Figure A.2 shows ten representative specimens from throughout the borehole. Most samples contained taxa that narrowed the identification of dinocyst zonations.

Six samples from 628 ft to 580 ft were found to occur in the *Sumatradinium soucouyantiae* Zone, or DN 2. Zone DN 2 occurs within the lower Miocene (de Verteuil and Norris, 1996). Samples at 628 ft and 620 ft contained *Cordosphaeridium cantharellus*, which has its highest occurrence within DN 2. Samples at 610 ft, 590 ft, and 580 ft all contained *Dinopterygium cladoides*, which has also its highest occurrence in DN 2 (De Verteuil and Norris, 1996). Because of this occurrence in the sample at 580 ft, all samples including and below had to have occurred in no higher than DN 2. The identification of *S. soucouyantiae* in the sample at 628 ft show that all of the samples from 628 ft to 580 ft also could be no lower than DN 2.

Nine samples from 570 ft to 459 ft were found to occur in the *S. soucouyantiae* Zone (DN 2) to no higher than the *Cousteaudinium aubryae* Zone, or DN 3. Positive identification of the taxon *Sumatradinium hamulatum* in samples at 570 ft, 560 ft, 548 ft, and 534 ft represents a highest occurrence at the top of DN 3 and a lowest occurrence at the base of DN 2. *Cousteaudinium aubryae* was identified in samples at 520 ft and 499 ft. *Operculodinium longispinigerum* was identified in samples at 499 ft, 471 ft, and 459 ft. Both of these taxa have their highest occurrences at the top of DN 4 and lowest occurrences in DN 2 (De Verteuil and Norris, 1996). However, the occurrence of *Sumatradinium druggi* in samples below, whose lowest occurrence is in DN 3, constrains the samples to no younger than DN 3. Given this, these samples are dated to the lower Miocene (de Verteuil and Norris, 1996). The sample at 485 ft contained no stratigraphically informative taxa.

Six samples from 449.7 ft to 377 ft were constrained to the *Cousteaudinium aubryae* Zone (DN 3). Samples at 449.7 ft and 417 ft contained *S. druggi*, which has its lowest occurrence at the base of DN 3. Samples at 410 ft, 400 ft, 388 ft, and 377 ft contained *Lingulodinium multivirgatum*. This taxa has its highest occurrence at the top of DN 3 (De Verteuil and Norris, 1996). These two taxa constrain these samples to zone DN 3, which is dated to the middle Miocene (de Verteuil and Norris, 1996).

The sample at 365 ft occurs no lower than the *C. aubryae* Zone (DN 3) and no higher than the *Distatodinium paradoxum* Zone, or DN 4. This is because of the identification of *S. druggi*, with a lowest occurrence at the base of DN 3, and *O. longispinigerum,* with a highest occurrence within DN 4. The sample at 356 ft ranges in age from the uppermost lower Miocene to the lowermost middle Miocene (de Verteuil and Norris, 1996). Samples at 354 ft, 342 ft, and 315 ft did not contain stratigraphically significant dinoflagellate cysts. However, the occurrence of *S. druggi* in samples below, as well as *O. longispinigerum* and *C. aubryae* in samples above, these samples are also constrained to now lower than DN 3 and no higher than DN 4.

Four samples from 302 ft to 275.1 ft occur within the *Distatodinium paradoxum* Zone (DN4). Zone DN4 has been dated from the very end of the lower Miocene to the lowermost middle Miocene (de Verteuil and Norris, 1996). Positive identification of *Labyrinthodinium t. modicum* in samples at 302 ft and 287 ft, along with a possible identification at 280 ft, constrain this section to no lower than DN4, due to this species having its lowest occurrence at the base of DN 4 (De Verteuil and Norris, 1996). Positive identification of two taxa, *O. longispinigerum* and *C. aubryae*, in the sample at 275.1 constrain this section to no higher than DN 4, because both of these taxa have their highest occurrences in DN 4.

The samples at 263.2 ft and 253.8 are within the *Batiacasphaera sphaerica* Zone, or DN 5. The positive identification of *Habibacysta tectata*, with a highest occurrence and lowest occurrence both in DN 5, constrain the sample at 263.2 ft to DN 5. Zone DN 5 has been dated to the middle Miocene (de Verteuil and Norris, 1996). The positive identification of *Apteodinium tectatum* (highest occurrence at the base of DN5), *Unipontidinium aquaeductum* (highest and lowest occurrences in DN 5), and the possible identification of *H. tectata* constrain the sample at 253.8 to DN 5 also (De Verteuil and Norris, 1996).

The five samples from 222 ft to 160 ft contained few dinoflagellate cysts. However, identification of a few taxa in these samples constrain this section to no lower than the *Batiacasphaera sphaerica* Zone (DN 5) and no higher than the top of the *Cannosphaeropsis passio* Zone, or DN 7. The presence of *Trinovantedinium harpagonium*, which has a lowest occurrence at the base of DN 5 (De Verteuil and Norris, 1996), in the sample at 222 ft constrain it to no lower than DN 5. Due to the occurrence of *H. tectata* in samples below, further evidence is offered that the section can be no older than the base of DN 5. No stratigraphically significant taxa were identified in the sample at 215.4 ft. Samples at 190 ft and 177 ft both contained *Trinovantedinium papulum*, which has a lowest occurrence at the base of DN 5 (De

Verteuil and Norris, 1996). There were also no stratigraphically significant taxa found in the sample at 160 ft. The occurrence of *Cannosphaeropsis passio*, with a highest and lowest occurrence in DN 7, in the next highest sample at 146 ft indicates that these samples can be no younger than the top of DN 7. Given this range, these samples were deposited between the middle Miocene (de Verteuil and Norris, 1996).

Five samples from 146 ft to 112 ft occur within the *Cannosphaeropsis passio* Zone (DN 7). The possible identification of *C. passio* at 146 ft, and the positive identifications at 146 ft, 136 ft, 127 ft, and 112 ft, place all of these samples within DN 7, due to the taxa having a highest occurrence and lowest occurrence in DN 7. Zone DN 7 has been dated to the uppermost middle Miocene (de Verteuil and Norris, 1996).

One sample at 96 ft was identified as occurring within the *Cannosphaeropsis passio* Zone (DN 7) or the *Palaeocystodinium golzowense* Zone, or DN 8 (De Verteuil and Norris, 1996). The sample contained *Cerebrocysta poulsenii*, which has a highest occurrence at the lower part of DN 8. These samples are found to be above occurrences of *C. passio*, therefore they can be no older than DN 7. Given these zones, the samples were deposited between the uppermost middle to lowermost late Miocene (de Verteuil and Norris, 1996).

The final sample at 74 ft can be placed between the base of the *Cannosphaeropsis passio* Zone (DN 7) to within the *Hystrichosphaeropsis obscura* Zone, or DN 9. The sample contained *Hystrichosphaeropsis obscura*, which has a highest occurrence at the top of DN 9 (De Verteuil and Norris, 1996). This constrains the upper limit of the sample to DN 9, while the lower limit can only be constrained to DN 7 because of the identification of *C. passio* in the samples below. The final sample is indicative of an age ranging from the uppermost middle Miocene to possibly as high as the upper Miocene (de Verteuil and Norris, 1996).

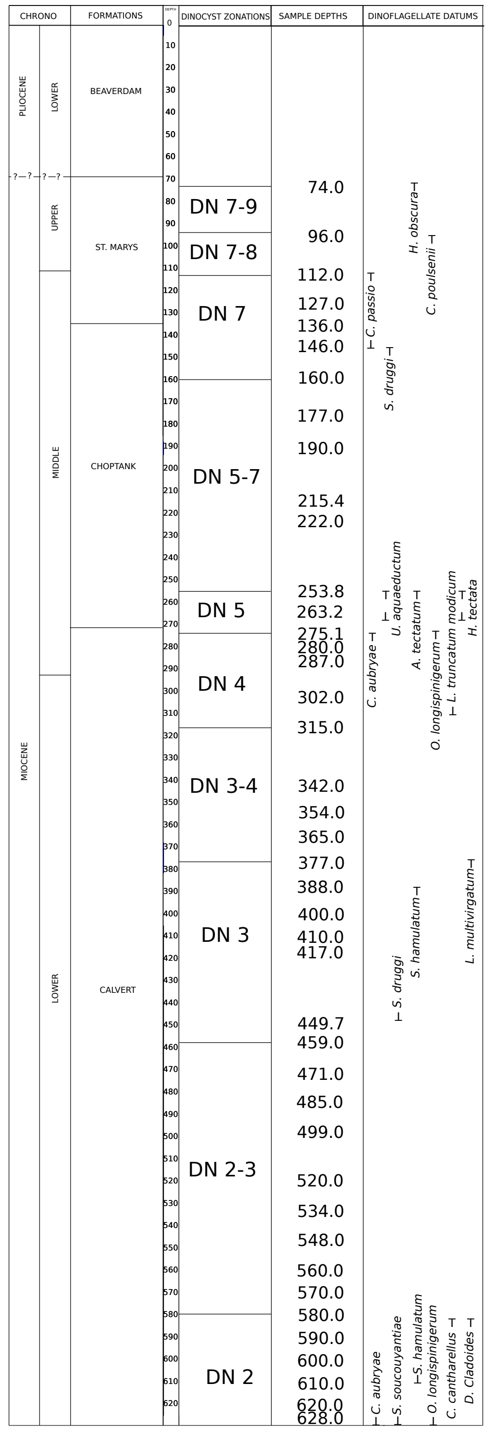

Figure 4.4: Dinoflagellate cyst zonation determined at Me22-25. Highest and lowest occurrences of zone specific taxa are found on the right.

Chapter 5

DISCUSSION AND INTERPRETATION

5.1 Depositional Environments

At Abbott's Mill, the sediments of borehole Me22-25 are interpreted to be a wave-dominated, sandy, shallow-marine shoreline environment. Sediments in the borehole are predominately quartz sands and silts with interbedded clays, commonly observed with carbonate shell material in some capacity. Depositional environments in this study follow the facies model put in place for the region by studies from McLaughlin et al. (2008) and Miller et al. (2003) (Figure 5.1), which are based on interpretations of lithofacies and geophysical logs. Figure 5.2 depicts the interpretations of depositional environments throughout the borehole. Throughout the Miocene section represented in this borehole, nine units have been identified, spanning the Calvert, Choptank, and Saint Marys Formations. These depositional units also represent stratigraphic sequences, in which environments shift within them.

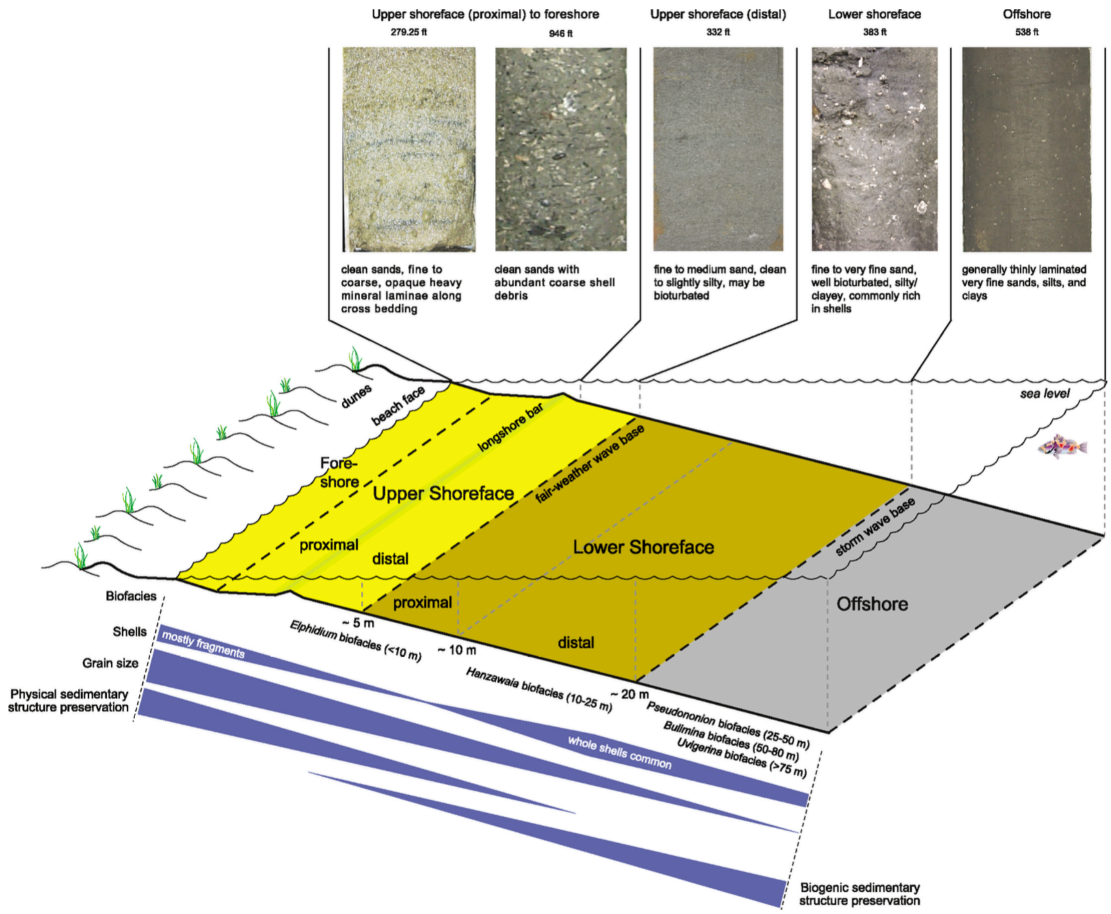

Figure 5.1: Generalized wave-dominated facies model, determined by Miller et al., 2003 and Browning et al., 2006 (McLaughlin et al., 2008).

Unit 1 encompasses sediments from the bottom of the borehole, at 630 ft, to 501.7 ft. It is noted to be the largest of the units found in the borehole and incorporates sediments from only the Calvert Formation. The package generally coarsens upwards, with slightly sandy silts, transitioning to sandy clay and finally muddy sands. Three distinct environmental sections are seen in this unit. The first section incorporates samples from 630 ft to 602.45 ft, and is comprised of silty sands with up to 20% shell fragments and whole shells. Carbonate material abundance varies throughout the section, down to 5% or less in some sections. Several burrows are preserved, including a spiral variety found at 604.1 ft. Silty sands may indicate churning of bioturbated sections. The top of this section is capped by a glauconite surface, where the composition reaches up to 20% of the lithology. Gamma values also peak at this depth. Given these notes, this unit represents a mainly shoaling upwards sequence, with minor oscillations in water depth. The upper part of the section is interpreted as a lower shoreface environment; however, the lower part of the sections represents minor shifts from more offshore to closer to foreshore environments.

From 602.45 ft up to approximately 540 ft, the lithology consists of clays interbedded with very fine grained sands. These sandy laminations become more prominent higher in the section. The clays are heavily bioturbated with some large burrows infilled by very fine grained sands. Small complete bivalve shells are present throughout, with generally up to 5% shell fragments present in the sediments. Gamma values stay relatively moderate, with a trend to slightly lower values, and resistivity values follow a reciprocal pattern, slightly increasing. The section is interpreted as an offshore environment with slight shoaling.

The upper section of unit 1, from 540 ft up to 501.7 ft, is interpreted to reflect shoaling associated with an advancing shoreline, from offshore to upper shoreface environments. The section is overall sandier than the middle part of Unit 1, coarsening upward from fine- to medium-grained muddy sands to cleaner medium- to coarse-grained sand.: Shells are conspicuous and become increasingly fragmented and less common, decreasing from approximately 30%, down to 5% at the top of the section. Gamma values show a sharp decrease, while resistivity values quickly increase, with two large peaks between. These peaks correlate to carbonate-cemented coarser sandy sections. This section is suggestive of a shoaling upwards trend in Unit 1 from offshore environments to upper shoreface environments.

Unit 2 begins at 501.7 ft up to 465.95 ft, and consists of a generally coarsening upwards package. Sediments consist of olive gray silts, transitioning upwards to gray medium to coarse grained sands. Gamma values and resistivity values remain relatively moderate throughout, so this section is interpreted as being a shoaling upwards from lower shoreface up to a distal upper shoreface environment, also given the lack of shell material (Miller et al., 2003). The top of this section is capped by a heavily bioturbated surface, with burrows being infilled by the overlying lithology. Sandy lithologies dominate from 482.8 ft to 465.95ft. The continuing increase in sand fractions, along with the increase in shelly material from the below section, provides evidence of a transition from upper shoreface to nearing foreshore environments.

Unit 3 is an overall coarsening-upward section, from 465.95 ft to 415.65 ft. Up to 447.1 ft, the lithology consists of heavily bioturbated clays. Gamma values are relatively high and resistivity logs are low, which further confirm the environment to be offshore.

The upper part of Unit 3, from 447 ft to 415. 65 ft consists of mainly muddy sands and sandstones. Much of this section must be interpreted from the geophysical logs, as through the depths between 420.65 and 445 ft, only small sections were recovered in each of the cores. It is presumed that sandstone blocked the rest of the core from being recovered. Sands and sandstones are muddy with 5% or less shell fragments. Burrows are found throughout. Phosphate pellets are also present in the sandstones. Overall for this section, the environment is indicative of a shoaling upwards sequence from lower shoreface up to foreshore. The muddy sands in the lower part of this unit are suggestive of lower shoreface environments of deposition; the bits of cemented sandstone with quartz pebbles and granules, as well as the peaks in the resistivity logs, support a foreshore interpretation at the top of the Unit.

Unit 4 encompasses sediments from 415.65 ft up to 371.3 ft. The contact with underlying Unit 3 is marked by dark silts over coarser sands represents an abrupt flooding event. Sediments from 415.65 ft to 387.1 ft consisted of mainly silts, generally very dark gray with high abundances of very fine grained sand fractions. Dark sandy silts in the lower part of this unit (415.65 ft to 387.1 ft) with a low percentage of shell material (less than 3%) and the frequent burrowing present are indicative of a distal upper shoreface environment.

The presence of cleaner and lithified sands from 387.1 ft to 371.3 with an increase in shell fragments may show a transition from the distal upper shoreface to the beginnings of a proximal upper shoreface environment.

Unit 5 is another coarsening upwards package from 371.3 ft up to 310.0 ft, consisting of dark grayish brown clays transitioning up to dark gray silty sands. The lower section of the unit, from 371.3 ft to 337.1 ft, is a sandy clay, with high percentages of organic material and shell material within the samples. Thin, interlaminated very fine sand, laminations occur throughout. The high abundance of organic material, along with the preserved laminations are common in low energy environments, and as such, this section is interpreted as an offshore environment.

There is a sharp transition to sand, interlaminated with sandy silt, at 337.1 ft, followed by an overall upward increase in grain size and abundance of thick sand fragments. Bioturbation is poorly preserved when present, indicating a high-energy environment. With this, a shoaling upwards sequence is seen from a nearly unrecognizable lower shoreface environment to a proximal upper shoreface or even foreshore environment.

Unit 6 occurs from 310.0 ft to 225.7 ft. This unit incorporates sediments from the top of the Calvert Formation into the Choptank Formation. The lower part of the unit, from 310.0 ft to 272.0 ft, consists of clay and silt transitioning to a higher silt constituent with increasing fine sand fractions up section. The increasing proportion of sand, decreasing abundance of shell fragments, as well as the transition from burrowing to cross-laminations, represents a transition from offshore to a distal upper shoreface environment.

The base of the Choptank Formation represents a distinct change from the lithologies directly below 272.0 ft. Sediments from this point up to 235.8 ft are slightly muddy fine sands coarsening to slightly gravelly sands starting at 250.5 ft. Shell fragments increase upward to 240 ft. Organic rich laminations are frequent up to 235.8 ft, but are not noted above this point. Gravel begins to become present above 235.8 ft, increasing upwards to 240 ft. The granule fraction indicates a shallow, high-energy environment. The very bottom of the unit contains similar compositional constituents compared to the top of Unit 6. Granules of rounded phosphate, glauconite, and quartz are present, and shell material constitutes over half of the composition in the sample at 235 ft. These factors determined that the environment was most likely upper shoreface to foreshore. Directly above, from 227.3 to 227.82, there is a sandstone surface, which may indicate the formation of a marine hardground. Above, sands become interlaminated with clays. Shell constituents drop in this section, indicating a possible deepening to a distal upper shoreface above a possible flooding surface at 225.7 ft. The upper part of Unit 6 represents a continuing shoaling upwards trend from distal upper shoreface to possibly foreshore environments, represented by the change from muddy fine sands to slightly gravelly sands with abundant shell fragments.

Sediments from 225.7 ft to 185.0 ft comprise Unit 7, which transition from clayey sand to silty, shelly sands. Sands with interlaminated clays continue to persist, however they become less frequent up towards the top of the unit. Sand grain sizes also increase from fine to a poorly sorted mix of fine to medium-coarse grains. Glauconite becomes present in samples at 205 ft and 192 ft, which is corroborated by a sharp peak in the gamma curve. The overall sandy nature of Unit 7, general increase in grain size and abundance of shell fragments, and the change from some interlaminated clays in the lower part to fewer in the upper part, represents a transition from the distal upper shoreface from below to a proximal upper shoreface.

Unit 8 occurs from 185.0 ft to 138 ft. The sediments in this unit consist of a coarsening upwards package from clayey, very slightly sandy silts to very fine-grained, silty sands. These sediments occur from the middle to the top of the Choptank Formation. Up to 167.2 ft, clay content is high and sands are found to be very fine grained. Lenticular cross-lamination is present. Horizontally deposited clams above 168.2 ft and larger sand sizes and abundances represent increasing energy. The environment for this section is interpreted as offshore to distal upper shoreface.

From 167.2 ft to 138 ft, the lithology becomes sandier, with cross-laminations of clay becoming less common towards the top of the unit. Shell fragments are noted to increase up section. The color transitions upwards, from very dark gray to light gray, and then back to greenish gray and greenish black at the top. Glauconite is present at the top of the Unit, indicating an erosional surface. Sands become cross-laminated at 157.75 ft, indicating wave interaction with the sediment surface. Sand grain sizes also increase from below to medium-grained quartz. Decreasing gamma levels and increasing resistivity corroborate with the coarsening trend of grain sizes, and with the above evidence, a shoaling upwards sequence is interpreted, from a proximal upper shoreface to a foreshore environment.

Unit 9 starts at the Choptank and Saint Marys Formation boundary at 138 ft, and continues the entirety of the Saint Marys Formation in this borehole to 70 ft. Peaks in the geophysical logs show several abrupt fine clay and silt sections throughout the unit, which is also seen in the lithology. The lower part of the unit begins as a very dark greenish gray silty sand up to 125.45 ft. This transitions into a clayey to silty, dark gray sand with decreasing shell fragments made up of thick bivalves. Towards 105.65 ft, colors alternate from dark greenish gray to gray, as sand grain size increases to more coarse fractions. Gravel begins to appear above 113 ft, consisting of quartz and glauconite granules, and rounded phosphate pebbles. The data for this lower section suggest an upper shoreface to estuarine environment.

The upper part of the section, from 125.45 ft to 70 ft, starts with an abrupt transition to interlaminated, dark gray clays and sands. This continues up to 93.5 ft, where above, the clay becomes sandier with gravel decreasing upwards until 91 ft, where gravel is no longer present. This may represent a flooding event where larger particles were transported away from the inland. Interlaminated sands and clays, which are heavily bioturbated, continue up through the rest of the unit, indicative of a low-energy estuarine environment.

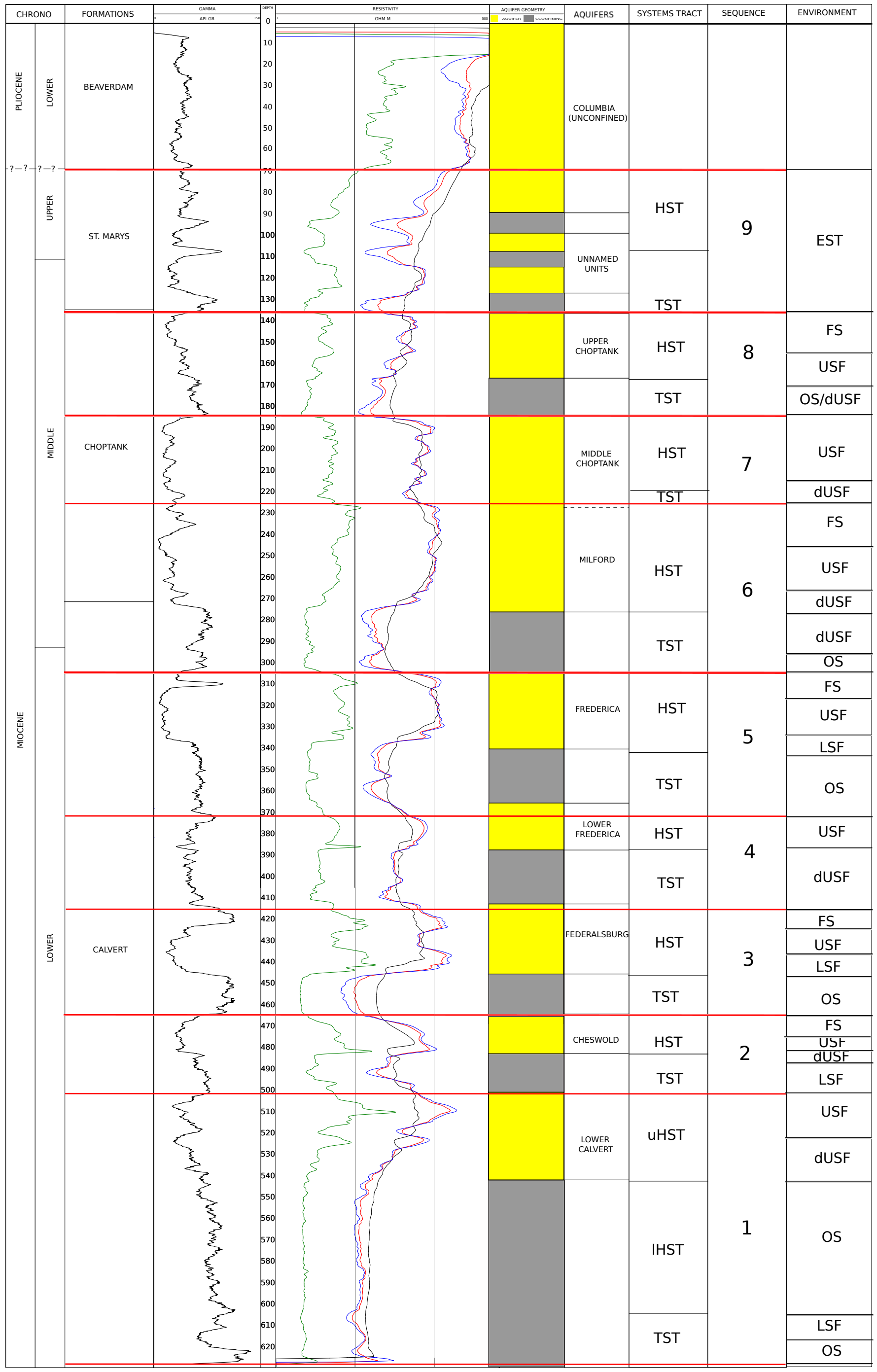

Figure 5.2: Depositional Environments and sequences identified at borehole Me22-25. Environments include: OS- offshore, LSF- lower shoreface, USF-upper shoreface, FS- foreshore, and EST- estuarine.

5.2 Palynological Environment and Climate Interpretation

Paleoenvironmental climate and environmental interpretations can be determined for the borehole at Abbott's Mill using the data from the pollen analysis. Vegetation migration and abundance can be heavily influenced by changes in the global and regional climate; however, responses to warming or cooling can be delayed for a period of time (Traverse, 2008). Other factors, including mountain-building events and natural catastrophes, can also affect plant taxa distribution and shifts in flora compositions (Davis, 1983). To determine a taxon's appropriate environmental preferences and distribution, modern taxa are used for comparison. This method takes the most morphologically similar modern species in order to draw conclusions about the fossil pollen identified in the borehole (Graham, 1999).

In the Abbott's Mill borehole, the palynology shows a warming trend though the early and into the middle Miocene. A shift to cooler climates is then noted, which corresponds to events after the Middle Miocene Thermal Optimum (Larsson et al., 2011). This cooling period, noted by Graham (1999) was the result of the growth of ice sheets in Antarctica. The cooling is followed by another warming trend, though regional temperatures most likely didn't reach that of the initial warming phase. These trends are noted to be similar to the global climate transition of the Miocene epoch, defined by Davis (1983).

5.2.1 Calvert Formation

Twenty-four samples were recovered across the entirety of the Calvert Formation in this borehole, forming a fairly complete representation of pollen assemblages at this location. The Calvert Formation was deposited during lower

Miocene, up into the early middle Miocene. Assemblage data of the Calvert Formation show a general climate regime of a warm-temperate to subtropical environment. In the upper part of the Calvert, there appears to be a shift towards a drier, cooler-temperate climate. The warm period coincides with the Miocene thermal optimum, where from around 21 Ma to 15 Ma, temperatures reached the highest levels compared the Middle Miocene and later (Graham, 1999).

The lower Miocene section, represented by the first nine samples taken from 630 ft to 548 ft, contains high abundances of *Quercus*, *Carya*, and *Pinus*. These taxa are representative of a temperate to subtropical environment (Groot, 1991). *Quercus* is commonly found in the region today, and is dominant across the eastern half of North America, in a wide range of environments (Sibley, 2009). *Carya* is found presently in several different environments from southern Canada to Florida along the eastern seaboard of North America (Sibley, 2009). *Pinus* is generally thought as a cooler-climate taxon; however, some species are localized to the southern half of the United States. These species are typically found in swampy lowlands or areas of moist soil (Sibley, 2009). Several exotic species that are now rare or non-existent in Delaware were also present in the lower Calvert section. *Engelhardia*, *Pterocarya*, and *Symplocos* each contributed up to 4% of the pollen sum in the samples. *Symplocos* and *Engelhardia* are found in areas of warm-temperate to tropical climates (Xie et al., 2010), while *Pterocarya* occurs in temperate to subtropical environments (Groot, 1991). *Symplocos* is found in the United States from the southern Delmarva Peninsula to central Florida, while *Engelhardia* and *Pterocarya* are extinct in this country. *Engelhardia* occurs in central America, while *Pterocarya* can be found in southeast Asia (Groot, 1991). Taxodiaceae-Cupressaceae-Taxaceae (TCT) also has relatively high abundances in this section, from 4 to 8 percent. TCT, particularly Cupressaceae, is prevalent in poorly drained, swampy and wet environments (Larsson et al., 2011) and has a modern range of no higher in latitude than the southern Delaware cypress swamps down towards the Gulf Coast (Sibley, 2009). The abundance of Cyperaceae is relatively high in all of the samples in this section compared to the rest of the borehole, as well. These non-arboreal, sedge plants grow in wet environments as well, indicative of higher precipitation levels (Graham, 1999). In general, this lower Calvert section is interpreted as a wet, subtropical to warm-temperate climate.

Through the middle Calvert section, from 520 ft to 354 ft, *Quercus* and *Carya* abundances stay generally the same compared to the lower Calvert. *Pinus*, however, shows a general increase, compared to the lower Calvert, towards the top of the middle Calvert section, which may indicate climatic cooling (Groot, 1991). This is corroborated by the appearance of *Abies* and the increase in *Tsuga* towards the top as well, which are both cold to cool climate taxa. Few species of *Abies* are found throughout central to eastern Canada, in moist coniferous forests, and *Tsuga* can be found in the Northeast and New England regions of the United States in moist lowlands (Sibley, 2009). *Engelhardia* abundances remain high, with the highest abundance of the borehole at 485 ft, along with up to 5% abundances of *Pterocarya* and *Symplocos*. TCT taxa abundances also remain relatively high. Mesophytic understory plants like Poeaceae, *Lycopodium*, and *Sphagnum* begin to increase in abundance in this section, which may indicate slightly drier conditions (Larsson et al., 2011). Climate at the beginning of the middle Calvert section is similar to that of the lower Calvert section, where there is evidence for a wet, subtropical to warm-temperate climate; however, a shift to a slightly more moderate-temperate climate with slightly drier conditions is noted at the top of the section.

The four samples that represent the upper Calvert section, from 354 ft to 272 ft, show an increase in *Carya* in the samples taken from 287 ft, 280 ft, and 275 ft, relative to the samples below. *Pinus* in these samples also increases, while *Quercus* decreases, compared to below. Cool-temperate to warm-temperate taxa begin to become more abundant, including *Alnus* and *Fagus* (Groot, 1991). *Liquidambar* becomes abundant, representing up to 5.5% of the samples. This taxon is mesothermic, preferring warm-temperate to subtropical conditions (Larsson et al., 2011, Groot, 1991). TCT pollen reaches its highest abundances in the upper Calvert section, up to 11.3%, and Poaceae continues to be present, indicating the prevalence of grasslands. The increased abundance of *Pinus* and *Picea* may show evidence of a continued cool period, compared to the lower Calvert section. Abundances of *Engelhardia* and *Symplocos* drop, with *Symplocos* not being present above 287 ft. This decline may represent the transition to an uninhabitable climate for these taxa (Groot 1991; McLaughlin 2008). The climate is interpreted to be a continuing cooling trend, albeit minor and slow to develop, with warm temperate to moderate temperate conditions. Precipitation is still variable, with plants from both wet and dry environments present in the assemblage.

5.2.2 Choptank Formation

The Choptank Formation is represented by seven samples recovered from between 272 ft and 138 ft. *Carya*, *Quercus*, and *Pinus* remain the most abundant constituents in samples, though similar to the upper Calvert section, *Carya* shows increased abundance. *Pinus* shows a general increase through the section. There is also a lower abundance, only up to 3%, of *Picea*, along with minor increases in *Abies* and *Tsuga* abundances. *Abies* and *Picea* are both representative of high-altitude forests or higher latitude, cool climates (Larsson et al., 2011), while all four of these taxa are found to grow in cool to cold climates (Groot, 1991). TCT pollen shows a consistent decline, from 8% at 222 ft to 2% at 146 ft. This, coupled with a decrease in Cyperaceae pollen, suggest a period of drying. *Pterocarya* abundances at 190 ft are the highest of the borehole at 8.8%; however other subtropical exotic taxa are either not present (*Symplocos*) or make up less than 1% of the abundance (*Engelhardia*). The samples show a slight decline in temperature and moisture, which corroborate with a known decline in global temperature during the middle Miocene around 15 Ma (Graham, 1999).

5.2.3 St. Marys Formation

Paleoenvironmental interpretation for the St. Marys Formation is based on five samples collected from 138 ft to 70 ft. *Carya*, *Quercus*, and *Pinus* remain the dominant taxa, representative of a warm temperate environment. *Picea* abundances drop compared to the Choptank Formation, and *Tsuga* is not present in either sample, which may be indicative of a slightly warmer climate trend. TCT, *Pterocarya* and *Engelhardia* are the only present exotic taxa; however, *Pterocarya* and *Engelhardia* abundances never reach over 3.2% and 1%, respectively. TCT abundances fall between 2 and 7 percent, which is consistent with abundances in the top of the Choptank Formation. Cyperaceae shows a very slight increase in abundance. *Nymphaea*, which is a freshwater taxon, is only identified in the St. Marys samples, at 127 ft and 74 ft (Larsson, 2011). Warm-temperate taxa, including *Ilex*, *Liquidambar*, *Quercus*, *Carya*, and *Ulmus*, are present in at least 4 of the 5 samples. The climate is interpreted to be generally warm-temperate and moderately moist, warmer than the Choptank Formation assemblage and slightly cooler than the Calvert Formation assemblages.

The transition from a warm-temperate, moist climate in the Calvert Formation, transitioning to a cooler, drier climate in Choptank Formation, and then to a warm-temperate, slightly moist climate in the St. Marys Formation is generally consistent with findings in previous studies by McLaughlin et al. (2008) and Fisher (2016). The relatively abrupt shift from tropical temperatures to cooler climates between the Calvert and Choptank seen in this sample is relatable to the Middle Miocene Climatic Optimum (Larsson et al., 2011), while the decline that was noted through the middle to upper Middle Miocene has also been noted previously (Graham, 1999).

5.3 Sequence Stratigraphy Interpretations

Sequence stratigraphic interpretations were determined based on lithologic changes, geophysical logs (gamma and resistivity), grain size trends, grain composition trends, and depositional environment interpretations. As noted previously, depositional environments in this study follow the wave-dominated shoreline facies model put in place for the region by studies from McLaughlin et al. (2008) and Miller et al. (2003), which was adapted from Bernard et al. (1962). Sequence stratigraphic interpretations from the Bethany Beach core (McLaughlin et al., 2008; Miller et al., 2003) provide a framework for interpretations made in this study at Abbott's Mill. Sequences identified can be found on Figure 2.3 under the column titled Sequences.

Sequence 1 occurs from 630 ft to 501.7 ft. The TS/SB (transgressive surface/sequence boundary) is assumed to occur below the depth where the borehole ends. Silty offshore sediments coarsen upward to lower shoreface silty sands between 630 and 610.5 ft. These sediments are considered to be the TST (transgressive systems tract). At 610.5, a burrowed surface is noted, which is interpreted as a flooding surface. Directly above, a shift to slightly finer sandy silts is found. These silts coarsen upwards to silty sands until 602.4 ft. The MFS (maximum flooding surface) is found at 602.45 ft, as a very fine grained, black, sandy, glauconitic surface, with heavy bioturbation. Above, the HST (highstand systems tract) occurs from 602.45 ft to 496.7 ft, and can be separated into a lHST (lower highstand systems tract) and an uHST (upper highstand systems tract). The lHST occurs from 602.45 ft to approximately 540 ft, where a transition from offshore sandy clays with interlaminations of fine sands, to silty sands with interlaminations of silts occurs above 540 ft. Above this point, sands become coarser-grained with high shell abundance, decreasing towards the top. Gamma values decrease slowly through the section, however there is a spike starting at 529 ft. Sediments also become siltier again at this point, so this transitional contact is noted to be a marine flooding surface. Therefore, the uHST is divided into two coarsening-upwards parasequence packages, with the flooding surface at 529 ft being the boundary between the two. The SB (sequence boundary) is located at 501.7 ft, where upper shoreface sands are overlain by offshore to upper shoreface silts.

Sequence 2 begins at 501.7 ft, up to 465.95 ft. The TST occurs from the base of the sequence at 501.7 ft, to 484.8. Clayey silts with very few shell fragments are persistent with very fine laminations of slightly sandier silts. Fine bioturbation is also present. The MFS is found at 484.8 ft, where glauconitized shell fragments and phosphate pellets are present, with a distinct drop in the gamma log above the surface. The HST occurs from 484.8 ft to the top of the sequence at 465.95 ft, where the marginal offshore silts abruptly transition to upper shoreface sands and lithified sandstones. Sands become coarser upwards as the environment transitions towards a foreshore environment. The sequence is capped by the sandy clay above the TS/SB of Sequence 3 above.

Sequence 3 occurs from 465.95 ft to 415.65 ft. The TST is present up to 447.1 ft, where the lithology consists of sandy offshore clays, with very fine grained sand fractions. The section is heavily bioturbated up to the MFS at 447 ft, where there is at 0.1 ft layer of cemented sand clusters and minor glauconite grains. With this, there is a sharp reduction in gamma value. The HST occurs up to 415.65 ft, where muddy lower shoreface sands transition to sandstones and then foreshore gravelly sands. Shell fragments and few burrows are present towards the bottom of the HST, while gravelly fractions increase towards the top starting at 420.65 ft. Phosphate granules begin to be observed at 420.65 ft, up to the top of the sequence, which can also be interpreted by peaks in the gamma log. Sequence 3 is capped by the TS/SB with the silty sands of a distal upper shoreface environment of Sequence 4.

At Sequence 4, from 415.65 ft to 371.3 ft, the TS/SB is marked by sandy silts marked by a peak in the gamma log. The TST occurs up to approximately 387.0 ft, based on the geophysical logs. The MFS is marked, then, at 387.0 ft. Above this surface, a HST is present up to 371.3 ft. The base of the HST is noted by a coarsening upwards sequence starting as silty sands transitioning to very fine sandstone at 387.1 ft. The very fine grained sandstone transitions to a fine, silty sand with increasing shell fragments towards the top and sparse bioturbation, indicating a shallowing of environments to a proximal upper shoreface.

Sequence 5 occurs from 371.3 ft to 303.6 ft. This sequence has a TS/SB with the silty sands of Sequence 4 below to offshore clays above, corroborated by slight gamma increase. The offshore clays of this TST continue up to 337.1 ft. Sand fractions slightly increase throughout, with grain sizes increasing from fine to medium-fine. The section is also laminated with slightly sandier laminations throughout, though the sand fraction increases upwards. At 337.1 ft, there is an abrupt transition to slightly silty sands, which is interpreted as the MFS. This is marked by a sharp decrease in gamma values. The medium to fine sands of a HST shoreface environment continue to the top of the sequence at 303.6 ft. Gravel begins to be present at 332.85 ft, and increases in abundance towards the top, where the environment shallows upwards to a near-foreshore environment. The sequence is capped by the TS/SB of Sequence 6, where above, interlaminated clays and silts of an offshore environment dominate.

Sequence 6 begins at the TS/SB at 303.6 ft, and continues up to 225.6 ft. Distal upper shoreface clays and silts of a TST occur from 303.6 to 272.0 ft. Thin shell beds are sparsely located towards the bottom of the section, which give way to larger, scattered horizontal burrows from 296.1 ft to 288 ft. Above, lenticular cross-lamination is common up to the top of the TST. Shell fragments are few to nonexistent above the lower shell beds. Though the MFS was not recovered in a sediment core, it can be interpreted to occur at 272 ft from the geophysical logs, where a steep drop in gamma values occur. This also marks the boundary between the Calvert Formation below and the Choptank Formation above. A HST is present up to the top of the sequence, from 272 ft to 225.6 ft, represented by a shoaling upwards sequence of environments from distal upper shoreface to foreshore. This is marked by a consistent transition from decreasingly silty sands to slightly gravelly sands. Gravelly fractions are comprised of quartz, phosphate and glauconite at the top of the HST.

Sequence 7 begins at the TS/SB found at 225.6 ft, though the boundary is not as sharp as the others in the borehole. The sequence ends at 185.0 ft. A very thin TST occurs from 225.6 ft to 223.0 ft, consisting of shelly, muddy distal shoreface sands. The MFS is noted at 223.0 ft, where sands transition into slightly deeper water, interbedded fine sands and clays with few shell fragments. The HST, from 223.0 ft to 185.0 ft, the interbedded lithologies transition to a proximal upper shoreface environment, based on larger sand grain sizes, and a greater increase in carbonate shell fragments. The TS/SB between Sequences 7 and 8 is marked by a transition from the silty, shelly sands to clayey silts of an offshore environment at 185.0 ft.

Sequence 8 occurs from 185.0 ft up to 138.0 ft. The TST, from 185.0 ft to 167.2 ft, consists of clays, continuously cross-laminated with siltier laminations. Upwards, the silt becomes more dominant, with laminations of clay. One thick whole bivalve shell is noted at 168.2 ft. This offshore environment abruptly changes at the MFS noted at 167.2 ft, where the lithology changes to shelly, fine to medium sands of an upper shoreface environment. This section to the top of the sequence is the HST. Lenticular cross-laminations remain persistent up to 145.3 ft, where shell fragments become larger, with a few scattered, disoriented, whole shells towards the top. The shallowing upwards trend this represents from 177.2 ft to 138 ft, is terminated by the TS/SB of Sequence 9. The surface at 138 ft is noted to contain small amounts of glauconite at the base, accompanied by a gamma log increase. This boundary is also the transition from the Choptank Formation below and the St. Marys Formation above.

The final sequence, Sequence 9, is found from 138 ft to 70 ft, and encompasses the entirety of the St. Marys Formation recovered in this borehole. In this sequence, the TST occurs from the base of the sequence up around 106.05 ft, where muddy sands with variable shell fragments are dominant. Thick shell hash and whole bivalve shells dominate the composition in several locations, representative of an upper shoreface to foreshore environment, to possibly an estuarine environment. A MFS is interpreted at 105.65 ft, where directly below, shell fragment abundance drastically drops, and granules of phosphate become notable. There is also a distinct color change to very dark gray above the MFS, with grain sizes decreasing to finely laminated sandy clays and silty sands. This is noted as the base of the HST, which continues up to 70 ft. The interlaminated clays and sands remain dominant through to the top of the sequence, with sparse sections of gravelly sands. The entirety of the HST is heavily bioturbated and little to no shell material is noted, and this is interpreted as an estuarine environment, with possible fluvial interactions based on intervals with gravelly fractions.

5.4 Correlation to Other Sites

In order to provide a stratigraphic framework for the region, the borehole at Abbott's Mill can be correlated to boreholes studied previously at Marshy Hope (Nb53-08) (Fisher, 2015) and Bethany Beach (Qj32-27) (Miller et al. 2003; Browning et al., 2006; McLaughlin et al., 2008), later reanalyzed and updated by McLaughlin et al. (2019). Geophysical logs (including gamma, spontaneous potential, and multipoint resistivity) and sedimentology of the borehole are the main determinants of sequence stratigraphic interpretations. Dinoflagellate zonations and pollen zonations from each of these studies are correlated within each sequence between the three sites.

Dinoflagellate zones are useful in determining an approximate age of the sequences, and pollen zones show vegetation dispersal across space and vegetation changes over time. Pollen assemblages appear to evolve from west to east through time, as assemblages at Marshy Hope change first, when compared to a particular correlated section. A map of the boreholes used for correlation can be found in Figure 5.3.

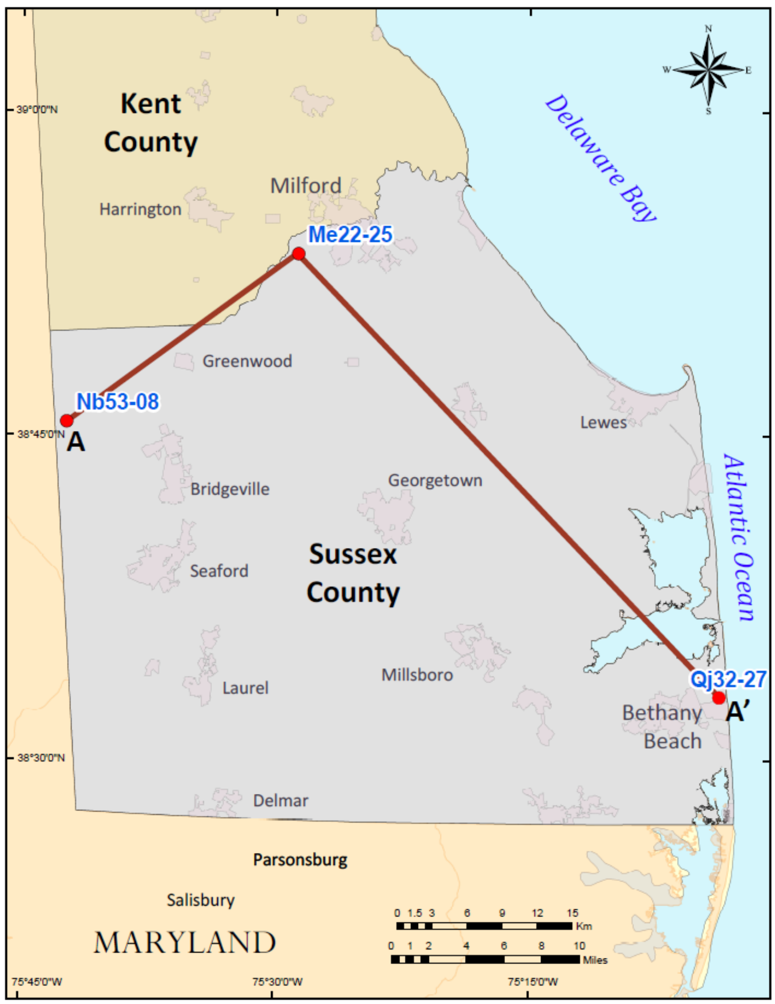

Figure 5.3: Map of Sussex County Delaware indicating the locations of the three correlated boreholes in this study. Nb53-08 represents Marshy Hope, Me22-25 represents Abbott's Mill, and Qj23-27 represents Bethany Beach.

Correlations of sequence stratigraphy are accomplished by comparing sequences identified at Abbott's Mill to sequences identified by Fisher (2016) from Marshy Hope, and the latest updates from the Bethany Beach borehole by McLaughlin et al. (2019). Generally, the nine sequences from Abbott's Mill correlate well with Sequences 1 to 7 at Marshy Hope and Sequences C1 to C9 at Bethany Beach. Sequence correlations are based on gamma and resistivity logs, and is typically corroborated by aquifer stratigraphy. As found with previous studies, stratigraphic layers dip downward towards the southeast. Dinoflagellate cyst and pollen zonations are also correlated in relation to the sequences. The correlations made between sights can be found in Figure 5.4.

Sequence 1, from 630 ft to 501.7 ft, correlates to Sequence C1 at Bethany Beach (1421.1 ft to 1153 ft) and Sequence 1 at Marshy Hope (527.3 ft to 431.6 ft). All three sequences are constrained within the lower Calvert Formation. The tops of each sequence are the upper limit of an aquifer sand. This study and the one conducted for Bethany Beach interpret the aquifer as the Lower Calvert Aquifer, where it is identified as the Lower Cheswold Aquifer at Marshy Hope. At Bethany Beach, the top of the Lower Calvert sand is dated to the early Miocene. This is matched by the dinocyst zone correlations, where across the correlation at Abbott's Mill and Marshy Hope, the dinoflagellate zonations fell within DN 2 to DN3. This is only slightly different from Bethany Beach, where the correlated section was in DN 2 to 4. In terms of pollen zones, Sequence 1 at Abbott's Mill fell within Zone 3, the correlation to Marshy Hope was represented by the bottom half of Zone 3. At Bethany Beach, the correlated section was represented by the bottom of Zone 6b. All three of these zones contain relatively high exotic taxa abundances, and high abundances of *Quercus*.

Sequence 2, from 501.7 ft to 465.95 ft, correlates to Sequences C2 and C3 at Bethany Beach (1153 ft to 981.3 ft) and most of Sequence 2 at Marshy Hope (431.6 ft to approximately 335 ft). The upper limit of the sequence is noted as the top of the Cheswold Aquifer at Abbott's Mill and Bethany Beach. The correlation from Abbott's Mill to Marshy Hope is not obvious, though it can be roughly estimated by log peaks in the sands of Sequence 2, which are also noted as the Cheswold Aquifer. The Cheswold sand at Marshy Hope is much thicker compared to the other sites. At Bethany Beach, the Cheswold Aquifer is dated to the lower Miocene (McLaughlin et al., 2019). Dinoflagellate Zones DN 2 to 3 are noted to fall within the correlated section for Abbott's Mill Sequence 2 at both Marshy Hope and Abbott's Mill. This same correlated section is represented by DN 2 to 8 at Bethany Beach. Zones DN 2 to DN 4 occur in the lower to lowermost middle Miocene. Sequence 2 fell within pollen Zone 3 at Abbott's Mill, whereas at Marshy Hope, the same section was represented by the top half of pollen zone 3 and the bottom part of pollen Zone 2. At Bethany Beach, pollen Zone 6b represented by the related section. These correlated pollen zones all still show relatively high exotic species with high *Quercus* abundance, though a transition to Zone 2 at Marshy Hope is noted in this correlation.

Sequence 3, from 465.95 ft to 415.65 ft, correlates to Sequence C4 at Bethany Beach (981.3 ft to 897.7 ft) and the top portion of Sequence 2 at Marshy Hope (335 ft to 302.1 ft). The top of all three sequences correlate to the top of the Federalsburg Aquifer, which is determined by a strong gamma spike just below the top of the sand, and are located in the middle Calvert Formation. At Bethany Beach, the top of the Federalsburg Aquifer has been dated to the uppermost lower Miocene (McLaughlin et al., 2019), which is corroborated by the correlated dinoflagellate zones. Across all three boreholes, the dinoflagellate zonations in this correlated section are noted to fall within DN 2 to DN 3, though at Bethany Beach, the zonation is broad, up to DN 8. Sequence 3 at Abbott's Mill is still within pollen Zone 3; however, the same related section falls within Zone 2 at Marshy Hope, and straddles Zones 6a and 6b at Bethany Beach. Zones 6a and 6b at Bethany Beach exhibit high abundances of *Quercus* and exotics, like the correlated section at Abbott's Mill. Marshy Hope Zone 2 shows a decrease in *Quercus* and an increase in *Pinus*, *Picea*, and *Carya*.

The upper limit of Sequence 4 (415.65 ft to 371.3 ft) at Abbott's Mill was the only sequence that did not correlate well with either of the other sites. The upper limit of the sequence was found to coincide with the Lower Frederica Aquifer, however this particular sand was not found at the other sites. It is possible that Sequences 4 and 5 at Abbott's Mill merge together at Marshy Hope and condense down towards Bethany Beach. Dinoflagellate found in this Sequence at Abbott's Mill range between DN 3 to DN 4. These zones represent an approximate age of the uppermost lower Miocene to lowermost middle Miocene.

Sequence 5, from 371.3 ft to 310 ft, correlates to Sequence C5 at Bethany Beach (897.7 ft to 787.1 ft) and Sequence 3 at Marshy Hope (302.1 ft to 242 ft). All three contain the Frederica Aquifer, located within the upper Calvert Formation in each borehole. At Bethany Beach, this aquifer has been dated to the lowermost middle Miocene (McLaughlin et al., 2019). Compared to the correlated sections, dinoflagellate zones range between DN 3 to DN 4 at Abbott's Mill. Marshy Hope and Bethany Beach provide broader ranges, from DN 2 to DN 5 and DN 2 to DN 8, respectively. Given these identified zones, the age is corroborated to that of the aquifer age at Bethany Beach, though slightly broader from the middle lower Miocene to middle middle Miocene. Almost the entirety of pollen zone 2B falls within Sequence 5 at Abbott's Mill, comparable to the middle of Zone 2 at Marshy Hope and most of the lower half of Zone 6a at Bethany Beach. Zone 2B at Abbott's Mill and Zone 2 at Marshy Hope exhibit similar assemblages, with increased *Pinus*, *Picea*, and *Carya*, and a decrease in the abundance of *Engelhardia*. Somewhat dissimilar, Zone 6a at Bethany Beach shows a relatively high abundance of exotic species and high levels of *Quercus*.

Sequence 6, from 310 ft to 225.7 ft, correlates to Sequence C6 at Bethany Beach (787.1 ft to 698.5 ft) and Sequence 4 at Marshy Hope (242 ft to 184 ft). At Abbott's Mill and Marshy Hope, the top of the correlated sequences coincides with the top of the Milford Aquifer. Conversely, the Milford Aquifer straddles two sequences at Bethany Beach, and the bottom half of the Aquifer is correlated to the sands at the other two sites. The Milford Aquifer is much thicker at Bethany Beach compared to the other locations. The base of this Aquifer is dated to the lowermost middle Miocene at Bethany Beach, which is corroborated roughly by the dinoflagellate zones represented at each site, though Abbott's Mill offers the most constrained Zone range. Sequence 6 contains dinoflagellates spanning DN 4 to DN 7, which spans the entirety of the middle Miocene. This is comparable to the related sections at Marshy Hope and Bethany Beach, which were noted to contain dinoflagellates from DN 2 to DN 7 and DN 2 to DN 8. Pollen Zone 2a is almost entirely contained within Sequence 6, aside from the top quarter. The comparable section at Marshy Hope contained the top of Zone 2 and the bottom of Zone 1, while at Bethany Beach, the sequence contained the upper middle section of Zone 6a. All three pollen zones correlated in these sections exhibit varying pollen abundances. Zone 1 at Marshy Hope shows a high abundance of *Quercus* and *Carya*, with slightly lower abundances of *Picea* and *Pinus*. At Abbott's Mill, the top of Zone 2 begins to see a slightly higher abundance of *Carya*, with lower levels of *Engelhardia* and *Symplocos*. Zone 6a at Bethany Beach still shows higher abundances of *Quercus* and exotic taxa.

Sequence 7, from 225.7 ft to 185 ft, correlates to Sequence C7 at Bethany Beach (698.5 ft to 649 ft) and Sequence 5 at Marshy Hope (184 ft to 150 ft). At Abbott's Mill, most of the sequence is made up of sand, interpreted as the Middle Choptank Aquifer. This correlates also to the Middle Choptank Aquifer at Bethany Beach. At Marshy Hope, the entirety of Sequence 5 is silts and clays, which could be interpreted as a change from sandy coastal facies to muddier estuarine facies across the three locations. All three of these sections occur within the middle Choptank Formation. Sequence 7 at Abbott's Mill and Sequence 5 at Marshy Hope contain dinoflagellates spanning DN 5 to DN 7. Sequence C8 at Bethany Beach, however, was found to contain dinoflagellates from DN 2 to DN 8. However, no dinoflagellates from within DN 5 or DN 6 were found in that study (McLaughlin et al., 2008). Based on the findings at Abbott's Mill and Marshy Hope, these correlated sequences have an approximate age within the middle to uppermost middle Miocene. The top of pollen Zone 2A and the very bottom of Zone 1 occur within Sequence 7, comparable to the lower middle section of Zone 1 at Marshy Hope, and the top of Zone 6a at Bethany Beach. At Marshy Hope, exotic taxa abundances are at their lowest in Zone 1, like the top part of the sequence at Abbott's Mill, where in Zone 1, little to no exotic species were found, and *Carya* and *Quercus* begin to increase in abundance again. These two locations correlate poorly to Bethany Beach's Zone 6a, where *Quercus* and exotic species are relatively high.

Sequence 8, from 185 ft to 138 ft, correlates to Sequence C8 at Bethany Beach (649 ft to 575.2 ft) and Sequence 6 at Marshy Hope (150 ft to 93.1 ft). Sequence 8 at Abbott's Mill incorporates the Upper Choptank Aquifer, which correlates across to the upper half of Sequence C8 at the Bethany Beach borehole. The bottom half of C8 incorporates nearly all of the Middle Choptank Aquifer. Sequence 6 at Marshy Hope is noted to be a generally sandy unit, consisting of a few unnamed aquifer sands. This could be interpreted as either including what is considered the Upper Choptank Aquifer, or the entirety of the unit may be the Upper Choptank Aquifer. It is possible that environmental factors caused interjections of muddier sections within the sequence. At Abbott's Mill and Marshy Hope, the top of the sequences also coincides with the contact between the Choptank Formation below and the St. Marys Formation above. The Upper Choptank Aquifer at Bethany Beach has been dated to the uppermost middle Miocene (McLaughlin et al., 2019). The top of Sequence 6 at Marshy Hope was also dated to approximately the uppermost middle Miocene (Fisher, 2016). At Bethany Beach, the boundary is interpreted as slightly above Sequence C8. Sequence 8 at Abbott's Mill, and Sequence 6 at Marshy Hope, contain dinoflagellates from DN 5 to DN 7. Similar to the sequence below, the correlated section at Bethany Beach was found to contain dinoflagellates identifying the section as DN 2 to 8. The zonation correlation at Marshy Hope and Abbott's Mill would give the sequences an age of approximately the middle to uppermost middle Miocene, which corroborates to the dated sediments at Marshy Hope. At Abbott's Mill, the sequence contains the lower section of pollen Zone 1, similar to Marshy Hope, which contains that study's middle section of Zone 1. As noted previously, both Zonations' Zone 1 contain little to no exotic taxa, with increasing abundances of *Quercus*, *Carya*, and *Pinus*. Sequence

C8 at Bethany Beach contains Zone 5b, which complements the correlated zones at the other two locations, with higher *Pinus* and *Carya* abundances and lower exotic species.

Sequence 9, from 138 ft to 70 ft, correlates with Sequence C9 at Bethany Beach (575.2 ft to 523.05 ft) and Sequence 7 at Marshy Hope (93.1 ft to 50.5 ft). At Bethany Beach and Marshy Hope, the sediments in the sequences are noted as being the St. Marys Confining Unit, which occurs continuously through the sediments of the St. Marys Formation. At Abbott's Mill however, Sequence 9 is made up of several unnamed aquifer sands and confining beds. This interpretation based on the lithologies and geophysical logs may represent a different environment of deposition compared to the other two sites. These sequences at all the locations encompass the entirety of the present St. Marys Formation. At Bethany Beach, the top of Sequence C9 is dated to roughly the middle upper Miocene. The final sequence at Abbott's Mill contains dinoflagellates spanning DN 7 to DN 9. The correlated sequence at Marshy Hope represents a slightly narrower range, containing dinoflagellates from DN 7 to DN 8. At Bethany Beach, the correlated section was noted to be within DN 2 to DN 8. Given the range, dinoflagellate zones across this correlation provide an age of uppermost middle to middle upper Miocene. The top of pollen Zone 1 is contained within Sequence 9 at Abbott's Mill, which is the same as the correlated sequence at Marshy Hope. The correlated section at Bethany Beach contains pollen Zone 5a. These three zonations correlate well across this section; all three exhibit increasing abundances of *Quercus*, relatively moderate abundances of *Carya*, and few exotic taxa present. At Abbott's Mill, only one or two specimens of *Engelhardia* were found in this section.

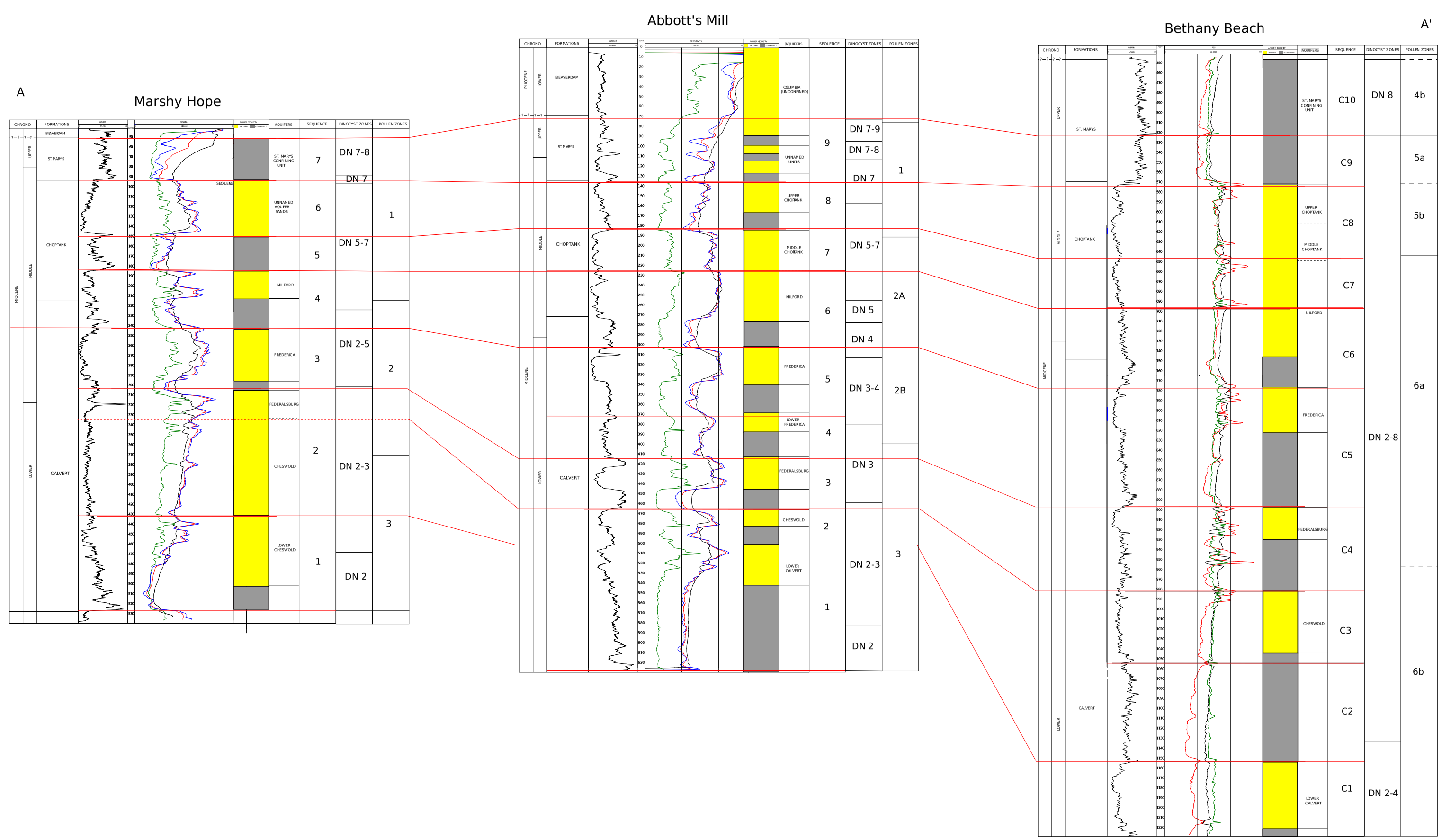

Figure 5.4: Correlation of sequences, pollen zones, and dinoflagellate zones between the Miocene formations at Abbott's Mill, Marshy Hope, and Bethany Beach. Solid red lines trace the sequences across the three boreholes.

Chapter 6

CONCLUSION

This thesis project has investigated the stratigraphy and palynology of three Miocene geologic units in the subsurface of Delaware: the Calvert, Choptank and St. Marys Formations. The study has examined, in detail, the stratigraphic record of these ancient shallow-marine units in detail in a nearly- continuous cored borehole at Abbott's Mill, southeast of Milford, Delaware.

The stratigraphic framework of the Abbott's Mill borehole was established by lithologic descriptions of the cores integrated with wireline geophysical logs. This study has documented the lithologies in detail and shown that the Miocene marine section of the Milford area is characterized by an alternation of permeable sands, which serve as aquifers, and less permeable silt- and clay-rich intervals, which serve as confining units. These lithologies reflect alternations between the shallower and deeper portions of an overall wave-dominated, sandy, shallow-marine shoreline environment. Aquifer sands are generally medium-grained quartz, with some sections containing coarser sands. Given the high abundance of shell fragments and whole specimens (bivalves, gastropods), these sands are interpreted to be deposits from intertidal to shoreface environments. Intercalated muds are indicative of deeper shelfal environments, confirmed by the presence of fine shell fragments, common bioturbation, and thin very-fine-grained sands with lenticular cross laminations.

Nine lithologic units were defined, which were used as the basis for sequence stratigraphy. The Calvert Formation contains five full coarsening upwards units, and the fine-grained section of the sixth unit. The Choptank Formation contains the coarser section of the sixth unit and two coarsening upward units above. The St. Marys Formation is made up of one unit, which is generally sandy with some sections of finer grained sediments. Overall, the Miocene section coarsens upward from the base to the top of the Calvert Formation, is sandiest in the Choptank Formation, and has more abundant mud in the thin interval of St. Marys Formation present in this borehole.

Based on the sedimentological interpretation, a sequence stratigraphy was established for the Abbott's Mill section. Nine sequences were recognized. Sequence boundaries are generally associated with the tops of shallow marine aquifer sands. Generally, these sequences contained thin transgressive systems tracts with thicker highstand systems tracts. No lowstand systems tracts were present. Most sequences were representative of an offshore to upper shoreface environment, shallowing upwards to a foreshore environment, except for in the St. Marys Formation, where the environment is more indicative of an estuarine to marsh environment.

Three hypotheses were tested in this study:

1. Palynological assemblages will correlate to palynological zonations determined at other boreholes around the region, namely Marshy Hope and Bethany Beach.

2. Dinocyst zones determined from this study are predicted to correlate to the Miocene dinocyst zonation created for the Salisbury Embayment by de Verteuil and Norris (1996).

3. These palynological data will help constrain the correlation of the hydrostratigraphic framework (aquifers and confining units) at Abbott's Mill to the hydrostratigraphy previously established for boreholes at Marshy Hope and Bethany Beach.

The results of this study confirm each of these hypotheses.

To test the first hypothesis, the palynological assemblages were analyzed in 37 samples that yielded usable palynomorphs. In total, 43 samples were taken from the borehole, however six of the samples contained less than 100 identifiable grains. This sample set included 25 samples from the Calvert Formation, 7 samples from the Choptank Formation, and 5 samples from the St. Marys Formation. Counts of the spores and pollen in each sample were analyzed and plotted for the section to show changes in relative abundance that could be used to establish a zonation as well as provide insights into paleoenvironments and paleoclimate. Using cluster analysis, three palynological zones were recognized, designated from the top to the bottom of the hole as Zones 1, 2, and 3. Zone 2 could be subdivided into two subzones. Zone 1 is characterized by little to no exotic taxa, as well as high abundances of *Carya* with increases in Cyperaceae, *Quercus*, and *Ilex*. Zone 2 is characterized abundances of *Pinus*, *Tsuga*, and *Picea*, with decreases in *Quercus* and *Carya*. Zone 3 contains the highest abundances of exotic species including *Engelhardia*, as well as high abundances in *Quercus* and Cyperaceae. These zones provide valuable stratigraphic constraints for subsurface correlation of the Miocene Formations and aquifers. Comparison to other boreholes with pollen stratigraphy indicate that Abbott's Mill Zone correlated fairly well to Zones 1 to 3 at Marshy Hope, and 5a to 6b at Bethany Beach.

In testing the second hypothesis, dinoflagellate assemblages present allow the section to be subdivided using the zonation of de Verteuil and Norris (1996). Of the 43 samples taken for dinoflagellate identification, 42 contained identifiable dinoflagellate cysts. The dinoflagellates at Abbott's Mill allow the highest resolution dinocyst zone results of any borehole examined yet in Delaware. Dinoflagellate Zones from DN 2 to

DN 9 were recognized in this section. Twenty-nine samples were taken from the Calvert Formation, and range from Zone DN 2 (lower Miocene) to DN 4 (lower to middle Miocene). Nine samples were taken from the Choptank Formation, and are indicative of Zones DN 5 to DN 7 (middle Miocene). Four samples were taken from the St. Marys Formation, and range from Zones DN 7 (uppermost middle Miocene) to possibly as high as Zone DN 9 (upper Miocene).

The third hypothesis was confirmed through integration of the palynological and dinoflagellate zonations with the lithostratigraphy and sequence stratigraphy established for the Abbott's Mill borehole. Generally, the nine sequences from Abbott's Mill correlate well with Sequences 1 to 7 at Marshy Hope and Sequences C1 to C9 at Bethany Beach. The stratigraphic layers dip towards the southeast, with sequences generally deepening from Marshy Hope to Abbotts Mill to Bethany Beach. Aquifers generally follow this pattern and become more confined from west to east. Whereas at Marshy Hope several aquifers appear to combine into one amalgamated sand unit, aquifers seen at Abbott's Mill and Bethany Beach have finer grained confining beds separating them. These confining beds are noted to thicken towards the east and south. The borehole at Abbott's Mill helps to clarify the aquifer distribution across Sussex County, Delaware.

The insight gained from this integrated stratigraphic and palynological study completed for the borehole at Abbott's Mill provides crucial information about the subsurface geology of southern Delaware. Results from palynological identifications and subsequent zonation creations aid in a better understanding of past vegetation changes and climate fluctuations during the Miocene in this region. Sedimentary descriptions done for this study provide detailed documentation of the geological characteristics of the aquifer sands and intervening confining mud beds, which help to create a better understanding of the geological controls on aquifer occurrence. Correlations to previously studied boreholes at Marshy Hope and Bethany Beach allow for a clearer understanding of aquifer and confining bed distribution and thickness variations across the state. Knowledge gained from this study can be used not only to further the details known about economically important aquifer units in the area, but also to better understand, from a scientific standpoint, the depositional and environmental history of this region during the Miocene epoch.

REFERENCES

Bernard, H.A., LeBlanc, R.J., and Major, C.F., 1962, Recent and Pleistocene geology of southeast Texas. In Rainwater, E.H., and Zingula, R.P. (Eds.), Geology of the Gulf Coast and Central Texas, Guidebook of Excursions: Houston, TX (Houston Geol. Soc.), p.175–224.

Browning, J.V., Miller, K.G., Sugarman, P.J., Barron, J., McCarthy, F.M.G., Kulhanek, D.K., Katz, M.E., and Feigenson, M.D., 2013, Chronology of Eocene-Miocene sequences on the New Jersey shallow shelf: Implications for regional, interregional, and global correlations: Geosphere, v. 9, no. 6, p. 1434–1456.

Browning, J.V., Miller, K.G., Sugarman, P.J., Kominz, M.A., McLaughlin, P.P., Kulpecz, A.A., and Feigenson, M.D., 2008, 100 Myr record of sequences, sedimentary facies and sea level change from Ocean Drilling Program onshore coreholes, US Mid-Atlantic coastal plain: Basin Research, v. 20, no. 2, p. 227–248.

Browning, J.V., Miller, K.G., McLaughlin, P.P., Kominz, M.A., Sugarman, P.J., Monteverde, D., Feigenson, M.D., and Hernandez, J.C., 2006, Quantification of the effects of eustasy, subsidence, and sediment supply on Miocene sequences, mid-Atlantic margin of the United States: Geological Society of America Bulletin, v. 118, no. 5-6, p. 567–588.

Coe, A.L., 2005, The Sedimentary Record of Sea-Level Change: Cambridge University Press, 288 p.

Davis, M.B., 1983, Quaternary history of deciduous forests of eastern North America and Europe: Annuals of the Missouri Botanical Garden, v. 70, No. 3, p. 550-563.

De Verteuil, L., and Norris, F., 1996, Miocene dinoflagellate stratigraphy and systematics of Maryland and Virginia: Micropaleontology, v. 42, 187 pp.

Dybkjær, K., and Piasecki, S., 2010, Neogene dinocyst zonation for the eastern North Sea Basin, Denmark: Review of Palaeobotany and Palynology, v. 161, no. 1-2, p. 1–29.

Fægri, K., and Iversen, J., 1989, Textbook of pollen analysis: 4th ed. by K. Fægri, P.E. Kaland & K. Krzywinski, The Blackburn Press, 328 p.

Fisher, K.A., 2016, Interpretation and Analysis of Sequence Stratigraphy and Palynomorph Assemblages of Miocene-Age Sediments in Southern Delaware [thesis], 118 pp.

Graham, A., 1999, Late Cretaceous and Cenozoic History of North American Vegetation: Oxford University Press, New York, NY, 350 pp.

Groot, J.J., 1992, Plant Microfossils of the Calvert Formation of Delaware: Delaware Geological Survey Report of Investigations no. 50, 14 p.

Groot, J.J., 1991, Palynological evidence for Late Miocene, Pliocene and Early Pleistocene climate changes in the middle U.S. Atlantic Coastal Plain: Quaternary Science Reviews, v. 10, p. 147-162.

Groot, J.J., Ramsey, K.W., and Wehmiller, J.F., 1990, Ages of the Bethany, Beaverdam, and Omar formations of southern Delaware: Delaware Geological Survey Report of Investigations No. 47, 19 p.

Harris, L.C., and Whiting, B.M., 2000, Sequence-stratigraphic significance of Miocene to Pliocene glauconite-rich layers, on- and offshore of the US Mid-Atlantic margin: Sedimentary Geology, v. 134, no. 1-2, p. 129–147.

Kidwell, S.M., 1997, Anatomy of Extremely Thin Marine Sequences Landward of a Passive-Margin Hinge Zone: Neogene Calvert Cliffs Succession, Maryland, U.S.A.: SEPM Journal of Sedimentary Research, v. 67, p. 322–340.

Kidwell, S.M., 1989, Stratigraphic Condensation of Marine Transgressive Records: Origin of Major Shell Deposits in the Miocene of Maryland: The Journal of Geology, v. 97, no. 1, p. 1–24.

Kidwell, S.M., 1984, Outcrop features and origin of basin margin unconformities in the Lower Chesapeake Group (Miocene), Atlantic Coastal Plain: American Association of Petroleum Geologists, v. 36, p. 37-58.

Kotthoff, U., Greenwood, D.R., McCarthy, F.M.G., Müller-Navarra, K., Prader, S., and Hesselbo, S.P., 2014, Late Eocene to middle Miocene (33 to 13 million years ago) vegetation and climate development on the North American Atlantic Coastal Plain (IODP Expedition 313, Site M0027): Climate of the Past, v. 10, no. 4, p. 1523–1539.

Kulpecz, A.A., Miller, K.G., Browning, J.V., Edwards, L.E., Powars, D.S., McLaughlin, P.P., Harris, A.D., and Feigenson, M.D., 2009, Postimpact deposition in the Chesapeake Bay impact structure: Variations in eustasy, compaction, sediment supply, and passive-aggressive tectonism: Geological Society of America Special Papers, v. 458, p. 811–837.

Larsson, L.M., Dybkjær, K., Rasmussen, E.S., Piasecki, S., Utescher, T., and Vajda, V., 2011, Miocene climate evolution of northern Europe: A palynological investigation from Denmark: Palaeogeography, Palaeoclimatology, Palaeoecology, v. 309, no. 3-4, p. 161–175.

Louwye, S., and De Schepper, S., 2010, The Miocene-Pliocene hiatus in the southern North Sea Basin (northern Belgium) revealed by dinoflagellate cysts: Geological Magazine, v. 147, p. 760-776.

McCartan, L., Tiffney, B.H., Wolfe, J.A., Ager, T.A., Wing, S.L., Sirkin, L.A., Ward, L.W., and Brooks, J., 1990, Late Tertiary floral assemblage from upland gravel deposits of the southern Maryland Coastal Plain: Geology, v. 18, p. 311-314.

McCarthy, F.M.G., Katz, M.E., Kotthoff, U., Browning, J.V., Miller, K.G., Zanatta, R., Williams, R.H., Drljepan, M., Hesselbo, S.P., Bjerrum, C.J., and Mountain, G.S., 2013, Sea-level control of New Jersey margin architecture: Palynological evidence from Integrated Ocean Drilling Program Expedition 313: Geosphere, v. 9, no. 6, p. 1457–1487.

McLaughlin, P.P., Tomlinson, J.L., and Lawson, A.K., 2019 (in press), Aquifers and Groundwater Withdrawals, Kent and Sussex Counties, Delaware, Delaware Geological Survey Report of Investigations, v. 83, 582 pp.

McLaughlin, P.P., Miller, K.G., Browning, J.V., Ramsey, K.W., Benson, R.N., Tomlinson, J.L., and Sugarman, P.J., 2008, Stratigraphy and correlation of the Oligocene to Pleistocene section at Bethany Beach, Delaware, Delaware Geological Survey Report of Investigations, v. 75, 40 pp.

McLaughlin, P.P., and Velez, C.C, 2006, Geology and extent of the confined aquifers of Kent County, Delaware: Delaware Geological Survey Report of Investigations, v. 72, 40 pp.

Miller, K.G., Kominz, M.A., Browning, J.V., Wright, J.D., Mountain, G.S., Katz, M.E., Sugarman, P.J., Cramer, B.S., Christie-Blick, N., and Pekar, S.F., 2005, The Phanerozoic Record of Global Sea-Level Change: Science, v. 310, p. 1293–1298.

Miller, K.G., McLaughlin, P.P., Browning, J.V., Benson, R.N., Sugarman, P.J., Hernandez, J., Ramsey, K.W., Baxter, S.J., Feigenson, M.D., Aubry, M.-P., Monteverde, D.H., Cramer, B.S., Katz, M.E., McKenna, T.E., Strohmeier, S.A., Pekar, S.F., Uptegrove, J., Cobbs, G., Cobbs, G., III, and Curtin, S.E., 2003a, Bethany Beach site report, in Miller, K.G., Sugarman, P.J., Browning, J.V., et al., Proceedings of the Ocean Drilling Program, Initial Reports, v. 174AX Supplement: College Station, TX, Ocean Drilling Program, p. 1-84.

Munsterman, D.K., and Brinkhuis, H., 2004, A southern North Sea Miocene dinoflagellate cyst zonation: Netherlands Journal of Geosciences, v. 83, p. 267-285.

Pazzaglia, F.J., 1993, Stratigraphy, petrography, and correlation of late Cenozoic middle Atlantic Coastal Plain deposits: Implications for late-stage passive-margin geologic evolution: Geological Society of America Bulletin, v. 105, no. 12, p. 1617–1634.

Pazzaglia, F.J., Robinson, R.A.J., and Traverse, A., 1997, Palynology of the Bryn Mawr Formation (Miocene): insights on the age and genesis of Middle Atlantic margin fluvial deposits: Sedimentary Geology, v. 108, no. 1-4, p. 19–44.

Shattuck, G.B., 1904, Geological and paleontological relations, with a review of earlier investigations: Maryland Geological Survey, Miocene Volume, p. 33-137

Shattuck, G. B., 1902, The Miocene formations of Maryland (abs.): Science, v. XV, no. 388, p. 906.

Sibley, D. A., 2009, The Sibley guide to trees, New York: Alfred A. Knopf, 464 p.

Sugarman, P.J., Miller, K.G., Browning, J.V., Kulpecz, A.A., McLaughlin, P.P., and Monteverde, D.H., 2005, Hydrostratigraphy of the New Jersey Coastal Plain: Sequences and facies predict continuity of aquifers and confining units: Stratigraphy, v. 2, no. 3, p. 259–275.

Sugarman, P.J., and Miller, K.G., 1997, Correlation of Miocene sequences and hydrogeologic units, New Jersey Coastal Plain: Sedimentary Geology, v. 108, no. 1-4, p. 3–18.

Sugarman, P. J., Miller, K.G., Owens, J.P., and Feigenson, M.D., 1993, Strontium-isotope and sequence stratigraphy of the Miocene Kirkwood Formation, southern New Jersey: Geological Society of America Bulletin, v. 105, no. 4, p. 423–436.

Traverse, A., 2008, Paleopalynology: Springer Netherlands, 772 p.

Wentworth, K., 1922, A Scale of Grade and Class Terms for Clastic Sediments: The Journal of Geology, v. 30, p. 377-392.

Appendix A

SUPPLEMENTAL MATERIAL

Table A.1: Grain size distribution for samples taken from borehole Me22-25.

	granule	vcg	cg	mg	fg	vfg	mud
DEPTH (ft)	2.0 mm	1.0 mm	500 micron	250 micron	125 micron	67 micron	<67 micron
77	0.00%	0.26%	0.78%	3.00%	68.36%	11.48%	16.11%
85	0.79%	2.15%	7.07%	17.52%	52.52%	6.28%	13.67%
92	6.60%	10.11%	17.86%	40.18%	10.65%	3.10%	11.50%
100	0.00%	1.68%	2.16%	16.83%	59.37%	3.92%	16.04%
106	7.20%	7.13%	15.73%	24.72%	28.41%	4.02%	12.79%
114	0.84%	1.24%	2.58%	19.97%	46.30%	2.73%	26.33%
119	1.14%	1.59%	1.50%	6.06%	71.82%	4.51%	13.38%
125	23.56%	8.75%	6.87%	14.68%	35.42%	3.88%	6.83%
132	0.00%	0.05%	0.60%	10.14%	45.72%	26.49%	17.00%
138	6.91%	7.49%	9.56%	18.73%	24.35%	15.76%	17.18%
144	0.91%	0.75%	1.77%	53.66%	31.18%	2.37%	9.35%
150	1.09%	2.03%	6.21%	44.37%	22.52%	3.75%	20.03%
162	2.99%	1.70%	3.91%	24.91%	33.27%	5.24%	27.99%
168	1.27%	1.83%	4.40%	36.03%	27.30%	4.89%	24.28%
174	0.00%	0.05%	0.15%	2.29%	33.11%	13.14%	51.25%
180	0.00%	0.06%	0.45%	2.35%	30.83%	17.93%	48.38%
192	14.38%	9.76%	20.41%	31.23%	10.21%	2.26%	11.75%
205	1.09%	1.16%	1.22%	10.93%	64.95%	6.30%	14.34%
210	9.57%	9.57%	17.17%	34.71%	16.42%	2.30%	10.27%
218	0.56%	0.45%	2.09%	67.27%	18.02%	1.36%	10.26%
224	40.33%	9.89%	7.22%	11.36%	10.20%	2.62%	18.37%
230	18.13%	13.02%	11.52%	11.89%	10.39%	6.28%	28.77%
235	51.54%	10.75%	9.01%	8.28%	7.88%	2.37%	10.18%
240	8.59%	11.56%	23.04%	30.56%	17.70%	1.46%	7.09%
246	5.61%	17.82%	30.58%	18.26%	11.65%	3.56%	12.52%
252	0.00%	0.10%	0.70%	41.58%	44.71%	5.12%	7.80%
262	0.00%	0.00%	0.05%	4.16%	46.60%	13.25%	35.94%
270	0.47%	28.59%	53.39%	6.46%	7.21%	1.22%	2.67%
275	0.00%	1.12%	2.68%	1.26%	8.77%	8.10%	78.07%
280	0.00%	0.00%	0.07%	0.15%	0.22%	0.22%	99.33%
284	0.00%	0.16%	0.26%	0.63%	12.81%	17.76%	68.37%
290	0.00%	0.00%	0.34%	1.01%	3.99%	21.90%	72.76%
297	0.00%	0.00%	0.56%	14.07%	26.45%	2.00%	56.91%
304	1.25%	6.15%	8.66%	34.68%	19.36%	2.35%	27.55%
310	37.64%	14.87%	15.08%	13.63%	7.52%	2.77%	8.50%
316	5.44%	8.78%	12.54%	28.79%	17.42%	7.41%	19.63%
323	17.98%	21.22%	29.12%	17.53%	7.00%	1.86%	5.29%
330	3.05%	37.55%	45.34%	9.16%	1.91%	0.23%	2.77%
336	0.00%	1.68%	8.29%	57.72%	25.30%	1.55%	5.46%
338	0.00%	0.00%	0.15%	1.10%	5.28%	21.94%	71.53%
343	0.00%	0.06%	0.34%	1.32%	1.37%	3.26%	93.65%
350	0.00%	2.46%	3.24%	1.38%	2.40%	9.83%	80.70%
354	1.10%	0.17%	0.33%	0.33%	0.22%	0.44%	97.40%
359	0.00%	0.06%	0.12%	0.24%	0.12%	0.24%	99.21%
365	0.00%	0.00%	0.39%	0.89%	1.08%	5.92%	91.72%
371	0.05%	0.66%	0.55%	0.98%	24.29%	32.55%	40.92%
377	0.00%	0.08%	0.19%	3.47%	74.81%	5.29%	16.17%
383	0.00%	0.05%	0.24%	0.44%	62.35%	12.74%	24.18%
390	0.00%	0.06%	0.22%	0.67%	6.61%	18.57%	73.87%
400	0.00%	0.19%	0.27%	1.01%	8.77%	14.79%	74.96%
410	0.00%	0.00%	0.55%	0.64%	11.13%	17.38%	70.29%
417	1.18%	0.61%	1.46%	31.41%	39.54%	7.21%	18.59%
420	3.22%	2.07%	4.07%	51.48%	21.91%	4.47%	12.79%
448	0.00%	0.00%	0.23%	2.21%	1.26%	0.83%	95.47%
454	0.00%	0.11%	0.43%	0.32%	31.60%	26.14%	41.40%
460	0.00%	0.00%	0.09%	0.65%	1.62%	0.83%	96.81%
465	0.10%	0.31%	1.61%	11.35%	5.34%	2.13%	79.16%
471	0.09%	0.42%	7.66%	48.07%	8.20%	4.52%	31.03%
477	0.67%	2.63%	12.18%	42.90%	7.96%	6.64%	27.02%
483	37.37%	9.13%	7.70%	10.59%	4.93%	3.44%	26.84%
489	0.00%	0.03%	0.12%	1.14%	60.99%	11.74%	25.98%
495	0.00%	0.28%	2.92%	8.63%	25.25%	11.18%	51.74%
501	0.52%	0.67%	4.64%	18.83%	54.66%	4.24%	16.44%
509	13.71%	3.75%	8.72%	50.22%	14.60%	1.56%	7.44%
515	11.24%	3.37%	5.91%	35.80%	19.90%	3.76%	20.02%
520	0.04%	0.09%	0.36%	3.69%	30.80%	12.19%	52.83%
525	10.60%	8.24%	8.13%	20.81%	29.55%	2.70%	19.98%
529	2.48%	2.06%	2.00%	11.97%	43.17%	3.74%	34.58%
534	0.04%	0.38%	0.75%	1.85%	66.88%	12.02%	18.09%
540	0.00%	0.10%	0.89%	2.47%	36.12%	16.58%	43.84%
546	0.00%	0.00%	0.28%	0.99%	4.09%	6.78%	87.86%
552	0.00%	0.05%	0.36%	0.99%	8.68%	9.22%	80.70%
558	0.00%	0.08%	0.32%	0.97%	8.60%	8.44%	81.58%
564	0.00%	0.08%	0.16%	0.43%	1.58%	5.95%	91.80%
570	0.00%	0.05%	0.10%	0.72%	5.27%	10.44%	83.41%
576	0.00%	0.09%	0.56%	1.29%	37.76%	11.94%	48.36%
582	0.00%	0.00%	1.14%	1.70%	12.71%	12.09%	72.37%
588	0.00%	0.00%	0.85%	1.73%	66.92%	9.18%	21.31%
594	0.00%	0.00%	0.14%	0.90%	17.60%	14.75%	66.61%
600	0.00%	0.16%	0.43%	1.12%	0.96%	1.54%	95.80%
606	0.00%	0.11%	0.63%	0.48%	0.71%	0.74%	97.33%
612	0.00%	0.05%	0.05%	0.05%	0.23%	0.32%	99.32%
618	0.05%	0.05%	0.05%	0.24%	0.10%	0.33%	99.19%
624	0.00%	0.14%	0.78%	3.46%	11.68%	8.76%	75.19%
630	1.05%	0.80%	16.95%	40.07%	16.52%	3.64%	20.96%

Table A.2: Grain composition data from samples taken at borehole Me22-25.

DEPTH	Quartz	Lithics	OHM	Mica	Carbonate	Feldspar	Forams	Organic	Glauconite	Phosphate
77	94%	1%	1%	2%	0%	0%	0%	2%	0%	0%
85	97%	1%	1%	0%	0%	1%	0%	0%	0%	0%
92	95%	0%	1%	0%	0%	1%	0%	0%	0%	3%
100	93%	0%	1%	0%	2%	3%	0%	1%	0%	0%
106	94%	3%	1%	0%	0%	0%	0%	0%	0%	2%
114	86%	0%	1%	0%	10%	0%	0%	0%	0%	3%
119	77%	0%	1%	1%	20%	0%	0%	1%	0%	0%
125	75%	0%	2%	0%	23%	0%	0%	0%	0%	0%
132	94%	0%	2%	0%	3%	1%	0%	0%	0%	0%
138	64%	0%	1%	0%	32%	0%	0%	0%	0%	3%
144	79%	0%	2%	0%	18%	0%	0%	0%	0%	1%
150	83%	0%	1%	0%	12%	1%	0%	0%	0%	3%
162	90%	0%	1%	0%	6%	0%	1%	0%	0%	2%
168	90%	0%	1%	0%	0%	1%	0%	0%	3%	5%
174	92%	0%	1%	2%	0%	0%	1%	4%	0%	0%
180	96%	0%	1%	2%	0%	0%	0%	1%	0%	0%
192	61%	0%	1%	0%	32%	0%	3%	0%	2%	1%
205	76%	0%	1%	2%	7%	0%	3%	0%	8%	3%
210	82%	1%	2%	0%	11%	0%	2%	0%	0%	2%
218	84%	0%	2%	0%	9%	1%	2%	0%	0%	2%
224	39%	0%	1%	0%	55%	0%	2%	0%	0%	3%
230	56%	0%	1%	0%	40%	0%	1%	0%	0%	2%
235	34%	1%	1%	0%	62%	0%	1%	0%	0%	1%
240	83%	0%	2%	0%	12%	0%	0%	0%	2%	1%
246	97%	0%	1%	0%	0%	0%	0%	0%	0%	2%
252	95%	0%	2%	2%	0%	0%	0%	0%	0%	1%
262	94%	0%	3%	1%	0%	0%	1%	1%	0%	0%
270	92%	5%	0%	0%	0%	2%	0%	0%	0%	1%
275	90%	0%	5%	0%	2%	1%	0%	2%	0%	0%
280	95%	0%	2%	1%	1%	0%	0%	1%	0%	0%
284	88%	0%	1%	3%	3%	0%	0%	5%	0%	0%
290	93%	0%	2%	4%	0%	0%	0%	1%	0%	0%
297	94%	0%	3%	2%	0%	0%	0%	0%	0%	1%
304	95%	0%	3%	0%	0%	1%	0%	0%	0%	1%
310	63%	1%	1%	0%	30%	0%	0%	0%	2%	3%
316	93%	1%	1%	0%	0%	2%	0%	0%	0%	3%
323	93%	0%	1%	1%	1%	1%	1%	1%	0%	1%
330	92%	6%	1%	0%	0%	0%	0%	0%	0%	1%
336	92%	1%	2%	3%	0%	1%	0%	1%	0%	0%
338	86%	0%	0%	4%	0%	0%	0%	10%	0%	0%
343	91%	3%	1%	1%	3%	1%	0%	0%	0%	0%
350	90%	2%	2%	3%	1%	1%	0%	1%	0%	0%
354	86%	3%	1%	1%	8%	0%	0%	0%	1%	0%
359	96%	0%	2%	2%	0%	0%	0%	0%	0%	0%
365	90%	3%	1%	2%	3%	0%	0%	1%	0%	0%
371	92%	0%	2%	0%	5%	0%	0%	1%	0%	0%
377	92%	0%	2%	0%	5%	0%	1%	0%	0%	0%
383	93%	0%	4%	0%	3%	0%	0%	0%	0%	0%
390	95%	1%	2%	1%	0%	0%	0%	1%	0%	0%
400	91%	0%	1%	3%	4%	0%	0%	1%	0%	0%
410	91%	0%	2%	3%	2%	0%	1%	1%	0%	0%
417	94%	0%	3%	1%	1%	0%	1%	0%	0%	0%
420	83%	0%	3%	1%	12%	0%	0%	1%	0%	0%
448	98%	0%	2%	0%	0%	0%	0%	0%	0%	0%
454	95%	0%	1%	2%	1%	0%	0%	1%	0%	0%
460	96%	0%	1%	0%	2%	0%	0%	1%	0%	0%
465	76%	3%	2%	1%	14%	1%	0%	0%	0%	3%
471	81%	1%	1%	3%	9%	0%	0%	0%	0%	5%
477	76%	5%	1%	0%	12%	0%	0%	0%	2%	4%
483	47%	10%	1%	0%	34%	0%	0%	0%	7%	1%
489	90%	1%	1%	2%	4%	0%	0%	1%	0%	1%
495	85%	1%	2%	3%	7%	1%	0%	0%	0%	1%
501	82%	1%	2%	2%	8%	0%	0%	0%	1%	4%
509	63%	1%	2%	0%	30%	0%	0%	0%	3%	1%
515	71%	3%	2%	0%	23%	0%	0%	0%	0%	1%
520	86%	2%	3%	4%	3%	1%	0%	1%	0%	0%
525	65%	1%	1%	0%	30%	1%	0%	0%	0%	2%
529	82%	2%	2%	2%	9%	0%	0%	3%	0%	0%
534	87%	3%	1%	3%	3%	1%	0%	2%	0%	0%
540	89%	0%	2%	5%	2%	1%	0%	1%	0%	0%
546	88%	0%	1%	5%	1%	0%	0%	2%	1%	2%
552	88%	1%	1%	5%	1%	0%	0%	4%	0%	0%
558	81%	2%	1%	6%	2%	0%	0%	8%	0%	0%
564	82%	1%	3%	4%	0%	1%	0%	4%	2%	3%
570	88%	1%	1%	5%	0%	1%	0%	1%	0%	3%
576	88%	0%	1%	6%	1%	0%	0%	2%	1%	1%
582	88%	1%	1%	5%	2%	0%	0%	2%	0%	1%
588	87%	0%	2%	3%	0%	3%	0%	2%	1%	2%
594	90%	0%	2%	4%	2%	0%	1%	1%	0%	0%
600	90%	0%	1%	5%	2%	0%	1%	1%	0%	0%
606	87%	3%	2%	2%	3%	0%	2%	1%	0%	0%
612	83%	0%	1%	4%	8%	0%	3%	1%	0%	0%
618	72%	0%	2%	3%	13%	2%	3%	4%	1%	0%
624	87%	2%	2%	2%	2%	1%	0%	0%	3%	1%
630	93%	0%	1%	1%	1%	1%	0%	0%	0%	3%

Table A.3: Raw pollen counts for the borehole Me22-25. Red lines indicate formational boundaries. Solid black lines indicate divisions between the lower, middle, and upper Calvert Formation. The dashed line divides the middle Calvert section between the upper and lower subdivisions.

Depth	AP	NAP	Coniferou	Deciduous	Exotics	Abies	Acer	Alnus	Ambrosia	Aster-type	Betula	Carya	Carpinus	Castanea	Cornus	Corylus	Cyperacea	Cyrilla	Engelhard	Fagus	Faxinus
74	94.12	5.88	28.43	65.69	8.82	0.00	3.92	0.00	0.00	0.00	0.00	13.73	0.00	0.00	0.00	0.00	1.96	0.00	0.00	0.00	0.00
82	92.23	7.77	13.59	77.67	4.85	0.97	1.94	1.94	0.00	0.00	0.00	17.48	0.97	0.00	0.00	0.00	3.88	0.00	0.97	1.94	0.00
112	93.00	7.00	12.00	81.00	4.00	0.00	1.00	1.00	1.00	0.00	0.00	13.00	0.00	0.00	0.00	0.00	2.00	0.00	0.00	0.00	0.00
127	92.23	7.77	22.98	68.28	8.09	1.29	1.94	1.29	0.00	0.00	0.00	14.56	0.00	0.00	0.00	0.00	2.91	0.00	0.97	1.62	0.00
136	93.55	6.45	16.77	77.42	5.16	0.65	1.29	4.52	0.00	0.00	0.00	16.13	0.00	0.00	0.00	0.00	4.52	0.00	0.00	0.65	0.00
146	93.07	6.93	21.78	73.27	8.91	0.99	1.98	0.99	0.00	0.00	0.00	14.85	0.00	0.00	0.99	0.00	2.97	0.00	0.99	0.00	0.00
160	94.00	6.00	7.00	87.00	6.00	0.00	3.00	2.00	0.00	0.00	0.00	15.00	0.00	0.00	0.00	0.00	4.00	0.00	0.00	0.00	1.00
171	94.17	4.85	25.24	68.93	2.91	1.94	3.88	0.00	0.00	0.00	0.00	12.62	0.00	0.00	1.94	0.97	1.94	0.00	0.97	0.00	0.00
177	97.06	2.94	14.71	84.31	6.86	0.98	1.96	0.98	0.00	0.00	0.00	14.71	0.98	0.00	2.94	0.00	2.94	0.00	0.00	0.00	0.00
190	88.24	11.76	19.61	69.61	12.75	0.00	2.94	1.96	0.00	0.00	0.00	17.65	0.98	0.00	0.00	0.00	7.84	0.00	0.00	1.96	0.00
215	91.39	7.62	15.89	75.50	11.92	0.66	1.32	0.99	0.33	0.33	0.00	12.58	0.00	0.66	0.33	0.99	1.99	0.00	0.00	1.32	0.00
222	93.33	5.00	16.00	77.33	13.33	1.33	1.00	3.67	0.67	0.00	0.00	11.00	0.00	0.33	0.67	1.67	0.00	0.00	0.00	0.00	0.00
275	88.32	10.31	16.49	70.10	18.21	2.41	1.37	2.75	1.03	0.69	0.00	15.12	0.00	0.00	0.00	1.37	4.47	0.00	1.72	1.03	0.00
280	90.35	8.36	12.22	77.17	16.72	0.64	1.93	2.57	0.96	0.00	0.32	18.01	0.00	0.00	0.64	1.29	2.89	0.00	0.96	0.00	0.00
287	95.28	4.72	13.21	76.42	20.75	0.94	2.83	0.00	0.00	0.00	0.00	17.92	0.00	0.00	0.94	0.00	2.83	0.00	4.72	6.60	0.00
302	89.22	10.46	5.23	76.47	17.97	0.33	0.33	1.96	0.65	0.33	0.00	9.80	0.00	0.00	0.65	0.33	5.88	0.00	6.21	4.25	0.00
354	90.38	9.62	25.00	50.96	25.96	2.88	0.00	1.92	0.00	0.00	0.96	9.62	0.00	0.96	0.00	0.00	2.88	0.00	10.58	0.00	0.96
365	84.62	15.38	24.04	53.85	21.15	0.96	0.00	0.00	0.00	0.00	0.00	7.69	0.00	0.96	1.92	0.00	6.73	0.00	7.69	1.92	0.00
377	89.03	10.32	21.29	65.16	16.13	0.00	1.94	0.65	1.29	0.00	0.00	7.10	0.00	1.29	1.94	0.65	3.87	0.00	1.29	3.23	0.00
388	83.17	12.87	27.72	52.48	17.82	0.00	1.98	0.99	0.00	0.00	0.00	9.90	0.00	0.00	0.00	3.96	5.94	0.00	3.96	0.99	0.00
400	82.69	14.42	13.46	59.62	20.19	0.00	0.96	0.00	0.00	0.00	0.00	6.73	0.00	0.00	0.00	2.88	2.88	0.00	5.77	0.96	0.96
417	89.11	10.89	6.93	79.21	11.88	0.00	0.99	0.99	0.00	0.00	0.00	10.89	0.00	0.00	0.00	0.00	3.96	0.00	2.97	0.00	0.99
450	84.05	15.28	6.64	75.08	15.61	0.00	1.99	1.00	0.00	0.00	0.00	9.63	0.00	0.33	1.33	0.66	2.66	0.00	0.00	1.00	0.00
459	86.69	12.99	7.14	78.90	12.99	0.00	1.95	3.25	0.32	0.00	0.00	7.47	0.00	0.65	1.62	0.32	5.52	0.00	0.97	0.65	0.65
471	87.42	12.58	17.88	69.21	15.89	0.00	2.32	2.98	0.66	0.33	0.00	8.28	0.00	0.33	0.99	0.00	4.30	0.33	1.32	1.32	0.00
485	89.40	10.60	8.28	69.54	25.50	0.00	1.66	1.66	0.00	0.00	0.33	8.94	0.33	0.00	0.00	0.00	6.62	0.00	11.59	0.99	0.00
499	89.71	10.29	7.40	79.42	15.76	0.00	1.61	1.29	0.32	0.32	0.00	6.75	0.00	0.00	1.93	0.00	5.47	0.00	2.89	0.00	0.32
520	92.53	7.47	12.01	71.43	23.05	0.00	0.97	1.30	0.00	0.00	0.00	11.36	0.00	0.00	0.97	0.00	3.25	0.00	10.06	0.32	0.32
548	84.89	15.11	10.61	71.06	12.22	0.00	1.93	0.64	0.32	0.00	0.00	9.97	0.00	0.00	1.61	0.00	8.04	0.64	3.54	0.00	0.32
560	82.33	17.67	17.21	63.26	13.49	0.00	2.33	1.40	0.47	0.00	0.00	8.37	0.00	0.00	0.93	0.00	9.77	1.40	3.72	0.00	0.00
570	80.67	19.33	11.67	67.00	16.00	0.00	1.67	2.00	0.67	0.33	0.00	11.00	0.00	0.00	2.00	0.00	10.00	0.67	2.67	1.00	0.00
580	87.95	12.05	7.17	78.50	13.03	0.00	1.95	0.98	0.00	0.00	0.00	9.45	0.00	0.65	1.63	0.00	8.14	0.65	2.93	2.28	0.33
590	85.76	14.24	12.62	72.49	12.94	0.00	1.62	0.97	0.32	0.00	0.00	10.68	0.00	0.97	3.56	0.00	7.77	0.00	1.62	0.97	0.00
600	89.72	10.28	13.40	68.85	16.51	0.00	0.62	1.56	0.62	0.00	0.00	11.21	0.00	0.93	2.80	0.00	6.85	0.00	5.92	1.25	0.62
610	86.05	13.95	10.96	76.08	11.30	0.00	1.00	1.33	0.00	0.00	0.00	8.64	0.00	0.00	2.66	0.00	8.97	0.00	0.00	0.66	0.33
620	88.04	11.96	9.30	75.08	15.95	0.00	1.66	1.66	0.33	0.00	0.00	7.97	0.00	1.00	1.66	0.00	6.98	0.00	1.33	1.33	0.33
628	90.20	9.80	11.11	73.20	15.69	0.00	2.94	0.98	0.00	0.33	0.00	8.82	0.00	0.00	1.96	0.00	6.21	0.00	2.61	0.98	0.33

Depth	Ilex	Juglans	Liquidamb	Lycopod	Myrica	Nymphaea	Pterocarya	Picea	Pinus	Poeacea	Polygonac	Polypod	Podocarpu	Quercus	Salix	Symplocos	Sphagnum	TCT	Tilia	Tsuga	Ulmus
74	0.00	0.98	0.00	0.00	0.00	0.98	1.96	1.96	26.47	0.00	0.00	2.94	0.00	34.31	0.00	0.00	0.00	6.86	0.00	0.00	3.92
82	0.00	0.97	0.97	0.00	0.97	0.00	1.94	0.97	11.65	1.94	0.00	1.94	0.00	45.63	0.00	0.00	0.00	1.94	0.00	0.00	0.97
112	1.00	0.00	5.00	0.00	0.00	0.00	2.00	0.00	12.00	0.00	0.00	4.00	0.00	53.00	0.00	0.00	0.00	2.00	1.00	0.00	2.00
127	4.21	3.56	1.94	0.00	0.00	1.62	3.24	1.29	20.39	1.94	0.00	1.29	0.00	32.04	0.00	0.00	0.00	3.88	0.00	0.00	0.00
136	3.87	1.29	1.29	0.00	0.00	0.00	1.94	1.94	13.55	1.94	0.00	0.00	0.00	40.00	0.65	0.00	0.00	3.23	0.00	0.65	1.94
146	1.98	1.98	0.99	0.00	1.98	0.00	5.94	1.98	15.84	0.99	0.00	2.97	0.00	35.64	0.00	0.00	0.00	1.98	0.00	2.97	0.99
160	3.00	0.00	9.00	0.00	0.00	0.00	5.00	1.00	6.00	2.00	0.00	0.00	0.00	46.00	0.00	0.00	0.00	1.00	0.00	0.00	2.00
171	1.94	0.97	1.94	0.00	0.00	0.00	1.94	1.94	20.39	2.91	0.00	0.00	0.00	38.83	0.00	0.00	0.00	0.00	0.00	0.97	3.88
177	1.96	0.00	2.94	0.00	0.00	0.00	4.90	0.98	10.78	0.00	0.00	0.00	0.00	47.06	0.00	0.00	0.00	1.96	0.00	1.96	1.96
190	0.00	0.00	0.00	0.00	0.00	0.00	8.82	2.94	15.69	2.94	0.00	0.98	0.00	29.41	0.00	0.00	0.00	3.92	0.00	0.98	0.98
215	1.32	0.66	2.32	0.33	0.00	0.00	4.30	2.65	12.58	1.66	0.33	2.65	0.00	41.06	0.66	0.00	0.00	7.62	0.00	0.00	0.33
222	1.67	0.67	3.67	0.00	0.00	0.00	5.33	2.33	12.33	2.67	0.00	1.67	0.00	40.33	0.67	0.00	0.00	8.00	0.33	0.00	0.00
275	1.03	0.34	5.50	0.69	0.00	0.00	5.84	2.06	12.03	2.06	0.00	1.37	0.00	25.09	0.34	0.00	0.00	10.65	0.69	0.00	0.34
280	2.57	0.96	2.57	0.32	0.00	0.00	3.86	3.22	7.40	2.25	0.00	1.93	0.96	29.90	0.32	0.00	0.00	10.93	0.96	0.00	1.61
287	0.00	0.00	4.72	0.00	0.00	0.00	3.77	2.83	9.43	1.89	0.00	0.00	0.00	28.30	0.00	0.94	0.00	11.32	0.00	0.00	0.00
302	0.65	0.00	0.98	0.33	0.00	0.00	1.96	1.31	2.94	1.31	0.00	1.63	0.00	45.10	1.31	1.96	0.33	7.84	0.33	0.65	0.65
354	1.92	0.00	0.00	0.00	0.00	0.00	2.88	5.77	15.38	2.88	0.00	3.85	0.96	23.08	0.00	3.85	0.00	7.69	0.00	0.00	0.96
365	0.00	0.00	1.92	0.00	0.00	0.00	1.92	3.85	14.42	4.81	0.00	3.85	1.92	25.96	0.00	1.92	0.00	7.69	0.00	2.88	0.96
377	3.87	0.00	0.00	1.94	0.00	0.00	0.65	1.94	17.42	0.65	0.00	2.58	0.00	30.32	0.00	3.23	0.00	10.97	0.65	1.94	0.65
388	0.00	0.00	0.00	0.00	0.00	0.00	0.99	2.97	19.80	1.98	0.00	4.95	0.00	22.77	0.00	3.96	0.00	8.91	0.99	4.95	0.00
400	1.92	0.00	0.00	0.00	0.00	0.00	0.00	0.96	10.58	0.96	0.00	6.73	0.96	36.54	0.00	4.81	3.85	8.65	0.00	0.96	1.92
417	1.98	0.00	0.00	0.99	0.00	1.98	2.97	0.00	4.95	2.97	0.00	0.99	0.99	53.47	0.00	0.99	0.00	3.96	0.00	0.99	1.98
450	0.66	0.00	0.00	1.66	0.00	0.00	3.32	1.00	4.65	1.99	0.00	7.64	0.00	43.52	0.33	3.32	1.33	8.97	0.00	1.00	1.99
459	1.62	0.97	0.97	0.00	0.00	1.30	1.62	0.65	4.87	1.95	0.00	3.57	0.65	44.48	0.32	0.65	0.32	9.09	0.00	0.97	2.60
471	1.32	0.99	1.32	0.00	0.00	0.00	1.32	1.99	12.91	2.32	0.00	4.64	0.66	33.44	0.00	1.32	0.00	11.26	0.00	2.32	0.99
485	0.00	0.66	0.99	0.00	0.00	0.00	4.64	1.66	4.97	0.66	0.00	3.31	0.66	38.08	0.00	0.99	0.00	7.62	0.00	0.99	2.65
499	1.29	0.64	0.64	0.00	0.00	0.00	2.57	0.32	5.47	0.96	0.00	2.89	0.32	49.52	0.96	1.29	0.32	8.68	0.00	1.29	1.93
520	3.90	0.00	1.30	0.00	0.00	0.00	3.90	0.97	8.44	1.62	0.00	1.62	0.65	34.74	0.32	0.97	0.97	7.47	0.00	1.95	2.60
548	1.93	0.00	0.64	0.00	0.00	0.00	2.57	1.61	7.40	0.64	0.00	3.22	0.64	45.34	0.32	0.64	2.25	4.82	0.00	0.96	0.00
560	3.26	0.00	1.86	0.00	0.00	0.00	2.79	1.40	12.09	0.00	0.47	3.26	0.47	32.09	0.00	1.40	2.33	5.12	0.00	3.26	1.86
570	1.33	0.00	1.00	0.33	0.00	1.33	4.33	1.67	7.33	0.00	1.33	3.00	0.67	32.67	0.00	1.33	1.67	7.00	0.00	2.00	1.00
580	1.63	0.33	0.33	0.00	0.00	0.00	3.58	0.33	4.56	0.33	0.00	2.61	0.65	47.23	0.00	0.98	0.33	4.89	0.00	1.63	1.63
590	1.62	0.32	1.29	0.00	0.00	0.65	2.91	1.62	8.41	0.32	0.00	3.56	0.97	37.86	0.32	0.65	1.62	6.80	0.00	1.62	0.97
600	1.87	0.62	0.93	0.00	0.00	0.00	2.49	1.56	9.66	0.62	0.00	2.18	0.93	35.83	0.62	2.80	0.00	4.36	0.00	1.25	1.87
610	1.66	0.66	1.33	0.00	0.00	0.00	1.99	0.66	8.31	0.00	0.00	1.99	0.33	43.52	0.66	0.66	2.99	8.31	0.00	1.66	1.66
620	2.66	1.00	1.00	0.00	0.00	0.00	3.99	1.00	7.64	0.33	0.00	2.33	0.33	40.86	0.66	2.66	1.99	7.64	0.00	0.33	1.33
628	3.59	0.65	0.65	0.00	0.00	0.00	4.58	1.31	8.17	0.00	0.00	1.96	0.65	42.16	0.00	4.25	1.31	3.59	0.33	0.98	0.65

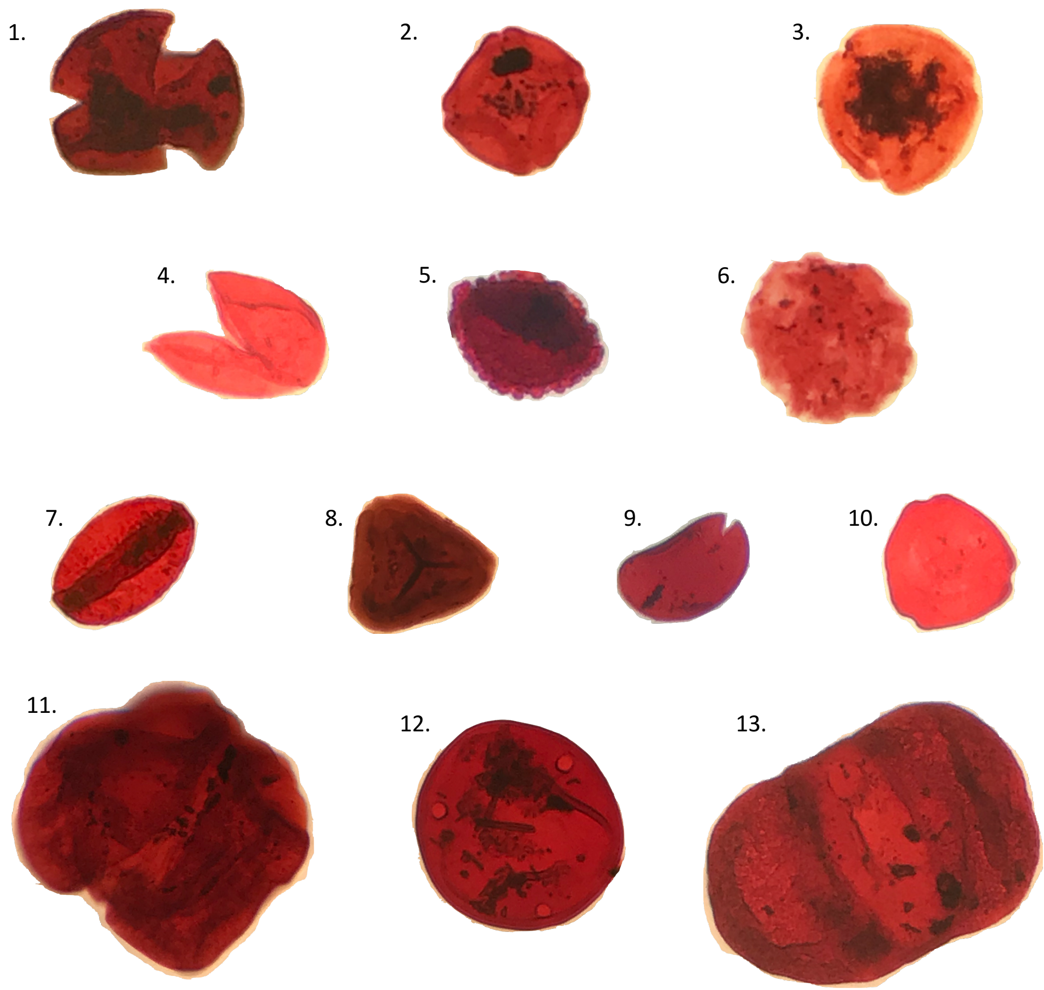

Plate 1

1. Acer sp.
2. Alnus sp.
3. Symplocos sp.
4. Taxodiaceae-Cupressaceae-Taxaceae
5. Ilex sp.
6. Liquidambar sp.
7. Quercus sp.
8. Sphagnum sp.
9. Polypodium sp.
10. Engelhardia sp.
11. Picea sp.
12. Carya sp.
13. Pinus sp.

Figure A.1: Common pollen taxa identified in the borehole Me22-25.

Table A.4: Dinoflagellate cyst occurrence data from borehole Me22-25. Positive identification is represented by “X” and possible identification is represented by “P.”

Sample ID	Depth	*Apteodinium tectatum*	*Cannosphaeropsis passio*	*Causteaudinium aubryae*	*Cerebrocysta poulsenii*	*Cordosphaeridium cantharellus*	*Cribroperidininium tenuitabulatum*	*Cyclopsiella elliptica/ granosa*	*Dinopterygium cladoides*	*Distatodinium paradoxum*	*Habibacysta tectatc*	*Hystrichosphaeropsis obscura*	*Impagidinium sp.*	*Labyrinthodinium t. modicum*	*Labyrinthodinium truncatum*	*Lejeunecysta sp.*	*Lingulodinium multivirgatum*	*Multipinula sp.*	*Operculodinium longispinigerum*	*Palaeocystodinum golzowense*	*Pyxidiniopsis fairhavenensis*	*Round Brown*	*Selenopemphix dionaeacysta*	*Spiniferites solidago*	*Sunatradinium druggi*	*Sumatradinium hamulatum*	*Sumatradinium soucouyantiae*	*Systematophora placantha*	*Trinovantedinium ferugnomatum*	*Trinovantedinium harpagonium*	*Trinovantedinium papulum*	*Tuberculodinium sp.*	*Unipontidinium aquaeductum*
116092	74											X	X									X	X							X			
116095	96				X																			X							X	X	
116097	112		X																					X					X				
116099	127		X					X					X					X													X		
116100	136		X										X					X											X		X	X	
116101	146		P																	X			X	X	X								
116103	160																							X					X				
116104	177												X																		X		
116106	190																														X	X	
116109	215.4																						X	X			X						
116110	222														X							X					X			X		X	
116118	253.8	X									P																						X
116120	263.2										X		X																				
116123	275.1			X											X				X			X		P								X	
116124	280												X	P	X									X					P				
116125	287			X									X	X																		X	
116127	302												X	X										X	X								
116129	315																	X															
116134	342																	X				X						X				X	
116135	354																			X					X								
116136	365												X						X					X	X			X				X	
116138	377			X													X	X				X										X	
116140	388									X						X	X	X	X			X		X		X							
116142	400			X						X							X	X	X	X				X	X								
116144	410			X						X							X	X						X	X		X	X					
116145	417			X						X									X			X			X							X	
116152	449.7						X						X			X					P				X								
116154	459	X																	X			X		X								X	
116156	471												X						X					X			X					X	
116160	485						X						X											X									
116161	499	X		X															X													X	
116166	520			X									X							X		X					X						
116168	534											X										X				X	X					X	
116169	548						X												X					X		X	X						
116170	560						X																			X						X	
116171	570											X														X	X						
116172	580								X												X	X		X		X						X	
116173	590								X			X														X	X					X	
116174	600											X					X		X							X						X	
116175	610								X									P	X		P	X				X							
116176	620					X												X									X						
116177	628					X						X										X		P			X						

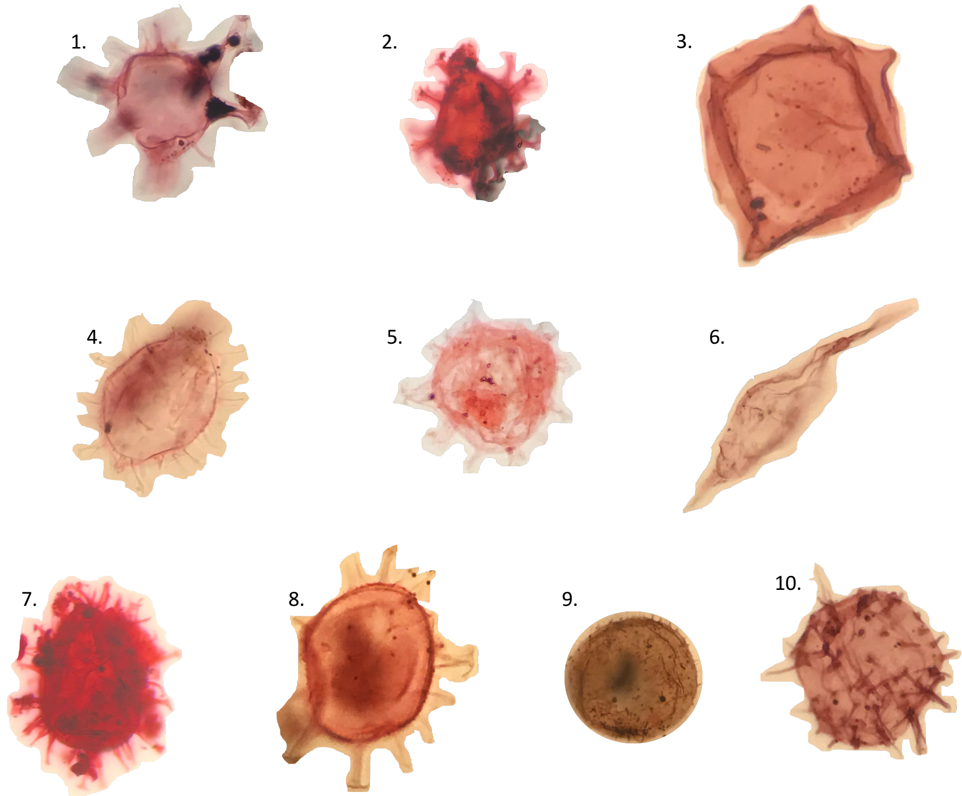

Plate 2

1. Cordosphaeridium cantharellus
2. Distatodinium paradoxum
3. Lejeunecysta sp.
4. Lingulodinium multivirgatum
5. Operculodinium longispinigerum
6. Palaeocysodinum golzownse
7. Selenopemphix dionaeacysta
8. Spiniferites solidago
9. Sumatradinium soucouyantiae
10. Trinovantedinium ferugnomatum

Figure A.2: Common dinoflagellate cyst taxa found in borehole Me22-25.

Table A.5: Total pollen and microsphere counts for the borehole Me22-25. Calculated pollen concentrations per gram of sediment can be found in the right column. Samples at 76.0 ft and 177.0 ft were omitted from this chart. The dry weight for the sample at 76.0 ft was not recorded, and there were no microspheres in the sample at 177.0 ft.

Sample ID	Depth	Tc (Total Pollen)	Lc (Total Microspheres)	Ms (microspheres added)	Wt (Dry Weight)	Pollen Concentration/g
116094-1.9-2.0	82	103	7	93900	47.78	28917.36
116097-1.9-2.0	112	100	56	93900	58.23	2879.59
116099-1.0-2.0	127	309	28	93900	44.36	23360.09
116100-5.9-6.0	136	155	13	93900	39.36	28444.54
116101-5.9-6.0	146	101	5	93900	57.21	33154.69
116103-0.0-0.1	160	100	3	93900	41.85	74790.92
116104-0.3-0.4	171	103	9	93900	50.98	21079.51
116106-0.0-0.1	190	102	9	93900	34.18	31135.17
116109-5.4-5.5	215	302	24	93900	62.63	18865.96
116110-1.9-2.0	222	300	13	93900	43.5	49814.32
116123-0.1-0.2	275	291	14	93900	37.63	51867.62
116124-0.0-0.1	280	311	12	93900	45.69	53262.75
116125-1.9-2.0	287	106	8	93900	30.69	40540.08
116127-1.9-2.0	302	306	26	93900	61.08	18093.17
116135-3.9-4.0	354	104	4	93900	36.71	66505.04
116136-9.9-10.0	365	104	5	93900	29.74	65673.17
116138-1.9-2.0	377	155	16	93900	59.74	15226.92
116140-1.9-2.0	388	101	11	93900	33.06	26079.03
116142-0.0-0.1	400	104	2	93900	50.57	96555.27
116145-1.9-2.0	417	101	2	93900	50.38	94123.66
116152-4.7-4.8	449.7	301	31	93900	48.3	18876.58
116154-4.9-5.0	459	308	30	93900	50.09	19246.16
116156-5.9-6.0	471	302	2	93900	48.68	291267.46
16160-0.0-0.1	485	302	14	93900	50.11	40422.21
116161-3.9-4.0	499	311	7	93900	50.38	82807.52
116166-0.0-0.1	520	308	7	93900	39.69	104096.75
116169-8.9-9.0	548	311	7	93900	38.69	107827.42
116170-9.9-10.0	560	215	5	93900	45.9	87967.32
116171-9.9-10.0	570	300	4	93900	44.24	159188.52
116172-9.9-10.0	580	307	20	93900	52.72	27340.00
116173-9.9-10.0	590	309	13	93900	50.65	44065.76
116174-9.9-10.0	600	321	6	93900	35.05	143328.10
116175-9.9-10.0	610	301	13	93900	30.71	70796.03
116176-9.9-10.0	620	301	9	93900	20.96	149829.83
116177-7.9-8.0	628	306	8	93900	54.75	65601.37